

Electronic Thesis and Dissertation Repository

1-31-2014

Pre-diabetes and sympathetic nervous system mediated microvascular dysregulation in skeletal muscle

Nicole M. Novielli
The University of Western Ontario

Supervisor
Dr. Dwayne Jackson
The University of Western Ontario

Graduate Program in Medical Biophysics
A thesis submitted in partial fulfillment of the requirements for the degree in Doctor of Philosophy
© Nicole M. Novielli 2014

Follow this and additional works at: <https://ir.lib.uwo.ca/etd>



Part of the [Circulatory and Respiratory Physiology Commons](#)

Recommended Citation

Novielli, Nicole M., "Pre-diabetes and sympathetic nervous system mediated microvascular dysregulation in skeletal muscle" (2014). *Electronic Thesis and Dissertation Repository*. 1888.
<https://ir.lib.uwo.ca/etd/1888>

This Dissertation/Thesis is brought to you for free and open access by Scholarship@Western. It has been accepted for inclusion in Electronic Thesis and Dissertation Repository by an authorized administrator of Scholarship@Western. For more information, please contact wlsadmin@uwo.ca.

*PRE-DIABETES AND SYMPATHETIC NERVOUS SYSTEM MEDIATED
MICROVASCULAR DYSREGULATION IN SKELETAL MUSCLE*

(Thesis format: Integrated Article)

by
Nicole Maria Novielli

Graduate Program in Medical Biophysics

*A thesis submitted in partial fulfillment
of the requirements for the degree of
Doctor of Philosophy*

*The School of Graduate and Postdoctoral Studies
The University of Western Ontario
London, Ontario, Canada*

© *Nicole Maria Novielli 2014*

Abstract

Pre-diabetes is associated with impairments in cardiovascular health that manifest prior to the onset of overt type 2 diabetes. Characterized by hyperinsulinemia and insulin resistance, pre-diabetes has been associated with increases in sympathetic nerve activity, which may result in augmented sympathetic control of the peripheral vasculature within skeletal muscle. Currently however, there are no studies investigating the impact of pre-diabetes on sympathetically-mediated vascular control. The primary study of this thesis investigated the effects of pre-diabetes on baseline sympathetic neuropeptide Y Y1 receptor (NPY Y1R) and alpha 1 adrenergic receptor (α 1R) control of hindlimb vascular tone. Experiments were carried out in anesthetized pre-diabetic Zucker Diabetic Fatty (ZDF) rats and control lean ZDF rats during drug delivery of sympathetic antagonists while measuring femoral artery blood flow (Q_{fem}) and calculated vascular conductance (VC). Despite similar baseline Q_{fem} and VC, Y1R, α 1R and dual Y1R+ α 1R blockade (via BIBP3226 and prazosin) elicited increases in Q_{fem} and VC that were greater in pre-diabetic rats compared to controls, demonstrating heightened Y1R and α 1R control of baseline vascular tone. These results were also supported by increased Y1R, α 1R and NPY expression in hindlimb tissue of pre-diabetic rats. In effort to determine whether pre-diabetes effects microvascular network function in contracting skeletal muscle, intravital microscopy was used to evaluate arteriolar rapid onset vasodilation (ROV) and steady-state vasodilation and blood flow responses to tetanic and rhythmic contraction of the gluteus maximus muscle in pre-diabetic (The Pound Mouse, c57bl6 background) and control mice (c57bl6). Baseline diameter and blood flow of arterioles were similar between groups; however, contraction-evoked vasodilatory and blood flow responses were blunted in pre-diabetic compared to control

mice. In addition, the magnitude of contraction-evoked dilation was greater in distal arterioles (3A and 4A) compared to proximal arterioles (2A) in GM arteriolar networks of control mice; however, such spatially-dependent differences in contraction-evoked dilation was disrupted in pre-diabetic mice. Blockade of Y1R and α 1R (via BIBP3226 and prazosin) restored ROV and steady-state vasodilation to tetanic and rhythmic contractions in pre-diabetic mice to levels similar to controls. Blockade of arteriolar sympathetic receptors also restored dilatory magnitude of distal arterioles in pre-diabetic mice. In conclusion, the results presented in this dissertation provide evidence that peripheral arteriolar Y1R and α 1R activation are enhanced in pre-diabetes, resulting in augmented sympathetic modulation of basal skeletal muscle blood flow and VC, as well as deficits in arteriolar vasodilation to skeletal muscle contraction.

Key words: pre-diabetes, diabetes, microcirculation, arterioles, neuropeptide Y, norepinephrine, Y1 receptor, adrenoceptor, sympathetic nervous system, skeletal muscle, muscle contraction, exercise, blood flow.

Co-Authorship Statement

The work contained herein was carried out by the author, under the supervision of Dr. Dwayne Jackson and the advice of Dr. Christopher Ellis and Dr. Daniel Goldman. This included conception, design, implementation, biochemical and data analysis and preparation of manuscripts.

In chapter 2, Baraa Al-Khazraji and Philip Medeiros assisted with Western blot analysis, and manuscript preparation. In chapter 5 and appendix A, Western blot analysis was performed by the author and Philip Medeiros.

Acknowledgments

The last five years of this academic journey cannot go without mention of several influential and supportive people:

Firstly, I would like to express greatest gratitude to my supervisor, Dr. Dwayne Jackson. Thank you for being my mentor and most importantly a dear friend. Thank you for giving me the opportunity to learn and grow as a young scientist, and providing me with many tools to ensure a successful future.

Thank you to my advisory committee members, Dr. Chris Ellis and Dr. Dan Goldman. Thank you for your contributions and guidance. I would also like to thank my thesis defense examiners, Dr. Kevin Shoemaker, Dr. Savita Dhanvantari, Dr. Greg Marsh, and Dr. Coral Murrant. I appreciate your time and efforts in evaluating my thesis and being part of my defense.

I would like to thank my fellow lab mates in the Jackson Lab: Phil Medeiros, Baraa Al-Khazraji and Nate Hayward. I cannot express what a joy it has been to work and overcome challenges together. You have made my time in graduate school unforgettable. I hold your friendships close to my heart, and cannot imagine the past five years without you. Thank you!

I would also like to acknowledge my most amazing friends/family for their continued support: Jenna Dasberg, Sonia Plusa, Christina Cicci, Nicole Wilson, Laura Fung, Allison Brazeau, Brittany Ballint, Lindsay Ringuette, Carolyn Crawford, Stephanie LoPresti, Franco LoPresti, Julie Guido. Thank you for always being there for me. You've all been such an important part of my life and I can't thank you enough.

To my family: Tonia, Dino and Bianca Novielli. You have been my biggest support group. Words cannot express how grateful and blessed I am to have such an amazing family. You have done absolutely everything for me. I love you all very much.

To my biggest cheerleader, Kyle Kuntz, thank you for your continued love and support. You have always believed in me and I cannot express how lucky I am to have you by my side. I love you, xo.

Table of Contents

Abstract.....	ii
Co-Authorship Statement.....	iv
Acknowledgments.....	v
Table of Contents.....	vi
List of Tables.....	ix
List of Figures.....	x
List of Appendices.....	xii
Preface.....	xiii
List of Abbreviations.....	xiv
Chapter 1 : Introduction.....	1
1.1. General introduction.....	1
1.2. Skeletal muscle microvasculature: The role of arterioles.....	6
1.3. The sympathetic nervous system: Peripheral neurovascular regulation.....	8
1.4. Skeletal muscle contraction, functional hyperemia and sympatholysis.....	17
1.5. Pre-diabetes and vascular dysregulation.....	18
1.6. Animal models of pre-diabetes.....	20
1.7. Rationale.....	21
1.8. Specific thesis objectives.....	24
1.9. Hypotheses.....	25
1.10. References.....	26
Chapter 2 : Pre-diabetes augments neuropeptide Y1- and α 1-receptor control of basal hindlimb vascular tone in young ZDF rats.....	40
2.1. Introduction.....	41
2.2. Materials and methods.....	43

2.3. Results.....	50
2.4. Discussion.....	66
2.5. Conclusions.....	70
2.6. Acknowledgements.....	70
2.7. References.....	72
Chapter 3 : Contraction-evoked vasodilation and functional hyperemia are compromised in branching skeletal muscle arterioles of young pre-diabetic mice	78
3.1. Introduction.....	79
3.2. Materials and methods	83
3.3. Results.....	95
3.4. Discussion.....	106
3.5. Conclusions.....	111
3.6. Acknowledgements.....	111
3.7. References.....	112
Chapter 4 : Y1- and α 1-adrenergic receptor activation attenuates contraction-evoked vasodilation in branching skeletal muscle arterioles of young pre-diabetic mice	120
4.1. Introduction.....	121
4.2. Materials and methods	125
4.3. Results.....	132
4.4. Discussion.....	150
4.5. Conclusions.....	158
4.6. References.....	159
Chapter 5 : Conclusions.....	167
5.1. Summary.....	167
5.2. Merit.....	168
5.3. Limitations and assumptions.....	171
5.4. Future Directions	174

5.5. References.....	179
Appendices.....	184
Curriculum Vitae	189

List of Tables

Table 2.1: Physical and physiological characteristics of CTRL and PD rats.	52
Table 2.2: Blood pressure and heart rate responses associated with each condition.	53
Table 2.3: Baseline values of hindlimb blood flow and vascular conductance before pharmacological treatments.	54
Table 2.4: Hindlimb blood flow and vascular conductance at baseline and following acetylcholine and sodium nitroprusside interventions.	55
Table 3.1. Body mass, fasting blood glucose and gluteus maximus dry/wet ratio for CTRL and PD.	96
Table 3.2. Gluteus maximus arteriolar baseline diameter, blood flow and responses to elevated O ₂ (21%).	99
Table 4.1. Gluteus maximus arteriolar baseline diameter and responses to elevated O ₂ (21%).	133
Table 4.2. Maximal diameter responses of gluteus maximus arterioles to sodium nitroprusside with and without sympathetic receptor blockade (10μM).	134

List of Figures

Figure 2.1: Representative hindlimb vascular conductance.	56
Figure 2.2. Sympathetic receptor blockade elicits greater vascular responses in PD.....	58
Figure 2.3: Percent change in hindlimb vascular conductance following Y1R and α 1R blockade.	59
Figure 2.4. Y1R and α 1R synergism is not observed in CTRL and PD.....	61
Figure 2.5. Skeletal muscle NPY concentration is elevated in PD.	63
Figure 2.6. Y1R expression is augmented in PD.	64
Figure 2.7. α 1R expression is augmented in PD.	65
Figure 3.1. Gluteus maximus 2A to 4A arteriolar segments.....	89
Figure 3.2. Second order arteriolar response to 800 ms tetanic contraction.	92
Figure 3.3. Second order arteriolar response to 8 Hz rhythmic contraction.	93
Figure 3.4. Rapid onset vasodilation and blood flow responses of arterioles following tetanic muscle contraction are blunted in PD.	100
Figure 3.5. Sensitivity of ROV responses to increasing tetanic contraction duration.	101
Figure 3.6. Percent diameter change of ROV at arteriolar orders.	102
Figure 3.7. Arteriolar dilation and blood flow responses are compromised in PD following rhythmic contraction.	104
Figure 3.8. Percent diameter change to rhythmic contraction at arteriolar orders.....	105
Figure 4.1. Sympathetic Y1R and α 1R blockade restores ROV in PD.	138
Figure 4.2. Sympathetic Y1R and α 1R activation attenuates ROV in CTRL.	139

Figure 4.3. Effects of Y1R and α 1R blockade on arteriolar branch order ROV responses following tetanic contraction in PD.	140
Figure 4.4. Sympathetic Y1R and α 1R blockade restores steady-state vasodilation in PD.	144
Figure 4.5. Sympathetic Y1R and α 1R activation attenuates steady-state vasodilation in CTRL.	145
Figure 4.6. Effects of Y1R and α 1R blockade on arteriolar branch order dilatory responses following sustained rhythmic contraction in PD.	146
Figure 4.7. Vasoconstriction of gluteus maximus arterioles to NPY.	148
Figure 4.8. Vasoconstriction of gluteus maximus arterioles to PE.	149
Figure 5.1. Glucose, insulin and leptin modifies vascular smooth muscle cell Y1R and α 1R expression in CTRL and PD.	178

List of Appendices

Appendix A.....	184
Appendix B.....	188

Preface

"To be what we are, and to become what we are capable of becoming, is the only end of life."-Robert Louis Stevenson.

List of Abbreviations

°C	Degrees Celcius
µg	Micrograms
µl	Microliters
2A	Second-order arteriole
3A	Third-order arteriole
4A	Fourth-order arteriole
α1R	Alpha 1 adrenergic receptor
α2R	Alpha 2 adrenergic receptor
AC	Adenyl cyclase
ACh	Acetylcholine
AEBSF	4-(2-Aminoethyl) benzenesulfonyl fluoride
APP	Amino peptidase P
αR	Alpha-adrenergic receptor
ATP	Adenosine triphosphate
β2R	Beta 2 adrenergic receptor
BIBP3226	N2-(diphenylacetyl)-N-[(4-hydroxyphenyl)-methyl]-D-arginine amide
βR	Beta-adrenergic receptor
BSA	Bovine serum albumin
cAMP	Cyclic adenosine monophosphate

CO ₂	Carbon dioxide
CTRL	Control group
D	Diameter
DMEM	Dulbecco's minimal essential medium
DPPIV	Dipeptidyl peptidase IV
EDTA	Ethylenediaminetetraacetic acid
FBS	Fetal bovine serum
FITC	Fluorescein isothiocyanate
fps	Frames per second
g	Grams
GM	Gluteus maximus
HBSS	Hank's buffered saline solution
HCl	Hydrochloric acid
hr	Hour
HR	Heart rate
HRP	Horseradish peroxidase
Hz	Hertz
IGEPAL	Octylphenoxypolyethoxyethanol
IP3	Inositol 1,4,5-triphosphate
i.v.	Intravenous

IVVM	Intravital video microscopy
kg	Kilograms
kHz	Kilohertz
L	Liter
L-NMMA	NG-monomethyl-L-arginine
LDCV	Large dense cored vesicles
MAP	Mean arterial pressure
mg	Milligrams
min	Minute
ml	Milliliters
mm	Millimeters
mM	Millimolar
mmHg	Millimeters of mercury
ms	Millisecond
MSNA	Muscle sympathetic nerve activity
N ₂	Nitrogen
N	Normal
NA	Numerical apperture
NaCl	Sodium Chloride
NE	Norepinephrine

nl	Nanoliters
ng	Nanograms
nm	Nanometers
NO	Nitric oxide
NOS	Nitric oxide synthase
NPY	Neuropeptide Y
NT	Neurotransmitter
O ₂	Oxygen
PD	Pre-diabetic group
PE	Phenylephrine
PE-10, -50 or -60	Polyethylene tubing 10, 50 or 60
pg	Picograms
Prazosin	(2-[4-(2-furoyl)- piperazin-1-yl]-4-amino-6,7-dimethoxyquinazolhinyedrochloride)
PSS	Physiological salt solution
Q _{fem}	Femoral blood flow
rpm	Revolutions per minute
RBC	Red blood cell
ROV	Rapid-onset vasodilation
SDCV	Small dense cored vesicles
SDS-PAGE	Sodium dodecyl sulfate poly-acrylamide gel electrophoresis

SE	Standard error
sec	Seconds
SEM	Standard error of the mean
SNA	Sympathetic nerve activity
SNP	Sodium nitroprusside
SNS	Sympathetic nervous system
SR	Sarcoplasmic reticulum
TBS	Tris-buffered saline
TH	Tyrosine hydroxylase
TMB	Tetramethylbenzidine
TTBS	Tris-buffered saline + Tween-20
VC	Vascular conductance
V_m	Mean velocity
V_{RBC}	Centerline red blood cell velocity
VSMC	Vascular smooth muscle cell
Y1R	Neuropeptide Y1 receptor
ZDF	Zucker diabetic fatty

Chapter 1 : Introduction

1.1. General introduction

Pre-diabetes is characterized by elevated blood glucose and insulin resistance, over-production of insulin and resultant hyperinsulinemia, affecting approximately 22% of the Canadian population (Canadian Diabetes Association, 2011). Cardiovascular disease, the most common diabetes-related co-morbidity, is prevalent in the pre-diabetic state prior to the onset of overt type 2 diabetes (Faeh, William, Yerly, Paccaud, & Bovet, 2007; Haffner, Stern, Hazuda, Mitchell, & Patterson, 1990). In the peripheral vasculature, specifically within skeletal muscle, compromised red blood cell (RBC) velocity and RBC supply rates in capillaries have been demonstrated under basal conditions (Ellis et al., 2010), suggesting functional deficits of upstream microvasculature. Skeletal muscle comprises approximately 30-40% of total body mass (Janssen, Heymsfield, Baumgartner, & Ross, 2000) and contains the largest proportion of the microvasculature responsible for tissue blood flow distribution, i.e. arterioles. However little is known of the impact of pre-diabetes on microvascular function within skeletal muscle.

Skeletal muscle microvasculature is comprised of arterioles, capillaries and venules. The arterioles are arranged in a network spanning the tissue, and are integral to distributing blood flow to the capillaries of active muscle fibers (via vasodilation) in an effort to meet metabolic demand (Fronek & Zweifach, 1975; Mackie & Terjung, 1983; Welsh & Segal, 1996). In contrast, concomitant arteriolar constriction in inactive tissues occurs to maintain resistance throughout the arteriolar network and redirect blood flow to sites of highest metabolic activity. Arteriolar constriction is achieved by the activation of

peripheral sympathetic nerve fibers innervating skeletal muscle arterioles through the release of sympathetic neurotransmitters (NT): norepinephrine (NE), neuropeptide Y (NPY) and adenosine triphosphate (ATP). These neurotransmitters interact with their respective sympathetic receptors (discussed in detail below) located on the arterioles to elicit vasoconstriction.

Changes in sympathetic outflow are mediated by the arterial baroreflexes in an effort to maintain overall systemic blood pressure on a moment-by-moment basis. The arterial baroreceptors are mechanoreceptors or ‘stretch’ receptors located in the aortic arch and carotid sinuses. Sudden increases or decreases in blood pressure deviating from the ‘operating point’, activate or inhibit baroreceptor activity. For example, a decrease in blood pressure elicits reciprocal increases in peripheral sympathetic outflow, causing vasoconstriction of the resistance vasculature, increasing peripheral resistance, and increasing blood pressure (Mosqueda-Garcia, 1996; Rowell, 1993). Under conditions of work or exercise however, arteriolar vasodilation in response to skeletal muscle contraction must occur to increase blood flow to the tissue, despite tonic arteriolar sympathetic activation. Thus, any dysregulation of arteriolar sympathetic control could deleteriously impact muscle microvascular supply at rest and under working conditions.

Although many diabetes-related vascular complications exist as a result of hyperglycemia, hyperinsulinemia in pre-diabetes may contribute to microvascular dysregulation, as insulin is known to stimulate sympathetic nerve activity (SNA). For example, elevated SNA recordings using microneurography have been shown to correlate with the degree of insulin resistance (E. A. Anderson, Balon, Hoffman, Sinkey, & Mark, 1992; DeFronzo & Ferrannini, 1991). Moreover, intracerebroventricular administration

of insulin elicits increases in peripheral SNA (Muntzel, Anderson, Johnson, & Mark, 1995). Insulin has also been shown to stimulate muscle sympathetic nerve activity, and in insulin resistant states, increased basal SNA has been reported (E. A. Anderson et al., 1992; Berne, Fagius, Pollare, & Hjendahl, 1992; Scherrer & Sartori, 1997). Interestingly, insulin exerts its sympathoexcitatory effects selectively. In humans, insulin stimulates increased SNA to skeletal muscle, but not to the skin, and in rats, insulin increases lumbar sympathetic outflow, but not adrenal SNA (Berne et al., 1992; Morgan, Balon, Ginsberg, & Mark, 1993). These findings may provide implications for peripheral sympathetic dysregulation of arterioles within limb skeletal muscle in pre-diabetes.

The regulation of sympathetic receptor activation at the arterial level is integral in maintaining resistance, tissue perfusion and blood pressure regulation at rest as well as during periods of physical activity. Enhanced activation in diseased states, such as pre-diabetes, could lead to impairments in sufficient skeletal muscle perfusion. This could occur via ‘hypersympathomodulation’ of skeletal muscle vasculature, where one or more of the components involved in sympathetic vascular regulation are increased. This may manifest as an increase in SNA, increased vascular sympathetic receptor expression, or greater sympathetic neurotransmitter production and release. Studies investigating basal sympathetic neurovascular control in the metabolic syndrome and obesity (conditions possessing overlapping characteristics to pre-diabetes) have demonstrated heightened alpha-adrenergic receptor (α R) contribution to basal vascular tone compared to lean controls. It was shown that blockade of α R caused greater increases in iliac and femoral vascular conductance (Frisbee, 2003; Naik, Xiang, Hodnett, & Hester, 2008), and that α R activation of hindlimb arteries and cremasteric arterioles elicited greater vasoconstrictor

responsiveness to adrenergic agonists (Naik et al., 2008; Stepp & Frisbee, 2002). Although these past studies illustrate augmented adrenergic vascular regulation under metabolic disease conditions, there is a paucity of studies that have investigated the independent and/or interactive role of NPY under such conditions.

NPY is a 36 amino acid peptide that is co-stored with NE within peripheral sympathetic nerves innervating skeletal muscle vasculature. It promotes potent and prolonged arteriolar constriction through activation of the NPY Y1 receptor (Y1R). Past studies have demonstrated that NPY is equally as important as NE in maintaining arteriolar blood flow and vascular conductance under baseline conditions in male Sprague Dawley rats (Jackson, Milne, Noble, & Shoemaker, 2005; Jackson, Noble, & Shoemaker, 2004). The effects of NPY on microvascular tone were shown to be both independent (via Y1R activation) (Jackson et al., 2004), and synergistic under conditions of Y1R and alpha 1 adrenergic receptor (α 1R) activation (Jackson et al., 2005). Neuronal NPY release and its effects on arteriolar constriction become even more apparent under conditions of elevated SNA (Bartfai, Iverfeldt, Fisone, & Serfozo, 1988; De Camilli & Jahn, 1990; Lundberg, Franco-Cereceda, Lou, Modin, & Pernow, 1994). Thus, it is reasonable to suspect that, under conditions of hyperinsulinemia and heightened baseline SNA (i.e., in pre-diabetes), NPY and NE would promote vascular dysregulation under baseline conditions, at the onset of exercise, and during steady state exercise. Remarkably, there have been no studies investigating the roles of NPY and NE on microvascular dysregulation pre-diabetes.

Under basal conditions, skeletal muscle is perfused with approximately 15% of cardiac output. In contrast however, under high intensity exercise conditions, the

proportion of cardiac output to working skeletal muscle can increase up to approximately 85% (Rowell, 1993), as increases in arteriolar diameter occur to increase blood flow to the tissue. Chronic sympathetic hyperactivity, occurring with hyperinsulinemia in pre-diabetes, could therefore compromise blood flow to exercising muscle. Deficits in skeletal muscle blood flow during exercise have indeed been reported in overt type 2 diabetes, metabolic syndrome and obesity in human and animal studies (Blain, Limberg, Mortensen, & Schrage, 2012; Frisbee, 2004; Karpoff et al., 2009; Kingwell, Formosa, Muhlmann, Bradley, & McConell, 2003; MacAnaney, Reilly, O'Shea, Egana, & Green, 2011; Vinet et al., 2011). Furthermore, enhanced arterial α R activation has been shown to compromise contraction-evoked blood flow responses in the metabolic syndrome (Frisbee, 2004). Such conclusions however, have been made based on hemodynamic changes measured at large conduit arteries (e.g. brachial and femoral arteries) with the use of Doppler ultrasound, venous occlusion plethysmography, transonic flow probes and thermodilution, providing a summation of arterial responses downstream in the muscle microvasculature. The large hyperemic response however is primarily encountered at the level of the arterioles within the muscle itself, therefore inferences regarding sympathetic vascular regulation, as well as dynamic changes of arteriolar diameter and blood flow in response to muscle contraction must be made. In an effort to deduce where potential sympathetic dysregulation within the arteriolar network occurs in the case of pre-diabetes, more invasive studies using animal models are needed.

Intravital studies of skeletal muscle microvasculature using animal models provide the ability to directly observe the microcirculation and determine regulatory mechanisms of blood flow within skeletal muscle. Stimulation of peripheral SNA has

shown to elicit variable vasoconstriction responses of arterioles depending on where they lie within the arteriolar network (J. M. Marshall, 1982), where constriction responses of smaller arterioles occurs to a greater extent compared to larger upstream arterioles (Boegehold & Johnson, 1988; Folkow, Sonnenschein, & Wright, 1971; VanTeeffelen & Segal, 2003). In an effort to drive capillary perfusion, distal arterioles have additionally demonstrated a greater ability to ‘overcome’ sympathetic constrictor restraint via vasodilation not only in resting, but also in active muscle (Folkow et al., 1971). Under circumstances of heightened SNA however, skeletal muscle arterioles may be affected differently depending on their location in the network. Therefore, in an effort to investigate whether pre-diabetes affects sympathetic skeletal muscle vascular function at the arteriolar level, an appropriate pre-diabetic model and skeletal muscle model for microvascular investigation is needed.

1.2. Skeletal muscle microvasculature: The role of arterioles

The skeletal muscle microcirculation is arranged in a network of blood vessels in order to continuously distribute blood flow throughout the tissue. Skeletal muscle blood flow is closely matched to metabolic demand of the tissue, where local changes in blood flow have been shown to occur specifically to fibers activated during muscle contraction (Mackie & Terjung, 1983). Dynamic changes in blood flow, based on metabolic need, occur as a result of changes in vessel diameter, particularly at the level of the arterioles. The arteriolar network is initiated at the feed artery entering the tissue, which bifurcates into daughter arterioles (termed first-order arterioles), giving rise to a branching arteriolar network (second order, third order arterioles, etc.) prior to reaching the terminal

arterioles, ultimately distributing RBCs and plasma to the capillaries. Arteriolar networks provide the greatest resistance to blood flow and, due to their branching architecture throughout the muscle and large capacity to constrict and dilate (Bevan, Halpern, & Mulvany, 1991; Tuma, Duran, & Ley, 2008), are essential to blood flow regulation and distribution of cardiac output.

The outer wall of arterioles consist of a layer of vascular smooth muscle cells (VSMC) surrounded by the external lamina or adventitia (Rhodin, 1967). The VSMCs are responsible for arteriolar contractility and can spatially control blood flow to capillary units supplying skeletal muscle fibers (Fuglevand & Segal, 1997). In resting skeletal muscle oxygen consumption is low, as is blood flow throughout the tissue. Reduced muscle perfusion under basal conditions occurs as a result of partial constriction of the resistance arterioles. The contractile properties of VSMCs maintaining basal arteriolar diameter are under a variable state of active shortening, referred to as “vascular tone” (Bevan et al., 1991; Rhodin, 1967). The contractile state of VSMCs is regulated by a balance of both vasodilator and vasoconstrictor control mechanisms. At rest, the need for vasodilation of skeletal muscle arterioles is rather low, however basal levels of putative dilators are necessary to negate increases in arteriolar resistance and preserve tissue perfusion in the face of partial arteriolar constriction. For example, nitric oxide (NO) and prostanoids, i.e., prostacyclin and prostaglandin E₂, have been implicated in the regulation of basal vascular tone within skeletal muscle (de Wit, von Bismarck, & Pohl, 1993; Radegran & Saltin, 1999).

In contrast to vasodilator mechanisms maintaining basal skeletal muscle blood flow, there are also vasoconstrictor influences maintaining the contractile state of

VSMCs, or “basal vascular tone”. A large contributor to maintaining partial constriction of arterioles is the sympathetic nervous system (SNS). The VSMC layer surrounding skeletal muscle arterioles is densely innervated with perivascular sympathetic nerve fibers that provide a constant outflow of sympathetic NTs. Sympathetic NTs interact with respective sympathetic receptors located on VSMCs, eliciting constitutive vasoconstrictive restraint on the arterioles and therefore maintaining resistance throughout the arteriolar network. Skeletal muscle is considered to have a high level of basal ‘vascular tone’ as it comprises a large proportion of the body, housing a substantial amount of the microvasculature, and therefore greatly influences basal blood pressure maintenance. In instances where metabolic demand of skeletal muscle increases however, such as during exercise, arterioles dilate to increase blood flow and support contractile activity of skeletal muscle.

1.3. The sympathetic nervous system: Peripheral neurovascular regulation

1.3.1. Sympathetic neurotransmission

The SNS plays an essential role in blood pressure maintenance and redistribution of blood flow during stress or exercise (Robertson, Biaggioni, Burnstock, Low, & Paton, 2012). Initiation of sympathetic outflow has been associated with central nervous system areas within the brain/brainstem such as the ventromedial and rostral ventrolateral medulla, caudal raphe nuclei, and paraventricular nucleus (Strack, Sawyer, Hughes, Platt, & Loewy, 1989). From the brain, supraspinal neurons project to cell bodies within the lateral horn of the spinal gray matter in the thoracolumbar spinal cord (T1-L2).

Sympathetic cell bodies give rise to pre-ganglionic neurons that innervate post-sympathetic neurons residing within the sympathetic ganglia (Robertson et al., 2012). Activation (or deactivation) of sympathetic outflow from supraspinal brain centers occurs on a moment-by-moment basis, entrained with the baroreflex (as discussed below), where neuronal impulses are stimulated and traverse to pre-ganglionic neurons. Upon activation, acetylcholine (ACh) is released from the pre-ganglionic neuron terminal, then binds to and activates nicotinic receptors of the post-ganglionic neurons at the sympathetic ganglion. Post-ganglionic neurons are unmyelinated and travel long distances, especially to the vasculature of the lower limbs, from the presynaptic ganglia to reach target organs. Excitatory impulses initiated by nicotinic receptor activation propagate along post-ganglionic nerve fibers to elicit exocytosis of vesicles containing NTs (Robertson et al., 2012). Post-ganglionic fibers supplying the vasculature of the lower body (pertaining to this thesis) originate from the lumbar and sacral paravertebral ganglia. These fibers come together into small bundles, forming a plexus within the adventitia of arterioles. This plexus then gives rise to a secondary plexus of fibers termed the terminal effector plexus, that resides on the surface of the medial layer of the vessel, where nerve fibres are then adjacent to the VSMCs (Robertson et al., 2012). The terminal effector plexus possesses varicosities, which contain small and large-dense cored vesicles (SDCV and LDCV) containing sympathetic NTs. These vesicles are generated near the golgi apparatus in the cell bodies and move by axonal transport within the axons to the nerve terminals of the terminal effector plexus. Sympathetic NT release from the vesicles is initiated by the release of pre-ganglionic ACh from nerve terminals that interacts with post-ganglionic nicotinic receptors, causing an increase in axon permeability to sodium. The increase in

sodium causes the opening of voltage-gated calcium channels, causing an influx of calcium, resulting in the fusion of vesicular and axonal membranes. The vesicle is then able to release its contents into the extracellular space close to the VSMCs, where NTs then interact with respective receptors located on the VSMCs, ultimately causing vasoconstriction (Robertson et al., 2012). For the purposes of this thesis, NE and NPY-mediated regulation of skeletal muscle vasculature will be addressed.

1.3.2. Norepinephrine

NE is the classically studied catecholamine involved in sympathetic vascular regulation. NE is found within adrenergic neurons, as well as in the chromaffin cells of the adrenal gland. Catecholamine synthesis begins with the uptake of the amino acid tyrosine into the cytoplasm of sympathetic neurons. Tyrosine hydroxylase, the rate limiting enzyme in the production of NE, then catalyses the conversion of tyrosine to dihydroxyphenyl-alanine. Dihydroxyphenyl-alanine is then converted to dopamine by the enzyme dopamine-decarboxylase. The aforementioned steps occur in the cytoplasm of the neuron, however dopamine-beta-hydroxylase catalyzes the conversion of dopamine to NE within the vesicles themselves. Once vesicles release NE into the extracellular space, NE interacts with respective α R and beta-adrenergic receptors (β R) located on the VSMCs. Binding of NE to the α 1R and alpha 2 adrenergic receptor (α 2R) causes calcium release from the sarcoplasmic reticulum within VSMCs, as well as increases VSMC membrane permeability to calcium. Increased intracellular calcium activates the calcium-calmodulin complex to cause VSMC constriction (Webb, 2003). Beta 2 adrenergic receptors (β 2R) are also present along VSMCs within skeletal muscle, which when activated by agonists such as isoproterenol, cause arteriolar vasodilation. Once the

β 2R is activated, production of intracellular cyclic adenosine monophosphate (cAMP) can inhibit calcium release from the sarcoplasmic reticulum and calcium entry into the cell, causing VSMC relaxation (Johnson, 2006). The effects of NE on β 2R activation are not resolvable unless the vasoconstrictor effects of α 1R and α 2R are blocked (Cowley & Franchini, 1996), demonstrating the predominant effect of NE on α R activation. Once NE disassociates from the respective receptor, it is inactivated by re-uptake via the Uptake-1 transporter into the axoplasm of the neuron where it can be stored into vesicles for future release or metabolized (Robertson et al., 2012). For the purposes of this thesis, focus will be on the α 1R.

1.3.2.1. Alpha 1 adrenergic receptor

Alpha 1 adrenergic receptors are long single-chain membrane-integrated glycoproteins and members of the G protein-coupled receptor superfamily. The receptor contains seven transmembrane alpha-helical domains, possessing three intracellular and three extracellular loops, and an intracellular juxtamembranous portion forming the eighth alpha-helix. The N-terminus of the receptor lies on the extracellular surface, where the C-terminus is located on the intracellular surface. Upon binding of NE to the receptor, $G_{\alpha q}$ -protein activation then activates second messenger protein pathways that contribute to increasing intracellular VSMC calcium levels (Robertson et al., 2012). $G_{\alpha q}$ -protein activation stimulates the activity of phospholipase C to hydrolyze phosphatidylinositol-bis-phosphate into inositol 1,4,5-triphosphate (IP₃) and diacylglycerol. IP₃ can directly initiate calcium signaling, as it interacts with calcium release channels on the sarcoplasmic reticulum (SR) (Somlyo & Somlyo, 2000). Increased calcium in the VSMC cytoplasm can also elicit calcium-induced calcium release from the SR, as well as

activate extracellular calcium entry through L-type calcium channels on the cell membrane (Hawrylyshyn, Michelotti, Coge, Guenin, & Schwinn, 2004; Wier & Morgan, 2003). Calcium binds to calmodulin, creating the calcium-calmodulin complex. This then activates myosin light chain kinase which phosphorylates myosin light chain, causing myosin cross-bridge activation and VSMC contraction (Wier & Morgan, 2003).

Endogenous α 1R regulation of the vasculature in this thesis was determined with the highly selective α 1R antagonist prazosin (2-[4-(2-furoyl)- piperazin-1-yl]-4-amino-6,7-dimethoxyquinazolinhydrochloride). Prazosin elicits hypotensive and vasodilatory effects by blocking the interaction between NE and the α 1R, and therefore interfering with sympathetically-activated VSMC contraction (Graham, Oates, Stoker, & Stokes, 1977; Oates, Graham, Stoker, & Stokes, 1976). Interestingly, the actions of prazosin have been predominantly identified at the level of the peripheral vasculature, where tissue distribution studies have also confirmed the majority of drug localization to the arterioles (Hess, 1975).

1.3.3. Neuropeptide Y

NPY is a 36 amino acid peptide that is co-stored and released with NE from peripheral sympathetic neurons (Ekblad et al., 1984). NPY was first isolated from the porcine brain (Tatemoto, Carlquist, & Mutt, 1982), and occurs abundantly in the mammalian central nervous system, as well as in the peripheral nervous system (Wahlestedt et al., 1990). Its composition is well conserved and is part of a family that includes peptide YY and pancreatic polypeptide. It is originally derived from a 97 amino acid precursor, pre-pro-NPY. Four post-translational enzymatic modifications follow in

order to synthesize the biologically active NPY₁₋₃₆. Prohormone convertase 1/3 cleaves proNPY, releasing a 30 amino acid c-flanking peptide of pre-proNPY and NPY₁₋₃₉ (Alfalah & Michel, 2004). Two amino acids of NPY₁₋₃₉ are then cleaved by a carboxypeptidase-like enzyme to form NPY₁₋₃₇. Finally, NPY₁₋₃₇ is amidated at its C-terminal by peptidyl-glycine- α -amidating monooxygenase to form the final biologically active peptide NPY₁₋₃₆. In the peripheral SNS, it is stored in post-ganglionic sympathetic neurons that innervate blood vessels, however NPY-containing neurons have been shown to be more abundant around resistance arterioles and proceed to innervate vessels in higher density as the arteriolar tree diverges into terminal branches (Sundler, Bottcher, Ekblad, & Hakanson, 1993). Although NPY is co-stored with NE, NPY is contained within LDCV of post-ganglionic sympathetic neurons, as opposed to SDCV that generally house NE. NPY release from these vesicles has been shown to occur to a greater extent under higher neuronal stimulation frequencies, however studies have confirmed that NPY is also released under lower stimulation frequencies (De Potter, Partoens, Schoups, Llona, & Coen, 1997), and is able to elicit vasoconstrictive effects under resting basal conditions (Bartfai et al., 1988; Jackson et al., 2004; Lundberg et al., 1994). When NPY is released from these neurons, it acts on its respective Y₁R to cause potent and prolonged vasoconstriction, a phenomenon initially discovered in cat skeletal muscle (Ekelund & Erlinge, 1997). NPY is degraded by enzymes dipeptidyl peptidase IV (DPPIV) to generate NPY₃₋₃₆, and amino peptidase P (APP) to generate NPY₂₋₃₆. DPPIV is a membrane-bound protease found on the cells of kidneys, liver, ileum, and also on endothelial cells, epithelial cells, astrocytes and T and B lymphocytes (Stange, Kettmann, & Holzhausen, 1996). It cleaves proline at the penultimate position, removing the tyr-pro

dipeptide from the N-terminus of NPY₁₋₃₆, generating NPY₃₋₃₆, which has less affinity for the Y1R (Grandt et al., 1993; Hopsu-Havu & Glenner, 1966). APP is found on astrocytes, endothelial cells, epithelial cells, neuronal cells and lung cells, and cleaves residues at the N-terminal to create NPY₂₋₃₆, also decreasing the affinity to Y1R binding.

1.3.3.1. Neuropeptide Y Y1 receptor

The NPY Y1R was the first NPY receptor identified and cloned from the rat cDNA library, having 90-96% overall identity across mammals (Eva, Keinanen, Monyer, Seeburg, & Sprengel, 1990; Larhammar et al., 1992). NPY Y1R expression has been detected in the brain, heart, kidneys, the gastrointestinal tract and skeletal muscle. Importantly, Y1Rs are located peripherally on arterioles where they mediate vasoconstrictive responses (Grundemar & Bloom, 1994). NPY Y1R is a G-protein coupled receptor. It is characterized by 7 trans-membrane spanning domains linked to a heterotrimeric G_{i/o}-protein. Activation of Y1R is specific to the full NPY₁₋₃₆ peptide. Truncated analogues of NPY at the N- and C-terminus, as well as modifications of central segments of the peptide result in significant decreases in NPY Y1R receptor affinity (Beck-Sickinger & Jung, 1995; Danho et al., 1988). The C-terminal region of NPY plays a main role in Y1R recognition as modifications to this end results in the greatest reductions in receptor affinity (Hoffmann, Rist, Videnov, Jung, & Beck-Sickinger, 1996). When NPY Y1R is activated, increases in intracellular calcium causes slow and long lasting depolarization of smooth muscle cells to elicit vasoconstriction (Dumont, Martel, Fournier, St-Pierre, & Quirion, 1992). Studies have reported that NPY can increase intracellular calcium via inhibition of ATP-sensitive potassium channels, activation of voltage-gated calcium channels and the inhibition of cAMP (Edvinsson,

1985; Edvinsson, Emson, McCulloch, Tatemoto, & Uddman, 1983; Motulsky & Michel, 1988; Tanaka et al., 1995). In support, NPY-induced vascular smooth muscle cell contraction can be inhibited by calcium channel antagonists (Lundberg et al., 1985).

In order to determine the endogenous Y1R-mediated effects of NPY on the vasculature, *N*2-(diphenylacetyl)-*N*-[(4-hydroxyphenyl)-methyl]-*D*-arginine amide (BIBP3226) was used in the studies described in this thesis. BIBP3226 is a highly potent and selective non-peptide Y1R antagonist, sharing similar Y1R molecular binding sites to NPY (Grundemar & Bloom, 1994). Past *in vivo* work in the rat has confirmed the ability of BIBP3226 to block the hypertensive response elicited by intravenous administration of NPY (Doods et al., 1995) and NPY induced vasoconstriction in rat skeletal muscle (Jackson et al., 2005).

1.3.4. Interactions between NPY and NE

Sympathetic postganglionic neurons release NE, NPY and ATP (Kasakov, Ellis, Kirkpatrick, Milner, & Burnstock, 1988). The release of each of these NTs can be modified as levels of SNA changes, allowing for a number of biological effects and interactions (e.g. slow, intermediary, and quick signaling) (Lundberg, 1996). For example, NPY produces a slow acting, potent and persistent increase in vascular tone. In contrast, NE-induced vasoconstriction occurs quickly and decays at a similar rate. Moreover, ATP induced vasoconstriction has been shown to be immediate and very short acting. It has been postulated that the duration of each transmitter's effects relies on the mode of deactivation/removal. For example, NE's vascular effects are removed quickly (NE reuptake via Uptake-1) compared to the prolonged duration of NPY induced vasoconstriction that is eliminated by enzymatic degradation of "free" NPY by DPPIV

and APP (Lundberg, 1996). In several investigations, NPY has been shown to potentiate α -adrenergic vasoconstriction *in vivo* (Dahlof, Dahlof, & Lundberg, 1985; Jackson et al., 2005; Linder, Lautenschlager, & Haefeli, 1996; Revington & McCloskey, 1988), as well as *in vitro* (Edvinsson, Ekblad, Hakanson, & Wahlestedt, 1984; Ekblad et al., 1984; Glover, 1985; Wahlestedt, Edvinsson, Ekblad, & Hakanson, 1985). The synergistic interaction between NPY and NE is receptor-mediated, as NPY has also been shown to enhance the vasoconstrictive response to sympathetic nerve stimulation and phenylephrine- (specific α 1R agonist) induced vasoconstriction (Dahlof et al., 1985). Additionally, NPY's endogenous contribution to basal vascular tone has been shown to act synergistically with endogenous NE. Upon simultaneous blockade of Y1R and α 1R of the hindlimb vasculature in male Sprague-Dawley rats, the increase in femoral artery vascular conductance was greater than the additive response elicited by independent blockade of each receptor (Jackson et al., 2004). It has been hypothesized that the interactive effects between Y1R and α 1R are due to consequent modification of specific receptor properties and/or second messengers (Franco-Cereceda & Liska, 1998). Both Y1R and α 1R are G-protein coupled receptors; therefore, cross talk between receptor-mediated changes in downstream signaling events may occur. Interestingly, the potentiating effects of NPY requires increased phospholipase C activity, which may further mobilize intracellular calcium (Wahlestedt et al., 1985; Wahlestedt et al., 1990). In addition, NPY may also inhibit adenylyl cyclase upon Y1R activation, decreasing downstream levels of cAMP (Kassis, Olasmaa, Terenius, & Fishman, 1987), thus reducing the relaxing effects of cAMP. Exact mechanisms behind potentiating effects of NPY however are not completely understood.

1.4. Skeletal muscle contraction, functional hyperemia and sympatholysis

Under basal conditions, there is a constant balance between arteriolar sympathetic activation and local vasodilator mechanisms (vascular tone). Increases in metabolic demand however elicits vasodilation of arterioles to increase blood flow to the working tissue and throughout the downstream capillary network – termed functional or exercise hyperemia (Bevan et al., 1991; Laughlin, Korthuis, Duncker, & Bache, 1996). Dilation of distal or terminal arterioles serving capillary units closest to activated muscle fibers initiates increases in blood supply, where modest adjustments of feed artery and proximal arteriole diameter occur. However in cases of intense exercise, muscle blood flow can increase up to 100-fold, constituting up to 90% of cardiac output (Saltin, Radegran, Koskolou, & Roach, 1998). High-intensity exercise elicits large vasodilatory responses within skeletal muscle, therefore providing an opportunity for large drops in arterial blood pressure (R. J. Marshall, Schirger, & Shepherd, 1961). To prevent a fall in blood pressure, SNA is increased (Rowell, 1993) as a result of the baroreflex. Heightened peripheral SNA therefore increases vasoconstrictor activity of the feed artery, proximal arterioles, and dilated terminal arterioles to maintain resistance throughout the arteriolar network of working tissue, as well as increase vasoconstriction to inactive tissues (Thomas & Segal, 2004). Increases in perivascular SNA has also been shown to suppresses conducted vasodilatory responses along skeletal muscle arterioles (Haug & Segal, 2005). The ability of arterioles to dilate, regardless of increased sympathetic neurovascular activation during exercise however, is termed ‘functional sympatholysis’ (Hansen, Sander, & Thomas, 2000; Remensnyder, Mitchell, & Sarnoff, 1962). Sympathetically-mediated skeletal muscle arteriolar constriction is greater at smaller

terminal arterioles feeding capillary units (J. M. Marshall, 1982); however, these arterioles have also been shown to undergo sympatholysis more readily compared to upstream vasculature during exercise (Folkow et al., 1971). Under such conditions, functional sympatholysis promotes distal arteriolar dilation to maximize perfusion of capillary networks supplying active muscle fibres (Folkow et al., 1971; Segal & Jackson, 2005). In diseased states where hypersympathomodulation of skeletal muscle vasculature occurs, such as pre-diabetes (Novielli, Al-Khazraji, Medeiros, Goldman, & Jackson, 2012), skeletal muscle arteriolar perfusion may become compromised as sympatholysis may occur to a lesser extent, especially in distal arterioles experiencing pronounced sympathetic vasoconstriction. Increased SNA has been confirmed in aged humans, and has been shown to reduce muscle blood flow at rest and during exercise (Dinenno, Jones, Seals, & Tanaka, 1999). More recently, this deficit in muscle blood flow has been attributed to hyperactivation of adrenergic receptors in aged animal models and humans (Casey & Joyner, 2012; Jackson, Moore, & Segal, 2010). Whether greater activation of sympathetic receptors (adrenergic and non-adrenergic) compromises arteriolar function and muscle blood flow in pre-diabetes remains to be investigated.

1.5. Pre-diabetes and vascular dysregulation

Pre-diabetes represents the initial stage of type 2 diabetic disease development, characterized by insulin resistance and elevated circulating insulin and glucose levels. As insulin resistance decreases tissue sensitivity to insulin, an overproduction of insulin results to promote glucose uptake and maintain near-normal blood glucose levels. Pre-diabetic disease progression to overt type 2 diabetes occurs when pancreatic beta cells

can no produce insulin to overcome insulin resistance, resulting in further hyperglycemia (Bock et al., 2006; Dinneen et al., 1998; Kanauchi, Kanauchi, Inoue, Kimura, & Saito, 2007; Meigs, Muller, Nathan, Blake, & Andres, 2003; Tirosh et al., 2005). Such pathological metabolic characteristics of pre-diabetes play a role in the initiation of cardiovascular complications that manifest prior to the onset of overt type 2 diabetes (Faeh et al., 2007; Gupta et al., 2012; Haffner et al., 1990; Schaefer et al., 2010; Shin, Lee, & Lee, 2011). Increased femoral intima media thickness, elevated blood pressure, augmented brachial-ankle pulse wave velocity, and impaired reperfusion hyperemia of the fingers have been reported in pre-diabetic humans, however there is a dearth of knowledge regarding the effects of pre-diabetes on microvascular function within skeletal muscle.

Although few, past studies have addressed modifications in arteriolar function as well as skeletal muscle capillary perfusion in pre-diabetic rats. Lesniewski *et al.* reported increases in vasoconstrictor responsiveness to NE and endothelin-1 in first order arterioles isolated from the gastrocnemius of normotensive pre-diabetic Zucker Diabetic Fatty (ZDF) rats (Lesniewski et al., 2008). In addition to pro-constrictor phenotypes of skeletal muscle arterioles, Ellis *et al.* demonstrated decreased RBC supply rate and decreased RBC velocity in capillary networks of the extensor digitorum longus muscle of the pre-diabetic ZDF rat (Ellis et al., 2010). These studies have demonstrated augmented arteriolar function of proximal arterioles and impaired capillary perfusion of skeletal muscle in early pre-diabetes; thus, it is reasonable to postulate that compromised arteriolar function occurs throughout the skeletal muscle microvascular network.

Studies directly investigating the impact of pre-diabetes on skeletal muscle microvascular control during exercise are limited. Certainly, human and animal studies have illustrated compromised blood flow regulation during exercise/muscle contraction in overt type 2 diabetes, the metabolic syndrome, and obesity (Blain et al., 2012, Vinet et al., 2011, Karpoff et al., 2009, Frisbee, 2003, Frisbee, 2004, MacAnaney et al., 2011, Kingwell et al., 2003). However, differences in the experimental models and methodological limitations constrain the current understanding of vascular control in metabolic diseases to bulk blood flow measures, i.e. femoral or brachial artery blood flow. Measures of bulk blood flow limits information on the site or nature of arteriolar dysregulation. Intravital techniques would be advantageous for directly addressing the microvascular network. Furthermore, models of overt type 2 diabetes, metabolic syndrome, and obesity are accompanied by chronic states of cardiovascular compromise and overt vascular disease; where early pre-diabetes represents the primary stage of diabetic disease, where vascular complications may not be as pronounced.

1.6. Animal models of pre-diabetes

1.6.1. The Zucker Diabetic Fatty rat

The ability to directly assess the effects of pre-diabetes on skeletal muscle vasculature can be performed using pre-diabetic animal models. The ZDF rat represents a model of progressive type 2 diabetes development. The ZDF rat has a genetic mutation of the leptin receptor, interrupting the interaction of leptin with its respective receptor. Leptin, a small adipose-derived hormone, is involved in the regulation of food intake via

a negative feedback loop upon binding to the leptin receptor (Clement et al., 1998; Lyssenko et al., 2005). Because of the dysfunctional leptin receptor in the ZDF rat, leptin is unable to signal cessation of food intake. When fed a high fat diet, the ZDF rat progressively develops programmed and consistent type 2 diabetes by the age of 8-9 weeks old. During the period prior overt type 2 diabetes development and pancreatic failure, the rat is considered to be in the pre-diabetic state. At 7-weeks-old, the ZDF rat demonstrates similar characteristics to the human condition of pre-diabetes; obesity, hyperinsulinemia, insulin resistance and elevated blood glucose –(Kim & Reaven, 2008; Lyssenko et al., 2005).

1.6.2. The Pound Mouse

Similar to the ZDF rat, the pound mouse also expresses a dysfunctional leptin receptor, in turn causing hyperphagia. The pound mouse is of the c57blk background and occurred as a spontaneous mutation at a Charles River facility. When fed a high fat diet, these mice exhibit obesity, hyperinsulinemia, insulin resistance and elevated blood glucose, similar to the pre-diabetic characteristics outlined for the human pre-diabetic condition. Unlike the ZDF rat however, the pound mouse does not go on to develop type 2 diabetes and pancreatic failure, rather it remains in a pre-diabetic state.

1.7. Rationale

Sympathetic neurovascular control is essential to the regulation of blood pressure and tissue perfusion due to its ability to modulate peripheral vascular resistance. It is especially important throughout skeletal muscle microvasculature, as skeletal muscle

makes up approximately 40% of body mass and comprises approximately 20% of total peripheral resistance under baseline conditions. NTs such as NE and NPY are released from perivascular nerve terminals and act post-junctionally on VSMC α 1Rs and Y1Rs to produce vasoconstriction. In states where peripheral sympathetic activation may be elevated, such as pre-diabetes, heightened sympathetic neurovascular modulation may result, leading to compromised skeletal muscle vascular control.

In pre-diabetes, SNA is suggested to be elevated, as hyperinsulinemia accompanying the disease is known to be sympathoexcitatory (E. A. Anderson et al., 1992; E. A. Anderson, Hoffman, Balon, Sinkey, & Mark, 1991; Rowe et al., 1981). In humans, hyperinsulinemia is associated with elevated SNA and correlates with the degree of insulin resistance (E. A. Anderson et al., 1992; DeFronzo & Ferrannini, 1991; Huggett, Hogarth, Mackintosh, & Mary, 2006). Moreover, systemic infusion of insulin in rats has been shown to preferentially increase lumbar SNA (Epstein & Sowers, 1992; Esler et al., 2001; Muntzel et al., 1995; Scherrer & Sartori, 1997). Increases in peripheral SNA accompanying pre-diabetes may therefore compromise skeletal muscle microvascular regulation under resting and active conditions via over-activation of arteriolar sympathetic receptors, however this is yet to be investigated.

Indeed studies investigating skeletal muscle vascular function under conditions of ageing, the metabolic syndrome and obesity have demonstrated increased basal vascular tone and compromised vasodilation of skeletal muscle vasculature as a result of heightened sympathetic vascular control (Casey & Joyner, 2012; Frisbee, 2004; Jackson et al., 2010; Naik et al., 2008). Such studies have only evaluated the contribution of α R

activation to sympathetically-mediated changes in vascular function; however, peptidergic NPY Y1R vascular control has not been considered. Under conditions of elevated SNA, sympathetic vascular modulation becomes more pronounced not only by NE-, but also NPY (Bartfai et al., 1988; De Camilli & Jahn, 1990; Lundberg et al., 1994). This provides implications for heightened adrenergic and peptidergic modulation of the vasculature in pre-diabetes, which may affect basal sympathetic vascular tone, as well as impinge on dilatory responses to skeletal muscle contraction.

Microvascular responses to skeletal muscle contraction are non-uniform throughout the arteriolar network, with greater (relative) arteriolar dilation occurring in distal versus proximal regions (Davis, Hill, & Kuo, 2008; Dodd & Johnson, 1991; J. M. Marshall & Tandon, 1984; VanTeeffelen & Segal, 2006). Distal arterioles are also able to dilate and overcome sympathetic activation (sympatholysis) more readily than proximal arterioles within the muscle (K. M. Anderson & Faber, 1991). Interestingly, studies have demonstrated differential distribution of sympathetic receptors at different arteriolar branch orders of arteriolar networks (K. M. Anderson & Faber, 1991; Moore et al., 2010). Furthermore, NPY-containing perivascular neurons have been shown to be more abundant around resistance arterioles and innervate distal arterioles of the microvascular network in higher density (Sundler et al., 1993). Under conditions of heightened SNA, i.e. in pre-diabetes, such distinct spatial sympathetic arteriolar control may be lost, where vasodilatory responses to skeletal muscle contraction may be compromised. Therefore, direct investigation of both adrenergic and peptidergic-mediated arteriolar network control is needed to address whether elevated SNA contributes to decrements in skeletal muscle microvascular function in pre-diabetes.

1.8. Specific thesis objectives

The overall objectives of this thesis research are the following:

Objective 1 – Manuscript 1: Chapter 2

To address whether basal endogenous Y1R and α 1R regulation of hindlimb vasculature is modified in pre-diabetic ZDF rats.

Objective 2 – Manuscript 2: Chapter 3

To establish and characterize the Pound mouse (pre-diabetic mouse model) and gluteus maximus muscle preparation as appropriate *in vivo* models to study skeletal muscle arteriolar function in pre-diabetes.

Objective 3 – Manuscript 2: Chapter 3

To determine whether pre-diabetes affects arteriolar vasodilation and blood flow responses to skeletal muscle contraction across arteriolar branches throughout the gluteus maximus microvascular network.

Objective 4 – Manuscript 3: Chapter 4

To determine if enhanced activation of sympathetic Y1R and α 1R affects arteriolar vasodilatory responses to muscle contraction in pre-diabetes.

1.9. Hypotheses

Overall hypothesis: Sympathetic vascular modulation is elevated in pre-diabetes.

Hypothesis 1: Endogenous Y1R and α 1R basal regulation of skeletal muscle vascular tone is greater in pre-diabetes compared to healthy controls.

Hypothesis 2: Arteriolar vasodilation and blood flow responses elicited by contraction of the gluteus maximus will be compromised in pre-diabetes compared to responses of healthy controls, where the greatest decrements in contraction-evoked vasodilation will occur in distal pre-capillary arterioles versus proximal arterioles.

Hypothesis 3: Blunted vasodilatory responses to gluteus maximus contraction observed in pre-diabetes are a result of an elevation in basal arteriolar smooth muscle cell activation of sympathetic arteriolar Y1R and α 1R.

1.10. References

- Alfalah, M., & Michel, M. C. (2004). *Neuropeptide Y and related peptides*. Berlin: Springer.
- Anderson, E. A., Balon, T. W., Hoffman, R. P., Sinkey, C. A., & Mark, A. L. (1992). Insulin increases sympathetic activity but not blood pressure in borderline hypertensive humans. *Hypertension*, *19*(6 Pt 2), 621-627.
- Anderson, E. A., Hoffman, R. P., Balon, T. W., Sinkey, C. A., & Mark, A. L. (1991). Hyperinsulinemia produces both sympathetic neural activation and vasodilation in normal humans. *J Clin Invest*, *87*(6), 2246-2252.
- Anderson, K. M., & Faber, J. E. (1991). Differential sensitivity of arteriolar alpha 1- and alpha 2-adrenoceptor constriction to metabolic inhibition during rat skeletal muscle contraction. *Circ Res*, *69*(1), 174-184.
- Bartfai, T., Iverfeldt, K., Fisone, G., & Serfozo, P. (1988). Regulation of the release of coexisting neurotransmitters. *Annu Rev Pharmacol Toxicol*, *28*, 285-310.
- Beck-Sickinger, A. G., & Jung, G. (1995). Structure-activity relationships of neuropeptide Y analogues with respect to Y1 and Y2 receptors. *Biopolymers*, *37*(2), 123-142.
- Berne, C., Fagius, J., Pollare, T., & Hjendahl, P. (1992). The sympathetic response to euglycaemic hyperinsulinaemia. Evidence from microelectrode nerve recordings in healthy subjects. *Diabetologia*, *35*(9), 873-879.
- Bevan, J. A., Halpern, W., & Mulvany, M. J. (1991). *The Resistance Vasculature*. New Jersey: Humana Press.
- Blain, G. M., Limberg, J. K., Mortensen, G. F., & Schrage, W. G. (2012). Rapid onset vasodilatation is blunted in obese humans. *Acta Physiol (Oxf)*, *205*(1), 103-112.

- Bock, G., Dalla Man, C., Campioni, M., Chittilapilly, E., Basu, R., Toffolo, G., et al. (2006). Pathogenesis of pre-diabetes: mechanisms of fasting and postprandial hyperglycemia in people with impaired fasting glucose and/or impaired glucose tolerance. *Diabetes*, 55(12), 3536-3549.
- Boegehold, M. A., & Johnson, P. C. (1988). Response of arteriolar network of skeletal muscle to sympathetic nerve stimulation. *Am J Physiol*, 254(5 Pt 2), H919-928.
- Canadian Diabetes Association (2011). Diabetes: Canada at the tipping point, Charting a new path. Toronto, Ontario, Canada
- Casey, D. P., & Joyner, M. J. (2012). Influence of alpha-adrenergic vasoconstriction on the blunted skeletal muscle contraction-induced rapid vasodilation with aging. *J Appl Physiol*, 113(8), 1201-1212.
- Clement, K., Vaisse, C., Lahlou, N., Cabrol, S., Pelloux, V., Cassuto, D., et al. (1998). A mutation in the human leptin receptor gene causes obesity and pituitary dysfunction. *Nature*, 392(6674), 398-401.
- Cowley, A. W., & Franchini, K. G. (1996). Neurogenic control of blood vessels. In D. Robertson, P. A. Low & R. J. Polinsky (Eds.), *Primer on the Autonomic Nervous System* (Vol. 1, pp. 49-58). San Diego: Academic Press Inc.
- Dahlof, C., Dahlof, P., & Lundberg, J. M. (1985). Neuropeptide Y (NPY): enhancement of blood pressure increase upon alpha-adrenoceptor activation and direct pressor effects in pithed rats. *Eur J Pharmacol*, 109(2), 289-292.
- Danho, W., Triscari, J., Vincent, G., Nakajima, T., Taylor, J., & Kaiser, E. T. (1988). Synthesis and biological evaluation of pNPY fragments. *Int J Pept Protein Res*, 32(6), 496-505.
- Davis, M. J., Hill, M. A., & Kuo, L. (2008). Local regulation of microvascular perfusion. In R. F. Tuma, W. N. Duran & L. Klaus (Eds.), *The Handbook of Physiology: Microcirculation* (2 ed., pp. 161-284). Boston: Elsevier/Academic Press.

- De Camilli, P., & Jahn, R. (1990). Pathways to regulated exocytosis in neurons. *Annu Rev Physiol*, *52*, 625-645.
- De Potter, W. P., Partoens, P., Schoups, A., Llona, I., & Coen, E. P. (1997). Noradrenergic neurons release both noradrenaline and neuropeptide Y from a single pool: the large dense cored vesicles. *Synapse*, *25*(1), 44-55.
- de Wit, C., von Bismarck, P., & Pohl, U. (1993). Mediator role of prostaglandins in acetylcholine-induced vasodilation and control of resting vascular diameter in the hamster cremaster microcirculation in vivo. *J Vasc Res*, *30*(5), 272-278.
- DeFronzo, R. A., & Ferrannini, E. (1991). Insulin resistance. A multifaceted syndrome responsible for NIDDM, obesity, hypertension, dyslipidemia, and atherosclerotic cardiovascular disease. *Diabetes Care*, *14*(3), 173-194.
- Dinenno, F. A., Jones, P. P., Seals, D. R., & Tanaka, H. (1999). Limb blood flow and vascular conductance are reduced with age in healthy humans: relation to elevations in sympathetic nerve activity and declines in oxygen demand. *Circulation*, *100*(2), 164-170.
- Dinneen, S. F., Maldonado, D., 3rd, Leibson, C. L., Klee, G. G., Li, H., Melton, L. J., 3rd, et al. (1998). Effects of changing diagnostic criteria on the risk of developing diabetes. *Diabetes Care*, *21*(9), 1408-1413.
- Dodd, L. R., & Johnson, P. C. (1991). Diameter changes in arteriolar networks of contracting skeletal muscle. *Am J Physiol*, *260*(3 Pt 2), H662-670.
- Doods, H. N., Wienen, W., Entzeroth, M., Rudolf, K., Eberlein, W., Engel, W., et al. (1995). Pharmacological characterization of the selective nonpeptide neuropeptide Y Y1 receptor antagonist BIBP 3226. *J Pharmacol Exp Ther*, *275*(1), 136-142.
- Dumont, Y., Martel, J. C., Fournier, A., St-Pierre, S., & Quirion, R. (1992). Neuropeptide Y and neuropeptide Y receptor subtypes in brain and peripheral tissues. *Prog Neurobiol*, *38*(2), 125-167.

- Edvinsson, L. (1985). Characterization of the contractile effect of neuropeptide Y in feline cerebral arteries. *Acta Physiol Scand*, 125(1), 33-41.
- Edvinsson, L., Ekblad, E., Hakanson, R., & Wahlestedt, C. (1984). Neuropeptide Y potentiates the effect of various vasoconstrictor agents on rabbit blood vessels. *Br J Pharmacol*, 83(2), 519-525.
- Edvinsson, L., Emson, P., McCulloch, J., Tatemoto, K., & Uddman, R. (1983). Neuropeptide Y: cerebrovascular innervation and vasomotor effects in the cat. *Neurosci Lett*, 43(1), 79-84.
- Ekblad, E., Edvinsson, L., Wahlestedt, C., Uddman, R., Hakanson, R., & Sundler, F. (1984). Neuropeptide Y co-exists and co-operates with noradrenaline in perivascular nerve fibers. *Regul Pept*, 8(3), 225-235.
- Ekelund, U., & Erlinge, D. (1997). In vivo receptor characterization of neuropeptide Y-induced effects in consecutive vascular sections of cat skeletal muscle. *Br J Pharmacol*, 120(3), 387-392.
- Ellis, C. G., Goldman, D., Hanson, M., Stephenson, A. H., Milkovich, S., Benlamri, A., et al. (2010). Defects in oxygen supply to skeletal muscle of prediabetic ZDF rats. *Am J Physiol Heart Circ Physiol*, 298(6), H1661-1670.
- Epstein, M., & Sowers, J. R. (1992). Diabetes mellitus and hypertension. *Hypertension*, 19(5), 403-418.
- Esler, M., Rumantir, M., Wiesner, G., Kaye, D., Hastings, J., & Lambert, G. (2001). Sympathetic nervous system and insulin resistance: from obesity to diabetes. *Am J Hypertens*, 14(11 Pt 2), 304S-309S.
- Eva, C., Keinanen, K., Monyer, H., Seeburg, P., & Sprengel, R. (1990). Molecular cloning of a novel G protein-coupled receptor that may belong to the neuropeptide receptor family. *FEBS Lett*, 271(1-2), 81-84.

- Faeh, D., William, J., Yerly, P., Paccaud, F., & Bovet, P. (2007). Diabetes and pre-diabetes are associated with cardiovascular risk factors and carotid/femoral intima-media thickness independently of markers of insulin resistance and adiposity. *Cardiovasc Diabetol*, 6, 32.
- Folkow, B., Sonnenschein, R. R., & Wright, D. L. (1971). Loci of neurogenic and metabolic effects on precapillary vessels of skeletal muscle. *Acta Physiol Scand*, 81(4), 459-471.
- Franco-Cereceda, A., & Liska, J. (1998). Neuropeptide Y Y1 receptors in vascular pharmacology. *Eur J Pharmacol*, 349(1), 1-14.
- Frisbee, J. C. (2003). Impaired skeletal muscle perfusion in obese Zucker rats. *Am J Physiol Regul Integr Comp Physiol*, 285(5), R1124-1134.
- Frisbee, J. C. (2004). Enhanced arteriolar alpha-adrenergic constriction impairs dilator responses and skeletal muscle perfusion in obese Zucker rats. *J Appl Physiol*, 97(2), 764-772.
- Fronek, K., & Zweifach, B. W. (1975). Microvascular pressure distribution in skeletal muscle and the effect of vasodilation. *Am J Physiol*, 228(3), 791-796.
- Fuglevand, A. J., & Segal, S. S. (1997). Simulation of motor unit recruitment and microvascular unit perfusion: spatial considerations. *J Appl Physiol*, 83(4), 1223-1234.
- Glover, W. E. (1985). Increased sensitivity of rabbit ear artery to noradrenaline following perivascular nerve stimulation may be a response to neuropeptide Y released as cotransmitter. *Clin Exp Pharmacol Physiol*, 12(3), 227-230.
- Graham, R. M., Oates, H. F., Stoker, L. M., & Stokes, G. S. (1977). Alpha blocking action of the antihypertensive agent, prazosin. *J Pharmacol Exp Ther*, 201(3), 747-752.

- Grandt, D., Dahms, P., Schimiczek, M., Eysselein, V. E., Reeve, J. R., Jr., & Mentlein, R. (1993). Proteolytic processing by dipeptidyl aminopeptidase IV generates receptor selectivity for peptide YY (PYY). *Med Klin (Munich)*, 88(3), 143-145.
- Grundemar, L., & Bloom, S. R. (1994). *Neuropeptide Y and drug development*. San Diego: Academic Press.
- Gupta, A. K., Ravussin, E., Johannsen, D. L., Stull, A. J., Cefalu, W. T., & Johnson, W. D. (2012). Endothelial Dysfunction: An Early Cardiovascular Risk Marker in Asymptomatic Obese Individuals with Prediabetes. *Br J Med Med Res*, 2(3), 413-423.
- Haffner, S. M., Stern, M. P., Hazuda, H. P., Mitchell, B. D., & Patterson, J. K. (1990). Cardiovascular risk factors in confirmed prediabetic individuals. Does the clock for coronary heart disease start ticking before the onset of clinical diabetes? *JAMA*, 263(21), 2893-2898.
- Hansen, J., Sander, M., & Thomas, G. D. (2000). Metabolic modulation of sympathetic vasoconstriction in exercising skeletal muscle. *Acta Physiol Scand*, 168(4), 489-503.
- Haug, S. J., & Segal, S. S. (2005). Sympathetic neural inhibition of conducted vasodilatation along hamster feed arteries: complementary effects of alpha1- and alpha2-adrenoreceptor activation. *J Physiol*, 563(Pt 2), 541-555.
- Hawrylyshyn, K. A., Michelotti, D. A., Coge, F., Guenin, S.-P., & Schwinn, D. A. (2004). Update on human alpha 1 adrenoreceptor subtype signaling and genomic organization. *Trends Pharmacol Sci*(25), 449-455.
- Hess, H. J. (1975). Prazosin: biochemistry and structure-activity studies. *Postgrad Med, Spec No*, 9-17.
- Hoffmann, S., Rist, B., Videnov, G., Jung, G., & Beck-Sickinger, A. G. (1996). Structure-affinity studies of C-terminally modified analogs of neuropeptide Y led to a novel class of peptidic Y1 receptor antagonist. *Regul Pept*, 65(1), 61-70.

- Hopsu-Havu, V. K., & Glenner, G. G. (1966). A new dipeptide naphthylamidase hydrolyzing glycyl-prolyl-beta-naphthylamide. *Histochemie*, 7(3), 197-201.
- Huggett, R. J., Hogarth, A. J., Mackintosh, A. F., & Mary, D. A. (2006). Sympathetic nerve hyperactivity in non-diabetic offspring of patients with type 2 diabetes mellitus. *Diabetologia*, 49(11), 2741-2744.
- Jackson, D. N., Milne, K. J., Noble, E. G., & Shoemaker, J. K. (2005). Gender-modulated endogenous baseline neuropeptide Y Y1-receptor activation in the hindlimb of Sprague-Dawley rats. *J Physiol*, 562(Pt 1), 285-294.
- Jackson, D. N., Moore, A. W., & Segal, S. S. (2010). Blunting of rapid onset vasodilatation and blood flow restriction in arterioles of exercising skeletal muscle with ageing in male mice. *J Physiol*, 588(Pt 12), 2269-2282.
- Jackson, D. N., Noble, E. G., & Shoemaker, J. K. (2004). Y1- and alpha1-receptor control of basal hindlimb vascular tone. *Am J Physiol Regul Integr Comp Physiol*, 287(1), R228-233.
- Janssen, I., Heymsfield, S. B., Baumgartner, R. N., & Ross, R. (2000). Estimation of skeletal muscle mass by bioelectrical impedance analysis. *J Appl Physiol*, 89(2), 465-471.
- Johnson, M. (2006). Molecular mechanisms of beta(2)-adrenergic receptor function, response, and regulation. *J Allergy Clin Immunol*, 117(1), 18-24; quiz 25.
- Kanauchi, M., Kanauchi, K., Inoue, T., Kimura, K., & Saito, Y. (2007). Surrogate markers of insulin resistance in assessing individuals with new categories "prehypertension" and "prediabetes". *Clin Chem Lab Med*, 45(1), 35-39.
- Karpoff, L., Vinet, A., Schuster, I., Oudot, C., Goret, L., Dauzat, M., et al. (2009). Abnormal vascular reactivity at rest and exercise in obese boys. *Eur J Clin Invest*, 39(2), 94-102.

- Kasakov, L., Ellis, J., Kirkpatrick, K., Milner, P., & Burnstock, G. (1988). Direct evidence for concomitant release of noradrenaline, adenosine 5'-triphosphate and neuropeptide Y from sympathetic nerve supplying the guinea-pig vas deferens. *J Auton Nerv Syst*, 22(1), 75-82.
- Kassis, S., Olasmaa, M., Terenius, L., & Fishman, P. H. (1987). Neuropeptide Y inhibits cardiac adenylate cyclase through a pertussis toxin-sensitive G protein. *J Biol Chem*, 262(8), 3429-3431.
- Kim, S. H., & Reaven, G. M. (2008). Isolated impaired fasting glucose and peripheral insulin sensitivity: not a simple relationship. *Diabetes Care*, 31(2), 347-352.
- Kingwell, B. A., Formosa, M., Muhlmann, M., Bradley, S. J., & McConell, G. K. (2003). Type 2 diabetic individuals have impaired leg blood flow responses to exercise: role of endothelium-dependent vasodilation. *Diabetes Care*, 26(3), 899-904.
- Larhammar, D., Blomqvist, A. G., Yee, F., Jazin, E., Yoo, H., & Wahlested, C. (1992). Cloning and functional expression of a human neuropeptide Y/peptide YY receptor of the Y1 type. *J Biol Chem*, 267(16), 10935-10938.
- Laughlin, M. H., Korthuis, R. J., Duncker, D. J., & Bache, R. J. (1996). *Handbook of physiology*. Bethesda: American Physiological Society.
- Lesniewski, L. A., Donato, A. J., Behnke, B. J., Woodman, C. R., Laughlin, M. H., Ray, C. A., et al. (2008). Decreased NO signaling leads to enhanced vasoconstrictor responsiveness in skeletal muscle arterioles of the ZDF rat prior to overt diabetes and hypertension. *Am J Physiol Heart Circ Physiol*, 294(4), H1840-1850.
- Linder, L., Lautenschlager, B. M., & Haefeli, W. E. (1996). Subconstrictor doses of neuropeptide Y potentiate alpha 1-adrenergic venoconstriction in vivo. *Hypertension*, 28(3), 483-487.
- Lundberg, J. M. (1996). Pharmacology of cotransmission in the autonomic nervous system: integrative aspects on amines, neuropeptides, adenosine triphosphate, amino acids and nitric oxide. *Pharmacol Rev*, 48(1), 113-178.

- Lundberg, J. M., Franco-Cereceda, A., Lou, Y. P., Modin, A., & Pernow, J. (1994). Differential release of classical transmitters and peptides. *Adv Second Messenger Phosphoprotein Res*, 29, 223-234.
- Lundberg, J. M., Saria, A., Franco-Cereceda, A., Hokfelt, T., Terenius, L., & Goldstein, M. (1985). Differential effects of reserpine and 6-hydroxydopamine on neuropeptide Y (NPY) and noradrenaline in peripheral neurons. *Naunyn Schmiedebergs Arch Pharmacol*, 328(3), 331-340.
- Lyssenko, V., Almgren, P., Anevski, D., Perfekt, R., Lahti, K., Nissen, M., et al. (2005). Predictors of and longitudinal changes in insulin sensitivity and secretion preceding onset of type 2 diabetes. *Diabetes*, 54(1), 166-174.
- MacAnaney, O., Reilly, H., O'Shea, D., Egana, M., & Green, S. (2011). Effect of type 2 diabetes on the dynamic response characteristics of leg vascular conductance during exercise. *Diab Vasc Dis Res*, 8(1), 12-21.
- Mackie, B. G., & Terjung, R. L. (1983). Blood flow to different skeletal muscle fiber types during contraction. *Am J Physiol*, 245(2), H265-275.
- Marshall, J. M. (1982). The influence of the sympathetic nervous system on individual vessels of the microcirculation of skeletal muscle of the rat. *J Physiol*, 332, 169-186.
- Marshall, J. M., & Tandon, H. C. (1984). Direct observations of muscle arterioles and venules following contraction of skeletal muscle fibres in the rat. *J Physiol*, 350, 447-459.
- Marshall, R. J., Schirger, A., & Shepherd, J. T. (1961). Blood pressure during supine exercise in idiopathic orthostatic hypotension. *Circulation*, 24, 76-81.
- Meigs, J. B., Muller, D. C., Nathan, D. M., Blake, D. R., & Andres, R. (2003). The natural history of progression from normal glucose tolerance to type 2 diabetes in the Baltimore Longitudinal Study of Aging. *Diabetes*, 52(6), 1475-1484.

- Moore, A. W., Jackson, W. F., & Segal, S. S. (2010). Regional heterogeneity of alpha-adrenoreceptor subtypes in arteriolar networks of mouse skeletal muscle. *J Physiol*, 588(Pt 21), 4261-4274.
- Morgan, D. A., Balon, T. W., Ginsberg, B. H., & Mark, A. L. (1993). Nonuniform regional sympathetic nerve responses to hyperinsulinemia in rats. *Am J Physiol*, 264(2 Pt 2), R423-427.
- Mosqueda-Garcia, R. (1996). Central Autonomic Regulation. In D. Robertson, P. A. Low & R. J. Polinsky (Eds.), *Primer on the Autonomic Nervous System* (Vol. 1, pp. 49-58). San Diego: Academic Press Inc.
- Motulsky, H. J., & Michel, M. C. (1988). Neuropeptide Y mobilizes Ca²⁺ and inhibits adenylate cyclase in human erythroleukemia cells. *Am J Physiol*, 255(6 Pt 1), E880-885.
- Muntzel, M. S., Anderson, E. A., Johnson, A. K., & Mark, A. L. (1995). Mechanisms of insulin action on sympathetic nerve activity. *Clin Exp Hypertens*, 17(1-2), 39-50.
- Naik, J. S., Xiang, L., Hodnett, B. L., & Hester, R. L. (2008). Alpha-adrenoceptor-mediated vasoconstriction is not involved in impaired functional vasodilation in the obese Zucker rat. *Clin Exp Pharmacol Physiol*, 35(5-6), 611-616.
- Novielli, N. M., Al-Khazraji, B. K., Medeiros, P. J., Goldman, D., & Jackson, D. N. (2012). Pre-Diabetes Augments Neuropeptide Y(1)- and alpha(1)-Receptor Control of Basal Hindlimb Vascular Tone in Young ZDF Rats. *PLoS One*, 7(10), e46659.
- Oates, H. F., Graham, R. M., Stoker, L. M., & Stokes, G. S. (1976). Haemodynamic effects of prazosin. *Arch Int Pharmacodyn Ther*, 224(2), 239-247.
- Radegran, G., & Saltin, B. (1999). Nitric oxide in the regulation of vasomotor tone in human skeletal muscle. *Am J Physiol*, 276(6 Pt 2), H1951-1960.

- Remensnyder, J. P., Mitchell, J. H., & Sarnoff, S. J. (1962). Functional sympatholysis during muscular activity. Observations on influence of carotid sinus on oxygen uptake. *Circ Res*, *11*, 370-380.
- Revington, M., & McCloskey, D. I. (1988). Neuropeptide Y and control of vascular resistance in skeletal muscle. *Regul Pept*, *23*(3), 331-342.
- Rhodin, J. A. (1967). The ultrastructure of mammalian arterioles and precapillary sphincters. *J Ultrastruct Res*, *18*(1), 181-223.
- Robertson, D., Biaggioni, I., Burnstock, G., Low, P. A., & Paton, J. F. R. (2012). *Primer on the Autonomic Nervous System* (Vol. 3). London: Academic Press Elsevier.
- Rowe, J. W., Young, J. B., Minaker, K. L., Stevens, A. L., Pallotta, J., & Landsberg, L. (1981). Effect of insulin and glucose infusions on sympathetic nervous system activity in normal man. *Diabetes*, *30*(3), 219-225.
- Rowell, L. B. (1993). *Human Cardiovascular Control*. New York: Oxford University Press.
- Saltin, B., Radegran, G., Koskolou, M. D., & Roach, R. C. (1998). Skeletal muscle blood flow in humans and its regulation during exercise. *Acta Physiol Scand*, *162*(3), 421-436.
- Schaefer, C., Biermann, T., Schroeder, M., Fuhrhop, I., Niemeier, A., Ruther, W., et al. (2010). Early microvascular complications of prediabetes in mice with impaired glucose tolerance and dyslipidemia. *Acta Diabetol*, *47*(Suppl 1), 19-27.
- Scherrer, U., & Sartori, C. (1997). Insulin as a vascular and sympathoexcitatory hormone: implications for blood pressure regulation, insulin sensitivity, and cardiovascular morbidity. *Circulation*, *96*(11), 4104-4113.
- Segal, S. S., & Jackson, W. F. (2005). Special edition of *Microcirculation* commemorating the 50th anniversary of the Microcirculatory Society, Inc. *Microcirculation*, *12*(1), 1-4.

- Shin, J. Y., Lee, H. R., & Lee, D. C. (2011). Increased arterial stiffness in healthy subjects with high-normal glucose levels and in subjects with pre-diabetes. *Cardiovasc Diabetol*, *10*, 30.
- Somlyo, A. P., & Somlyo, A. V. (2000). Signal transduction by G-proteins, rho-kinase and protein phosphatase to smooth muscle and non-muscle myosin II. *J Physiol*, *522 Pt 2*, 177-185.
- Stange, T., Kettmann, U., & Holzhausen, H. J. (1996). Immunoelectron microscopic single and double labelling of aminopeptidase N (CD 13) and dipeptidyl peptidase IV (CD 26). *Acta Histochem*, *98*(3), 323-331.
- Stepp, D. W., & Frisbee, J. C. (2002). Augmented adrenergic vasoconstriction in hypertensive diabetic obese Zucker rats. *Am J Physiol Heart Circ Physiol*, *282*(3), H816-820.
- Strack, A. M., Sawyer, W. B., Hughes, J. H., Platt, K. B., & Loewy, A. D. (1989). A general pattern of CNS innervation of the sympathetic outflow demonstrated by transneuronal pseudorabies viral infections. *Brain Res*, *491*(1), 156-162.
- Sundler, F., Bottcher, G., Ekblad, E., & Hakanson, R. (1993). *The biology of Neuropeptide Y and related peptides*. Totowa: Humana Press.
- Tanaka, Y., Nakazawa, T., Ishiro, H., Saito, M., Uneyama, H., Iwata, S., et al. (1995). Ca²⁺ handling mechanisms underlying neuropeptide Y-induced contraction in canine basilar artery. *Eur J Pharmacol*, *289*(1), 59-66.
- Tatemoto, K., Carlquist, M., & Mutt, V. (1982). Neuropeptide Y--a novel brain peptide with structural similarities to peptide YY and pancreatic polypeptide. *Nature*, *296*(5858), 659-660.
- Thomas, G. D., & Segal, S. S. (2004). Neural control of muscle blood flow during exercise. *J Appl Physiol*, *97*(2), 731-738.

- Tirosh, A., Shai, I., Tekes-Manova, D., Israeli, E., Pereg, D., Shochat, T., et al. (2005). Normal fasting plasma glucose levels and type 2 diabetes in young men. *N Engl J Med*, 353(14), 1454-1462.
- Tuma, R. F., Duran, W. N., & Ley, K. (2008). *Handbook of physiology: Microcirculation*. San Diego: Academic Press.
- VanTeeffelen, J. W., & Segal, S. S. (2003). Interaction between sympathetic nerve activation and muscle fibre contraction in resistance vessels of hamster retractor muscle. *J Physiol*, 550(Pt 2), 563-574.
- VanTeeffelen, J. W., & Segal, S. S. (2006). Rapid dilation of arterioles with single contraction of hamster skeletal muscle. *Am J Physiol Heart Circ Physiol*, 290(1), H119-127.
- Vinet, A., Karpoff, L., Walther, G., Startun, A., Obert, P., Goret, L., et al. (2011). Vascular reactivity at rest and during exercise in middle-aged obese men: effects of short-term, low-intensity, exercise training. *Int J Obes (Lond)*, 35(6), 820-828.
- Wahlestedt, C., Edvinsson, L., Ekblad, E., & Hakanson, R. (1985). Neuropeptide Y potentiates noradrenaline-evoked vasoconstriction: mode of action. *J Pharmacol Exp Ther*, 234(3), 735-741.
- Wahlestedt, C., Grundemar, L., Hakanson, R., Heilig, M., Shen, G. H., Zukowska-Grojec, Z., et al. (1990). Neuropeptide Y receptor subtypes, Y1 and Y2. *Ann N Y Acad Sci*, 611, 7-26.
- Webb, R. C. (2003). *Smooth muscle contraction and relaxation*. Bethesda. Document Number)
- Welsh, D. G., & Segal, S. S. (1996). Muscle length directs sympathetic nerve activity and vasomotor tone in resistance vessels of hamster retractor. *Circ Res*, 79(3), 551-559.

Wier, W. G., & Morgan, K. G. (2003). Alpha1-adrenergic signaling mechanisms in contraction of resistance arteries. *Rev Physiol Biochem Pharmacol*, 150, 91-139.

Chapter 2 : Pre-diabetes augments neuropeptide Y1- and α 1-receptor control of basal hindlimb vascular tone in young ZDF rats

A form of this manuscript has been published:

Novielli, N. M., Al-Khazraji, B. K., Medeiros, P. J., Goldman, D., & Jackson, D. N. (2012). Pre-Diabetes Augments Neuropeptide Y(1)- and alpha(1)-Receptor Control of Basal Hindlimb Vascular Tone in Young ZDF Rats. *PLoS One*, 7(10), e46659.

2.1. Introduction

In the peripheral vasculature, sympathetic neurons regulate arteriolar tone through the release of norepinephrine (NE) and neuropeptide Y (NPY). NE has been considered the primary neurotransmitter in maintenance of baseline arteriolar tone (Z. Zukowska-Grojec, 1995) through its interaction with alpha-adrenergic receptors (α R) located on vascular smooth muscle cells, causing vasoconstriction. NPY is co-stored and co-released with NE and acts on neuropeptide Y1 receptors (Y1R), to cause potent and prolonged vasoconstriction (Ekelund & Erlinge, 1997; Malmstrom, 1997; Z. Zukowska-Grojec & Wahlestedt, 1993). Interestingly, post-synaptic co-activation of Y1R and α 1R by NPY and NE leads to synergistic vasoconstrictive effects (Z. Zukowska-Grojec & Wahlestedt, 1993). Although recent evidence has shown that NPY contributes modestly to baseline vascular tone in skeletal muscle of male rats (Jackson, Noble, & Shoemaker, 2004), its effects are suggested to predominate under conditions of elevated sympathetic nerve activity (Bartfai, Iverfeldt, Fisone, & Serfozo, 1988; De Camilli & Jahn, 1990; Lundberg, Franco-Cereceda, Lou, Modin, & Pernow, 1994).

A large proportion of the body's resistance vasculature lies within skeletal muscle, which is highly regulated by sympathetic nerve activity (SNA) to maintain blood pressure and blood flow distribution under healthy conditions. However, in type 2 diabetes, sympathetic regulation of vascular tone can become augmented, leading to alterations in normal blood flow control. Type 2 diabetes is commonly associated with vascular disease; however, recent findings indicate that cardiovascular complications may be initiated in the pre-diabetic state, before the diagnosis of type 2 diabetes (Faeh,

William, Yerly, Paccaud, & Bovet, 2007; Haffner, Stern, Hazuda, Mitchell, & Patterson, 1990). Pre-diabetes is characterized by the concomitant presence of hyperinsulinemia, impaired glucose tolerance and insulin resistance and occurs prior to overt pancreatic β -cell failure. Of note, hyperinsulinemia stimulates SNA and may play a role in autonomic and vascular dysfunction associated with the disease (Mancia, Grassi, Giannattasio, & Seravalle, 1999). In humans, hyperinsulinemia is associated with elevated SNA and correlates with the degree of insulin resistance (Anderson, Balon, Hoffman, Sinkey, & Mark, 1992; DeFronzo & Ferrannini, 1991; Huggett, Hogarth, Mackintosh, & Mary, 2006). Moreover, systemic infusion of insulin in rats has been shown to preferentially increase lumbar SNA (Epstein & Sowers, 1992; Esler et al., 2001; Muntzel, Anderson, Johnson, & Mark, 1995; Scherrer & Sartori, 1997). Studies using animal models of pre-diabetes and the metabolic syndrome have reported augmented α -adrenergic vascular responsiveness to adrenergic agonists in isolated vascular preparations (Lesniewski et al., 2008; Okon, Szado, Laher, McManus, & van Breemen, 2003). As noted above, NPY-mediated vascular modulation becomes more pronounced under conditions of elevated SNA (Bartfai et al., 1988; De Camilli & Jahn, 1990; Lundberg et al., 1994); however, to date, studies addressing NPY/Y1R-mediated vascular control in pre-diabetes are lacking. Furthermore, there have been no studies investigating NPY and α -adrenergic co-modulation of vascular control in pre-diabetes.

The overall aim of the present study was to investigate if pre-diabetes modifies sympathetic Y1R and α 1R control of basal skeletal muscle blood flow (Q_{fem}) and vascular conductance (VC). Thus, we tested the independent and dependent (synergistic) functional contributions of endogenous Y1R and α 1R activation on Q_{fem} and VC *in vivo*

and hypothesized that pre-diabetes augments Y1R and α 1R vascular modulation. Concurrently, we hypothesized that skeletal muscle NPY concentration and Y1R and α 1R expression would be upregulated in pre-diabetic rats.

2.2. Materials and methods

All animal procedures were approved by the Council on Animal Care at The University of Western Ontario (protocol number: 2008-066). All invasive procedures were performed under α -chloralose and urethane anesthetic, and all efforts were made to minimize animal suffering.

2.2.1. Animals

Nine seven-week-old male ZDF rats (PD) and 8 age-matched lean controls (CTRL) (Charles River Laboratories, Saint-Constant, Quebec, Canada) were used in this study. The inbred ZDF rat is affected by a homozygous mutation of the leptin receptor (fa/fa), therefore leptin is unable to suppress appetite (Leonard, Watson, Loomes, Phillips, & Cooper, 2005). When fed a high fat diet (i.e., Purina 5008 rat chow), these animals become obese, hyperinsulinemic, insulin resistant and hyperglycemic by 7 weeks of age (Leonard et al., 2005; Lesniewski et al., 2008), characteristic of the pre-diabetic condition in humans (Kim & Reaven, 2008a, 2008b). This phenotype is absent in the ZDF lean rats heterozygous for the leptin receptor mutation (fa/+), and thus served as the control group in this study. Animals were housed in animal care facilities in a temperature (24°C) and light (12-hour cycle)-controlled room, fed Purina 5008 rat chow

(Ralston Purina, St. Louis, MO, USA) and allowed to eat and drink water *ad libitum*. Prior to surgery, animals were anesthetized with an intraperitoneal injection of α -chloralose (80 mg/kg) and urethane (500 mg/kg). This anesthetic was ideal for this study as it leaves autonomic, cardiovascular and respiratory function intact (Soma, 1983). Internal body temperature was monitored via a rectal temperature probe and maintained at 37°C with the use of a thermally controlled water-perfused heating pad.

2.2.2. Surgery

A mid-neck incision was made and a tracheal cannula was introduced to facilitate spontaneous respiration. End-tidal CO₂ and O₂ measures were made from expired air between pharmacological perturbations throughout the experiment using a breath-by-breath gas analyzer (ADInstruments, Colorado Springs, CO, USA). The left common carotid artery was cannulated (PE-50 tubing) to allow for recording of arterial blood pressure via the amplified signal of a pressure transducer using a PowerLab system (model ML118 PowerLab Quad Bridge Amplifier; model MLT0699 BP Transducer, ADInstruments, Colorado Springs, CO, USA). The right jugular vein was cannulated to maintain a constant infusion of anesthetic to the animal (α -chloralose: 8-16 mg/kg/hr, urethane: 50-100 mg/kg/hr).

Through a midline abdominal incision, gut contents were carefully moved aside within the abdominal cavity and covered with sterile gauze moistened with sterile saline (0.9% NaCl). Sterile cotton swabs were then used to expose the descending aorta and right iliac artery, isolating it from the right iliac vein and its surrounding fat. The right iliac artery was cannulated (PE-50 tubing) and the cannula was advanced to the

bifurcation of the descending aorta. This cannula was used for localized drug delivery to the left hindlimb. Following cannulation, gauze was removed and care was taken to reposition the gut. Incisions were closed with sterile wound clips (9 mm stainless steel wound clips). A blood sample was then taken from the carotid cannula in order to evaluate blood glucose levels, lactate levels, and pH using an iSTAT portable clinical analyzer (Abbott Laboratories, Abbott Park, IL, USA).

Using microscopic assistance, the left femoral artery was carefully isolated from surrounding nerves and vessels. Q_{fem} was measured beat-by-beat using a Transonic flow probe (0.7 PSB) and flowmeter (model TS420 Perivascular Flowmeter Module; Transonic Systems, Ithica, NY, USA). The flow probe was placed around the left femoral artery ~3 mm from the femoral triangle and innocuous water-soluble ultrasound gel was applied over the opened area of the left hindlimb to keep tissue hydrated and to maintain adequate flow signal.

2.2.3. Experimental protocol

Once surgery was completed, animals recovered for 1 hour. Prior to drug treatments, vehicle (160 μl of 0.9% saline) was delivered, followed by a 15-minute recovery period. Baseline data were recorded for 5 minutes followed by five separate drug infusions (Jackson, Ellis, & Shoemaker, 2010; Jackson, Milne, Noble, & Shoemaker, 2005a, 2005b; Jackson et al., 2004). Using a repeated measures design, drug infusions were delivered at a rate of 16 $\mu\text{l}/\text{sec}$ in the following order: 1) 250 μl of 0.2 $\mu\text{g}/\text{kg}$ acetylcholine chloride (ACh, Sigma-Aldrich, St. Louis, MO, USA), 2) 160 μl of 100 $\mu\text{g}/\text{kg}$ BIBP3226, a specific Y_1R antagonist (TOCRIS, Ellisville, MO, USA), 3) 160

μl of 20 $\mu\text{g}/\text{kg}$ prazosin, a specific $\alpha_1\text{R}$ antagonist (Sigma-Aldrich, St. Louis, MO, USA), 4) combined 100 $\mu\text{g}/\text{kg}$ BIBP3226 + 20 $\mu\text{g}/\text{kg}$ prazosin, and 5) 160 μl of 5 $\mu\text{g}/\text{kg}$ sodium nitroprusside (SNP, i.v., sodium nitroprussiate dihydrate, Sigma-Aldrich, St. Louis, MO, USA). Since the hemodynamic effects of prazosin are long lasting, BIBP3226 (Y1R antagonist) was administered first in all experiments. When hemodynamic variables returned to baseline (30-40 minutes), prazosin ($\alpha_1\text{R}$ antagonist) was infused. Once responses to prazosin peaked and stabilized (~ 5 minutes), combined blockade (Y1R + $\alpha_1\text{R}$ antagonist) was achieved by a subsequent infusion of BIBP3226 (100 $\mu\text{g}/\text{kg}$). In a previous study (using a similar protocol), we addressed the effects of randomized versus fixed delivery of BIBP3226 and prazosin and reported no effect of randomization (Jackson et al., 2005a).

2.2.4. Insulin immunoassay

Insulin levels were determined from plasma samples using an ELISA and by following manufacturer's instruction (ALPCO Immunoassays, Salem, NH, USA). All samples and standards (10 μl) were distributed in duplicate in the provided 96-well immunoplate. Seventy-five microliters of horseradish peroxidase (HRP)-labeled monoclonal anti-insulin antibody was added to each well and incubated at room temperature for 2 hours. The immunoplate was then washed 6 times with assay wash buffer. Following washing, 100 μl of tetramethylbenzidine (TMB) peroxidase substrate solution was added to each well and incubated for 15 minutes at room temperature. The reaction was then terminated with 100 μl of stop solution, and the optical absorbance of each well was read at 450 nm (Bio-Rad iMark Microplate Reader, Bio-Rad, Hercules, CA, USA).

2.2.5. NPY immunoassay and Western blotting

Analyses were carried out on two different skeletal muscle groups known to contain differing expression of slow-twitch oxidative (SO), fast-twitch glycolytic (FG), and fast-twitch oxidative-glycolytic (FOG) fiber types. The use of skeletal muscle groups expressing differing ratios of fiber types was based on early work by others showing that blood flow to such muscles is distributed differently at rest (Terjung & Engbretson, 1988) and during exercise (Armstrong & Laughlin, 1984; Terjung & Engbretson, 1988). We chose to analyze vastus muscle, as it comprises the bulk of muscle tissue in the hindlimb and plays a major role in locomotion. With the animal under deep surgical anesthesia, skeletal muscle samples were taken from red vastus (RV; expressing FOG > FG > SO fibers) and white vastus (WV; expressing FG > FOG) (Armstrong & Phelps, 1984; Laughlin & Armstrong, 1983) and were flash-frozen in liquid nitrogen. Animals were euthanized after tissue harvesting by an overdose of anesthetic. The same muscle tissue samples were used in all assays (NPY immunoassay and Western blot).

NPY concentration was determined in whole muscle tissue homogenates (from white and red vastus; see below for preparation of homogenate and total protein determination) and standards (50 μ l duplicate samples) using a competitive immunoassay (Bachem Bioscience, King of Prussia, PA, USA). All samples were incubated at room temperature for 2 hours. The immunoplate was then washed 5 times with 300 μ l per well of assay buffer. Wells were incubated at room temperature with 100 μ l of streptavidin-HRP for 1 hour. The immunoplate was washed again 5 times with 300 μ l per well of assay buffer. Following washing, 100 μ l of a TMB peroxidase substrate solution was added to all wells. After a 40 minute incubation at room temperature the reaction was

terminated by the addition of 100 μ l 2 N HCl. Finally, the optical absorbance of each well was read at 450 nm (Bio-Rad Ultramark Microplate Imaging System, Bio-Rad, Hercules, CA, USA). Absorbance measures were converted to NPY concentration by comparison with the 10-point standard curve. Results are given as a ratio of pg NPY (per μ g tissue), relative to protein concentration, as computed from amount of total protein loaded per well. The assay has a minimum detectable concentration of 0.04–0.06 ng per ml or 2–3 pg per well (manufacturer's data).

White and red vastus skeletal muscle tissue was removed from the hindlimb and flash frozen in liquid nitrogen. Approximately 100 mg of tissue was cut from the whole muscle and homogenized in 2 mL of radioimmunoprecipitation assay lysis buffer (50 mM Tris-HCl pH 7.4, 150 mM NaCl, 1% IGEPAL, 1% Sodium deoxycholate, 0.1% SDS, 100 mM EDTA) containing protease inhibitor cocktail (104 mM AEBSF, 80 mM aprotinin, 2.1 mM leupeptin, 3.6 mM betastatin, 1.5 mM pepstatin A, 1.4 mM ME-64, Sigma-Aldrich, St. Louis, MO, USA). Samples were then centrifuged at 4°C for 25 minutes at 14000 rpm and supernatant was collected and then stored at -80°C until ready for use. Protein concentration was determined using the Bradford protein assay (Bradford, 1976). Fifty micrograms of protein from each sample was loaded on a 4% to 12% gradient gel and separated by SDS-PAGE. After electrophoresis, proteins were transferred at a constant voltage to polyvinylidene fluoride membranes. Membranes were blocked in 5% milk in tris-buffered saline + Tween20 (0.5%) (TTBS) at 4°C for 5 hours. Membranes were washed in TTBS and incubated overnight at 4°C in one of two primary antibodies in 5% milk in TTBS, specific to rat, human or mouse: 1) Y1R (rabbit polyclonal to NPY1R, Cat no. ab73897, Abcam, Cambridge, MA, USA), and 2) α 1R

(rabbit polyclonal to alpha 1 adrenergic receptor, Cat no. ab3462, Abcam, Cambridge, MA, USA). After incubation, membranes were washed in TTBS then incubated in secondary antibody conjugated to HRP (goat anti-rabbit IgG, Cat no. A0545, Sigma Aldrich, St Louis, MO, USA) in 5% milk in TTBS for 1 hour at room temperature. Membranes were washed and bands were detected using Immun-Star WesternC[®] chemiluminescent kit (Bio-Rad, Hercules, CA, USA) and imaged with a ChemiDoc XRS System (Bio-Rad, Hercules, CA, USA). Membranes were immediately washed, stripped, and blocked in 5% bovine serum albumin for 1 hour at room temperature. Membranes were washed and incubated in primary antibody specific to β -actin (loading control, anti-beta actin, rabbit polyclonal, Cat no. ab16039, Abcam, Cambridge, MA, USA) for 1 hour at room temperature. Membranes were then washed, incubated in secondary antibody and imaged (as above). Densitometric band analysis was performed with Quantity One 1-D Analysis Software (Bio-Rad, Hercules, CA, USA). Quantified protein expression values were normalized to β -actin.

2.2.6. Data acquisition and statistical analyses

All data were collected at 1 kHz with the use of the PowerLab data acquisition system (AD Instruments, Colorado Springs, CO, USA) coupled to a computer. Heart rate (HR) and mean arterial pressure (MAP) were calculated from arterial blood pressure recordings. VC was calculated as a ratio of Q_{fem}/MAP . For all conditions, Q_{fem} , VC, MAP and HR were calculated as a 5 minute stable average during baseline (Baseline) and as a 1 minute average at the peak of drug response (Drug).

Statistical analyses were performed using Prism (version 4, GraphPad Software Inc, La Jolla, CA, USA) and differences were accepted as statistically significant when p

< 0.05 . Effect of treatment on MAP and HR within each group was analyzed using a paired t-test, and between groups at baseline and drug using an unpaired t-test with a Bonferroni correction (2 comparisons; $p < 0.025$). Effects of each drug perturbation on Q_{fem} and VC between CTRL and PD were analyzed using unpaired t-tests. The potential synergy between Y1R and $\alpha 1R$ activation was assessed by comparing the sum of the drug responses from the BIBP3226 and prazosin conditions against those of the BIBP3226 + prazosin condition using a paired t-test. Unpaired t-tests were used to compare cellular data (from Western blot and immunoassay) between groups. Pearson's Correlation was used to assess correlation between body mass and Q_{fem} or VC. Data are presented as mean values \pm standard error (SE).

2.3. Results

Body mass, blood glucose, insulin, lactate, mean end tidal CO_2 and respiratory rate were significantly greater in PD *versus* CTRL ($p < 0.001$, Table 2.1); however, expired O_2 and blood pH were similar between groups (Table 2.1). At baseline, both groups displayed similar MAP (85-95 mmHg); however, HR was greater in PD *versus* CTRL ($p < 0.025$, Table 2.2).

Baseline Q_{fem} and VC were similar between groups and similar before each drug perturbation (Table 2.3). This observation was independent of body mass, as there was no correlation between body mass and Q_{fem} or VC ($r = 0.11$, $p = 0.65$). Vehicle infusion of saline had no effect on MAP, HR, Q_{fem} or VC in either group.

The magnitude of vascular responses to bolus infusions of ACh and SNP were similar between groups, indicating that endothelial and smooth muscle cell functionality

were preserved in PD (Table 2.4). Representative tracings of mean hindlimb vascular conductance to pharmacologic interventions are shown for a CTRL and PD rat in Figure 2.1.

Table 2.1: Physical and physiological characteristics of CTRL and PD rats.

	CTRL	PD
Body mass (g)	196 ± 4	253 ± 5*
Blood glucose (mmol/L)	9.3 ± 0.6	14.1 ± 0.9*
Insulin (nmol/L)	0.1 ± 0.03	5.6 ± 0.7*
Blood lactate (mmol/L)	1 ± 0.1	2 ± 0.1*
Expired CO ₂ (mmHg)	35 ± 0.5	39 ± 0.5*
Expired O ₂ (%)	17 ± 0.1	17 ± 0.1
Respiratory rate (breaths/min)	68 ± 2	82 ± 2*
Blood pH	7.4 ± 0.01	7.4 ± 0.01

Values are mean ± SE. CTRL, control, n=7-8; PD, pre-diabetic, n=7-9. * $p < 0.001$ vs. CTRL.

Table 2.2: Blood pressure and heart rate responses associated with each condition.

		BIBP3226		Prazosin		BIBP3226+Prazosin	
		CTRL	PD	CTRL	PD	CTRL	PD
Mean arterial pressure (mmHg)	Baseline	95 ± 2	102 ± 6	88 ± 4	102 ± 5	88 ± 4	102 ± 5
	Drug	89 ± 4	94 ± 8	72 ± 5*	76 ± 6*	71 ± 3*	71 ± 6*
Heart rate (beats/min)	Baseline	375 ± 7	414 ± 7†	371 ± 6	409 ± 8†	371 ± 6	409 ± 8†
	Drug	379 ± 6	430 ± 11*†	368 ± 7	413 ± 10†	368 ± 8	406 ± 7†

Values are mean ± SE. CTRL, control, n=8; PD, pre-diabetic, n=9. * $p < 0.05$ vs. Baseline. † $p < 0.025$ vs. CTRL.

Table 2.3: Baseline values of hindlimb blood flow and vascular conductance before pharmacological treatments.

	BIBP3226		Prazosin		BIBP3226+Prazosin	
	CTRL	PD	CTRL	PD	CTRL	PD
Hindlimb blood flow (μ l/min)	385 \pm 69	364 \pm 42	364 \pm 61	358 \pm 34	364 \pm 61	358 \pm 34
Vascular conductance (μ l/min/mmHg)	4.0 \pm 0.6	3.7 \pm 0.5	4.1 \pm 0.6	3.6 \pm 0.4	4.1 \pm 0.6	3.6 \pm 0.4

Values are mean \pm SE. CTRL, control, n=8; PD, pre-diabetic, n=9.

Table 2.4: Hindlimb blood flow and vascular conductance at baseline and following acetylcholine and sodium nitroprusside interventions.

		Acetylcholine		Sodium Nitroprusside	
		CTRL	PD	CTRL	PD
Hindlimb blood flow ($\mu\text{l}/\text{min}$)	Baseline	380 ± 50	395 ± 30	385 ± 66	377 ± 47
	Drug	$708 \pm 66^*$	$760 \pm 93^*$	$503 \pm 72^*$	$582 \pm 53^*$
Vascular conductance ($\mu\text{l}/\text{min}/\text{mmHg}$)	Baseline	4.2 ± 0.6	3.7 ± 0.5	4.2 ± 0.7	3.6 ± 0.6
	Drug	$10 \pm 1^*$	$10 \pm 1^*$	$12 \pm 2^*$	$11 \pm 2^*$

Values are mean \pm SE. CTRL, control, n=6-8; PD, pre-diabetic, n=6-8. $*p < 0.05$ vs. Baseline.

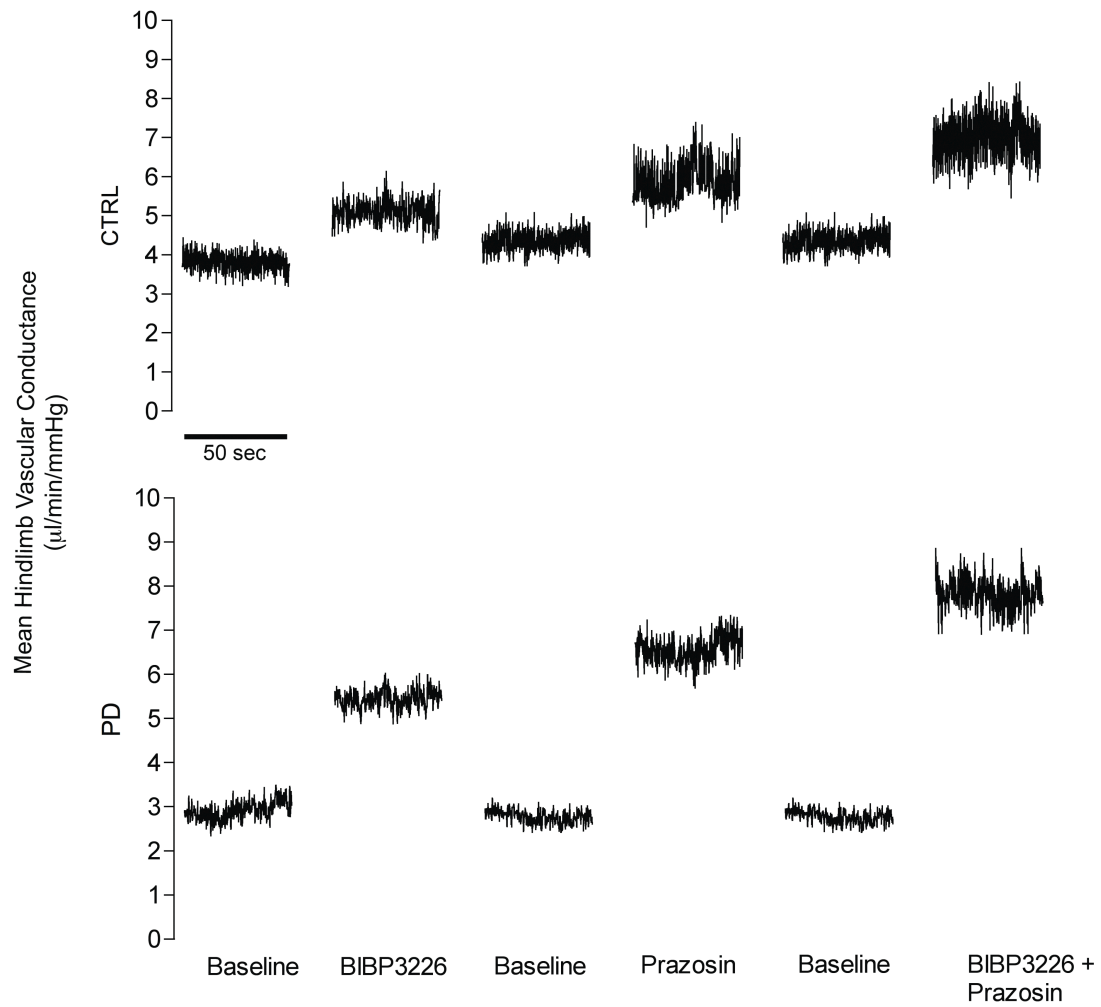


Figure 2.1: Representative hindlimb vascular conductance.

Representative mean vascular conductance (0.1 second averaging of 1 kHz beat-by-beat tracing) over 50 seconds for BIBP3226, prazosin and BIBP3226 + prazosin treatments in CTRL (top) and PD (bottom).

2.3.1. Functional effects of local Y1R and α 1R blockade

2.3.1.1. Effect of local Y1R blockade (BIBP3226)

Following Y1R antagonism, MAP was unchanged for both groups, however HR increased from baseline in PD ($p < 0.05$, Table 2.2). Q_{fem} and VC increased from baseline in CTRL ($\Delta Q_{\text{fem}} = 70 \pm 17 \mu\text{l}/\text{min}$; $\Delta\text{VC} = 1.0 \pm 0.2 \mu\text{l}/\text{min}/\text{mmHg}^{-1}$) and PD ($\Delta Q_{\text{fem}} = 190 \pm 45 \mu\text{l}/\text{min}$; $\Delta\text{VC} = 2.8 \pm 0.8 \mu\text{l}/\text{min}/\text{mmHg}$) ($p < 0.05$), however the increase in Q_{fem} and VC following Y1R blockade was greater in PD compared to CTRL ($p < 0.05$, Figure 2.2). Percent change in VC was greater in PD ($75 \pm 13\%$) *versus* CTRL ($31 \pm 12\%$) ($p < 0.05$, Figure 2.3).

2.3.1.2. Effect of local α 1R blockade (prazosin)

Following α 1R antagonism, MAP decreased 15 ± 2 and 26 ± 5 mmHg, for CTRL and PD respectively ($p < 0.05$, Table 2.2) and HR was unchanged from baseline (Table 2.2). Q_{fem} and VC increased from baseline in CTRL ($\Delta Q_{\text{fem}} = 39 \pm 13 \mu\text{l}/\text{min}$; $\Delta\text{VC} = 1.5 \pm 0.3 \mu\text{l}/\text{min}/\text{mmHg}$) and PD ($\Delta Q_{\text{fem}} = 149 \pm 37 \mu\text{l}/\text{min}$; $\Delta\text{VC} = 3.2 \pm 0.4 \mu\text{l}/\text{min}/\text{mmHg}$), where the increase in Q_{fem} and VC was greater in PD compared to CTRL ($p < 0.05$, Figure 2.2). Percent change in VC was greater in PD ($94 \pm 11\%$) *versus* CTRL ($41 \pm 9\%$) ($p < 0.05$, Figure 2.3).

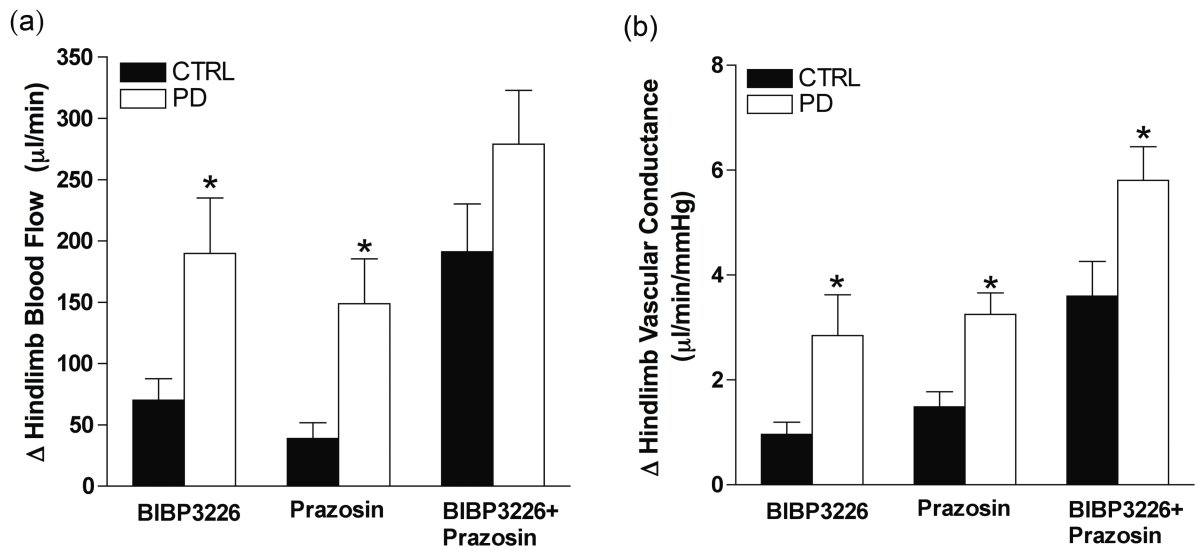


Figure 2.2. Sympathetic receptor blockade elicits greater vascular responses in PD.

Panel a: Change in hindlimb blood flow (Qfem) and Panel b: vascular conductance (VC) from baseline following Y1R and α 1R blockade. With Y1R blockade, the increase in Qfem and VC was greater in PD (n=9) versus CTRL (n=8) (p < 0.05). α 1R blockade elicited an increase in Qfem, as well as an increase in VC that was greater in PD compared to CTRL (p < 0.05). * Indicates different from CTRL (p < 0.05).

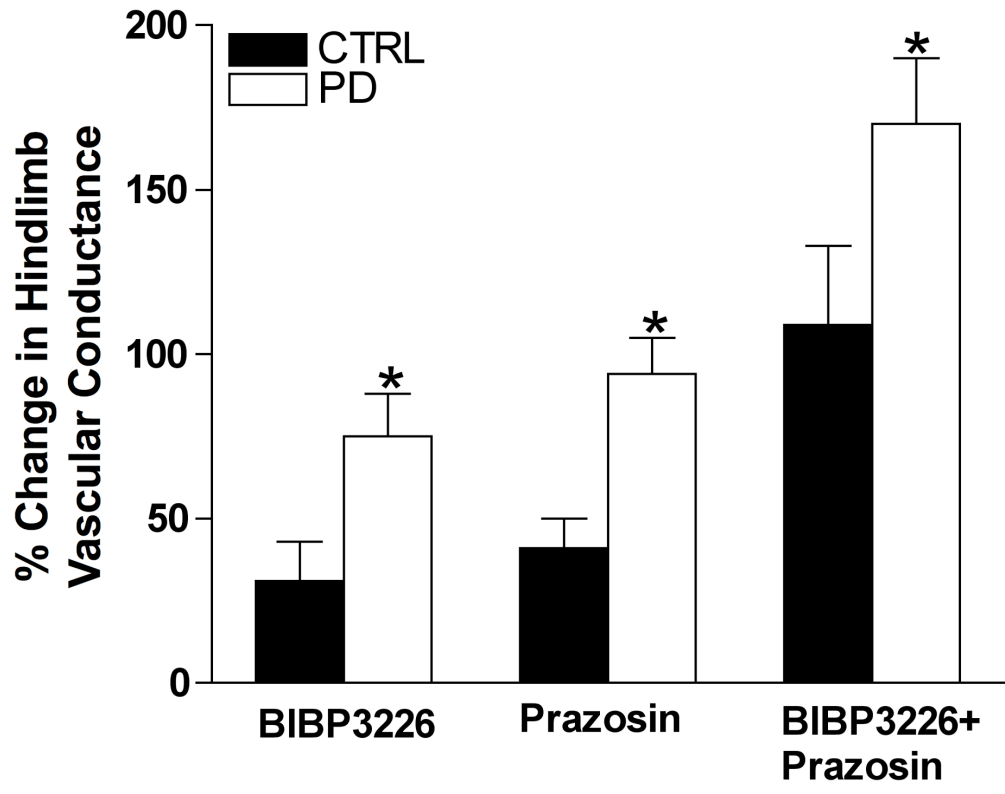


Figure 2.3: Percent change in hindlimb vascular conductance following Y1R and α 1R blockade.

The percent increase in VC following BIBP3226, prazosin and BIBP3226 + prazosin treatments was greater in PD (n=9) compared to CTRL (n=8). *Indicates different from CTRL (p < 0.05).

2.3.1.3. Effect of simultaneous Y₁R and α ₁R blockade (BIBP3226 + prazosin)

Following combined Y₁R and α ₁R antagonism, MAP decreased 17 ± 3 and 31 ± 6 mmHg, for CTRL and PD respectively ($p < 0.05$, Table 2.2), whereas HR remained unchanged. Q_{fem} and VC increased from baseline in CTRL ($\Delta Q_{fem} = 191 \pm 39$ μ l/min; $\Delta VC = 3.8 \pm 0.7$ μ l/min/mmHg) and PD ($\Delta Q_{fem} = 279 \pm 44$ μ l/min; $\Delta VC = 5.8 \pm 0.6$ μ l/min/mmHg) ($p < 0.05$), however the increase in Q_{fem} and VC following combined Y₁R and α ₁R blockade was greater in PD compared to CTRL ($p < 0.05$, Figure 2.2). Percent change in VC was greater in PD ($170 \pm 20\%$) *versus* CTRL ($109 \pm 24\%$) ($p < 0.05$, Figure 2.3).

To determine the potential synergistic interaction between endogenous Y₁R and α ₁R activation, the sum of the VC responses from the BIBP3226 and prazosin conditions was compared to the VC responses elicited by combined Y₁R and α ₁R blockade within each group. Compared to the sum of the independent effects of BIBP3226 and prazosin infusion, combined blockade resulted in a similar increase in VC within groups (Figure 2.4).

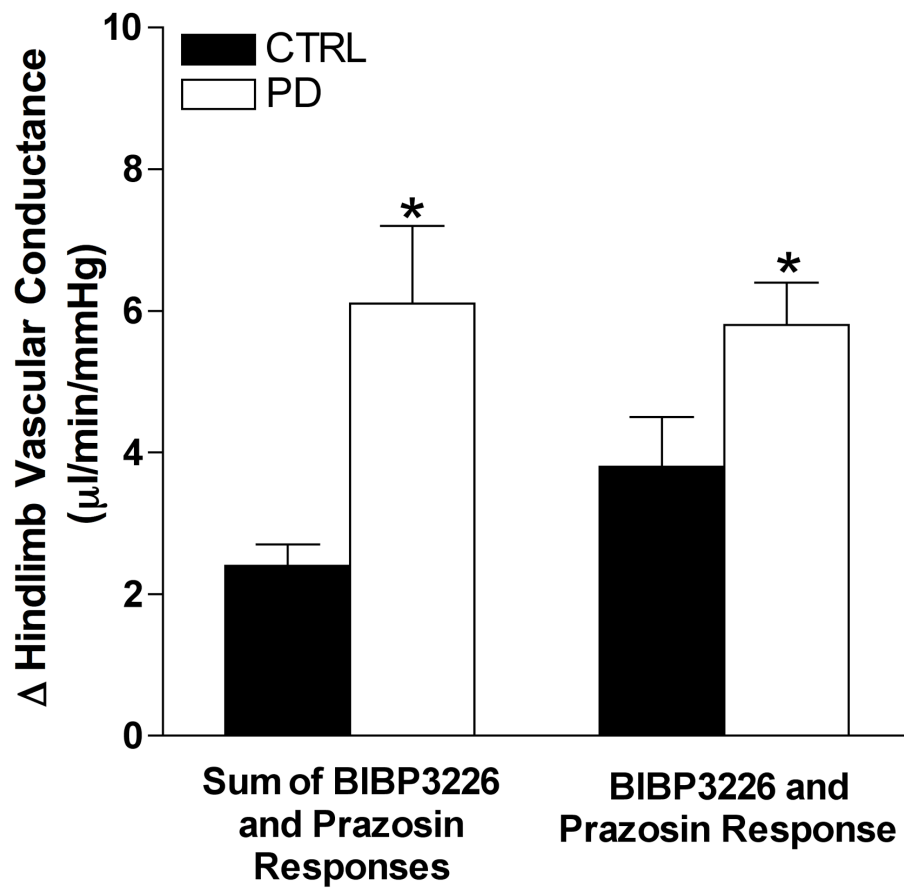


Figure 2.4. Y1R and α 1R synergism is not observed in CTRL and PD.

Comparison of the change in hindlimb vascular conductance between CTRL (n=8) and PD (n=9) for the sum of responses from BIBP3226 and prazosin conditions and the BIBP3226 + prazosin condition. * Indicates different from CTRL ($p < 0.05$).

2.3.2. Tissue NPY concentration and Y1R and α 1R expression

2.3.2.1. Tissue NPY concentration

NPY concentration was $155 \pm 32\%$ and $68 \pm 32\%$ greater in white and red vastus respectively in PD compared to CTRL ($p < 0.05$, Figure 2.5).

2.3.2.2. Tissue Y1R and α 1R

Compared to CTRL, Y1R protein expression was $43 \pm 15\%$ and $30 \pm 9\%$ greater in PD white and red vastus muscle respectively ($p < 0.05$, Figure 2.6). α 1R expression was $94 \pm 43\%$ greater in PD compared to CTRL in red vastus muscle ($p < 0.05$), however expression in white vastus muscle was similar between groups (Figure 2.7).

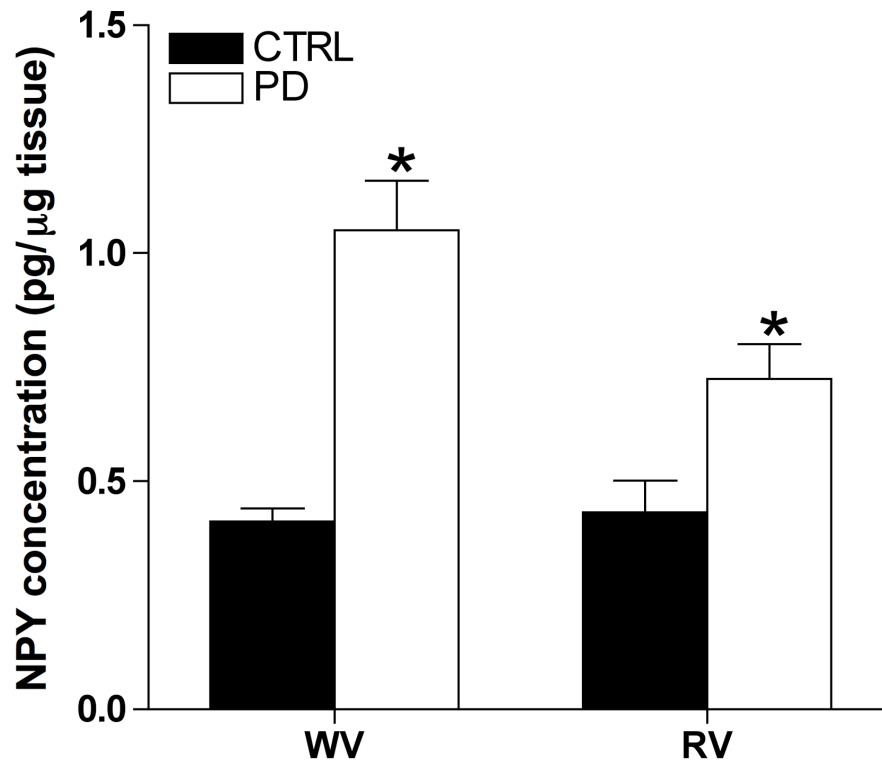


Figure 2.5. Skeletal muscle NPY concentration is elevated in PD.

NPY concentration normalized to total protein for whole muscle homogenate of white vastus (WV) and red vastus (RV). PD (n=6 per muscle group) tissue had greater NPY concentration compared to CTRL (n=6 per muscle group). * Indicates different from CTRL (p < 0.05).

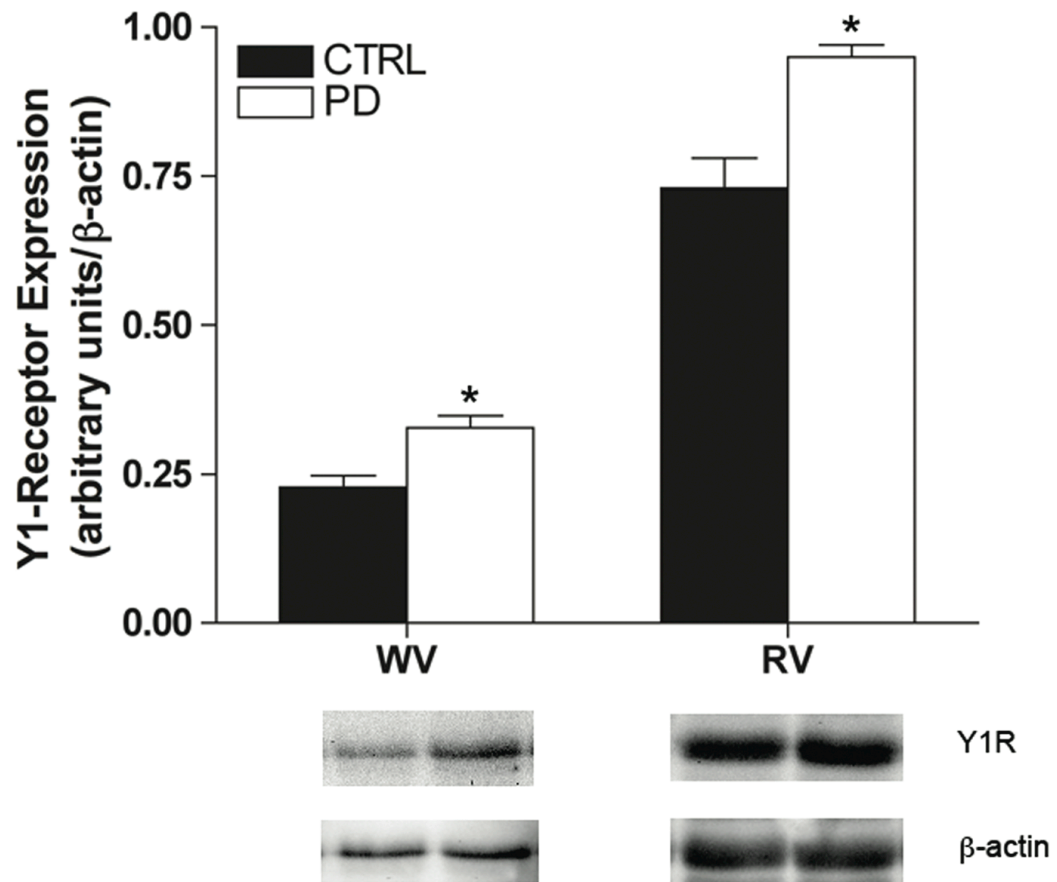


Figure 2.6. Y1R expression is augmented in PD.

Western blot analysis of Y1R expression (~43 kDa) in hindlimb muscle homogenate of CTRL (n=6 per muscle group) and PD (n=6 per muscle group). PD had greater overall expression of Y1R in both white and red vastus muscles. * Indicates different from CTRL (p < 0.05).

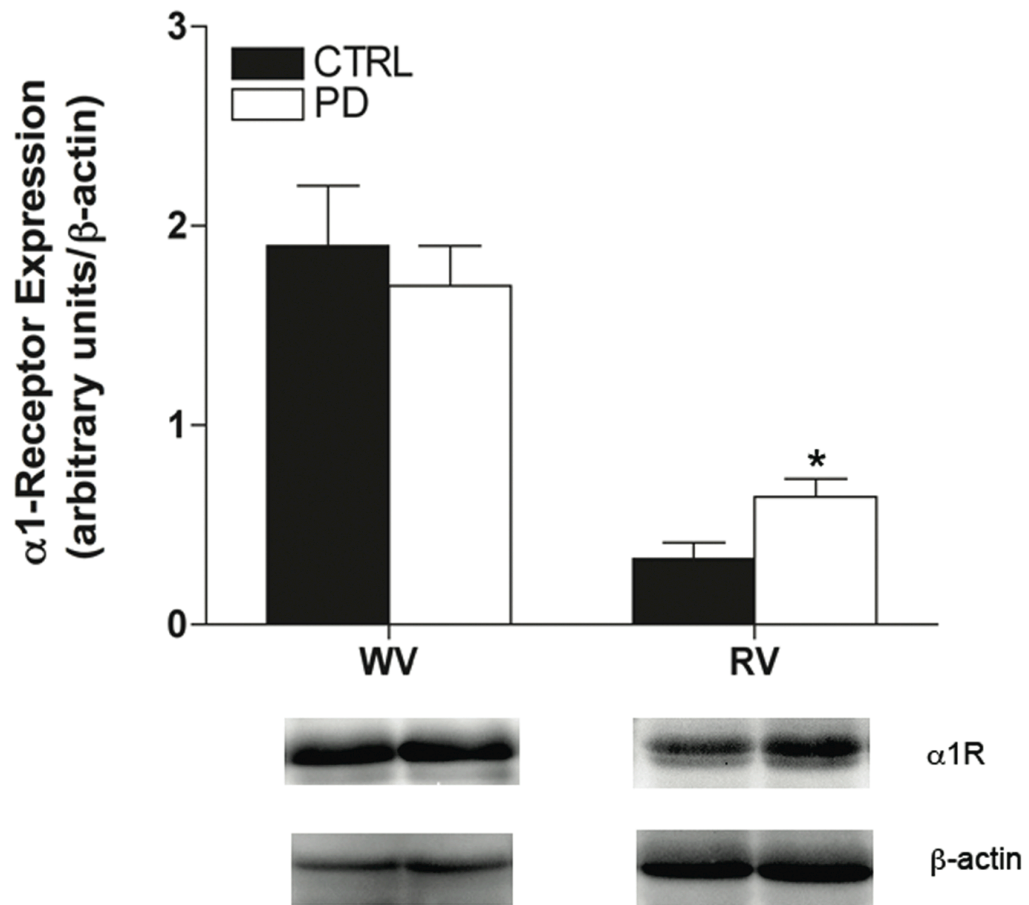


Figure 2.7. $\alpha 1$ R expression is augmented in PD.

Western blot analysis of $\alpha 1$ R expression (~42 kDa) in hindlimb muscle homogenate of CTRL (n=6 per muscle group) and PD (n=6 per muscle group). PD had greater $\alpha 1$ R expression in red vastus muscle, compared to CTRL. * Indicates different from CTRL (p < 0.05).

2.4. Discussion

As hypothesized, we observed heightened sympathetic influences on baseline vascular control in pre-diabetes, as blockade of sympathetic receptors elicited greater Q_{fem} and VC responses in PD compared to CTRL. This is the first study to report that pre-diabetes promotes an overall increase in Y1R and α 1R vascular control under baseline conditions. Accordingly, increases in skeletal muscle NPY concentration and Y1R expression were observed in PD. However, in contrast to our hypothesis, we did not unmask Y1R and α 1R synergistic effects on VC with combined receptor blockade.

In the current study we demonstrated that modifications in sympathetic vascular control occur before the manifestation of endothelial and/or vascular smooth muscle dysfunction generally observed in overt type 2 diabetes. Our current data are supported by past studies (using the same model of pre-diabetes) showing no differences in responses to ACh or SNP in PD versus CTRL (Ellis et al., 2010; Lesniewski et al., 2008). These data indicate that endothelium dependent and independent responses to such pharmacological stimuli (ACh and SNP) are intact in PD, supporting the hypothesis that vascular dysregulation in early pre-diabetes is mainly due to modifications in sympathetic control.

Past work from our group suggests that sympathetic vascular control involves interactions between Y1R and α 1R (Jackson et al., 2005a). Until presently, there was a lack of research investigating the role of NPY in pre-diabetic vascular dysfunction. In fact, past investigations addressing augmented sympathetic vascular control in pre-diabetes have relied predominantly on the functional responses to infusion/application of α -adrenergic agonists *in vivo*, or responses of isolated vascular preparations treated with

these agents (Frisbee, 2004; Lesniewski et al., 2008). Although essential for determining the existence of receptors and their independent function(s) within physiological systems, the infusion of agonists does not address autogenous ligand–receptor interactions. In the current investigation highly selective Y1R and α 1R antagonists (BIBP3226 and prazosin respectively) were delivered alone and in combination to address endogenous independent and synergistic Y1R/ α 1R control under baseline conditions. Although responses to Y1R, α 1R, and combined blockade were markedly augmented in PD, we did not unmask endogenous Y1R and α 1R synergism in either CTRL or PD (Figure 3.3). This was surprising, as we have previously reported endogenous synergy between Y1R and α 1R in adult male Sprague Dawley rats (Jackson et al., 2005a). Thus, it seems that such receptor interactions are not present in the young ZDF rat or they were not robust enough to resolve in the current study.

Despite similar baseline Q_{fem} and VC among groups, we observed that both Y1R and α 1R sympathetic antagonist treatments resulted in greater vascular responses in PD. Under conditions of heightened sympathetic influence, it seems unexpected that similarities in baseline Q_{fem} and VC would exist. However, our observations are supported by other work where isolated vessels from pre-diabetic rats (with similar baseline tone) demonstrated greater responses to sympathetic agonists compared to controls (Lesniewski et al., 2008). Thus, in the current study, it appears that compensatory dilatory mechanisms served to maintain normal blood flow under baseline conditions in PD. The presence of high blood lactate (a potent vasodilator, (Chen, Wolin, & Messina, 1996)) in PD likely contributed to buffering the effects of augmented sympathetic vascular modulation. In support of our data, others have shown that insulin

resistance (Lovejoy, Newby, Gebhart, & DiGirolamo, 1992) and type 2 diabetes (Crawford et al., 2010) are associated with heightened lactate levels.

Our observations of augmented baseline Y1R and α 1R activation in PD are complemented by our findings that PD had greater NPY concentration and Y1R and α 1R expression in hindlimb skeletal muscle. Neuropeptide Y is produced in sympathetic neuronal cell soma and packaged into secretory large dense-cored vesicles and undergoes axonal transport (the rate of which is SNA level dependent) to the axon terminal where it is released and eventually degraded by enzymes in the synaptic cleft (Lundberg, 1996). This is in contrast to NE, which is produced in sympathetic nerve terminal, released, and eventually taken back up into the nerve terminal (Eisenhofer, Goldstein, & Kopin, 1989). Based on the unique origin and fate of NPY, it can be reasonably inferred that increased skeletal muscle NPY concentration measured in PD was a result of one or a combination of the following: i) augmented sympathetic neuronal density; ii) increased production and axonal transport of NPY; and/or iii) increased NPY release into skeletal muscle interstitium. This line of reasoning falls in line with work by others who reported sympathetic nerve hyperactivity in insulin resistant and type 2 diabetic subjects, as well as heightened plasma NPY levels in type 2 diabetic patients (Huggett et al., 2003; Matyal et al., 2011). Beyond this, *in vivo* studies investigating NPY levels and Y1R/ α 1R expression in pre-diabetes are limited; however, increased Y1R mRNA expression has been reported in cardiac tissue of diabetic rats (Chottova Dvorakova et al., 2008) and it was shown that rat vascular smooth muscle cells treated with high levels of insulin resulted in upregulation of α 1R (Hu, Shi, & Hoffman, 1996).

2.4.1. Limitations

We used hindlimb muscle homogenate in order to quantify the receptors located along downstream resistance arterioles, as these vessels are responsible for modulating flow at the level of the femoral artery. Previous work indicates that peripheral Y1Rs are predominantly associated with vasculature (Franco-Cereceda & Liska, 1998). In contrast, α_1 Rs have been identified on skeletal muscle fibers in rats; however, the density of those located in muscle fibers is negligible compared to α_1 R expression on resistance arterioles (Martin, Tolley, & Saffitz, 1990). Based on past reports and the internal consistency between our functional and cellular data, we are confident that our reported differences in ligand concentration and receptor expression reasonably reflect what is occurring at the level of the vasculature.

We measured skeletal muscle tissue NPY concentration instead of plasma NPY levels for several reasons. Indeed, repeated blood sampling poses the risk of evoking hypotension and increases in sympathetic nerve activity. As well, plasma NPY levels represent a mixed sample originating from several sources throughout the body. In contrast, the skeletal muscle samples used in this study were promptly harvested from anesthetized animals (with minimal hemodynamic stress) under the same conditions that functional data were acquired. Thus, we feel that our reported NPY levels are an accurate representation of the local skeletal muscle environment under baseline conditions.

Due to limitations in detection, NE levels were not measured in the current study. However, this investigation and previous from our group (Jackson et al., 2010; Jackson et al., 2005a) used a sensitive enzyme immunoassay optimized to detect NPY in skeletal

muscle homogenates. NPY is co-released and co-stored with NE (Zofia, Zukowska-Grojec & Wahlestedt, 1993) and plasma NPY release correlates with NE release (Z. Zukowska-Grojec, Konarska, & McCarty, 1988), especially under conditions of elevated sympathetic nerve activity; thus, it is reasonable to postulate that our measures of increased skeletal muscle NPY concentration in PD reflect a concomitant increase in skeletal muscle NE.

2.5. Conclusions

In conclusion, we provide the first report that Y1R and α 1R vascular regulation is augmented in the hindlimb of pre-diabetic ZDF rats. Our findings are supported by increased skeletal muscle NPY concentration and Y1R/ α 1R expression in PD *versus* CTRL. Future studies are required to ascertain the long-term cardiovascular consequences of our findings and their functional significance in contracting skeletal muscle.

2.6. Acknowledgements

We would like to thank Elizabeth Bowles of Dr. Randy Sprague's laboratory (Department of Pharmacological and Physiological Science, Saint Louis University School of Medicine, Saint Louis, MO, USA) for the insulin ELISA, as well as Stephanie Milkovich for technical assistance and Dr. Christopher Ellis for his valuable advice (Department of Medical Biophysics, Schulich School of Medicine & Dentistry, *The University of Western Ontario*, London, ON, Canada).

2.7. References

- Anderson, E. A., Balon, T. W., Hoffman, R. P., Sinkey, C. A., & Mark, A. L. (1992). Insulin increases sympathetic activity but not blood pressure in borderline hypertensive humans. *Hypertension*, *19*(6 Pt 2), 621-627.
- Armstrong, R. B., & Laughlin, M. H. (1984). Exercise blood flow patterns within and among rat muscles after training. *Am J Physiol*, *246*(1 Pt 2), H59-68.
- Armstrong, R. B., & Phelps, R. O. (1984). Muscle fiber type composition of the rat hindlimb. *Am J Anat*, *171*(3), 259-272.
- Bartfai, T., Iverfeldt, K., Fisone, G., & Serfozo, P. (1988). Regulation of the release of coexisting neurotransmitters. *Annu Rev Pharmacol Toxicol*, *28*, 285-310.
- Bradford, M. M. (1976). A rapid and sensitive method for the quantitation of microgram quantities of protein utilizing the principle of protein-dye binding. *Anal Biochem*, *72*, 248-254.
- Chen, Y. L., Wolin, M. S., & Messina, E. J. (1996). Evidence for cGMP mediation of skeletal muscle arteriolar dilation to lactate. *J Appl Physiol*, *81*(1), 349-354.
- Chottova Dvorakova, M., Wiegand, S., Pesta, M., Slavikova, J., Grau, V., Reischig, J., et al. (2008). Expression of neuropeptide Y and its receptors Y1 and Y2 in the rat heart and its supplying autonomic and spinal sensory ganglia in experimentally induced diabetes. *Neuroscience*, *151*(4), 1016-1028.
- Crawford, S. O., Hoogeveen, R. C., Brancati, F. L., Astor, B. C., Ballantyne, C. M., Schmidt, M. I., et al. (2010). Association of blood lactate with type 2 diabetes: the Atherosclerosis Risk in Communities Carotid MRI Study. *Int J Epidemiol*.
- De Camilli, P., & Jahn, R. (1990). Pathways to regulated exocytosis in neurons. *Annu Rev Physiol*, *52*, 625-645.

- DeFronzo, R. A., & Ferrannini, E. (1991). Insulin resistance. A multifaceted syndrome responsible for NIDDM, obesity, hypertension, dyslipidemia, and atherosclerotic cardiovascular disease. *Diabetes Care*, *14*(3), 173-194.
- Eisenhofer, G., Goldstein, D. S., & Kopin, I. J. (1989). Plasma dihydroxyphenylglycol for estimation of noradrenaline neuronal re-uptake in the sympathetic nervous system in vivo. *Clin Sci (Lond)*, *76*(2), 171-182.
- Ekelund, U., & Erlinge, D. (1997). In vivo receptor characterization of neuropeptide Y-induced effects in consecutive vascular sections of cat skeletal muscle. *Br J Pharmacol*, *120*(3), 387-392.
- Ellis, C. G., Goldman, D., Hanson, M., Stephenson, A. H., Milkovich, S., Benlamri, A., et al. (2010). Defects in oxygen supply to skeletal muscle of prediabetic ZDF rats. *Am J Physiol Heart Circ Physiol*, *298*(6), H1661-1670.
- Epstein, M., & Sowers, J. R. (1992). Diabetes mellitus and hypertension. *Hypertension*, *19*(5), 403-418.
- Esler, M., Rumantir, M., Wiesner, G., Kaye, D., Hastings, J., & Lambert, G. (2001). Sympathetic nervous system and insulin resistance: from obesity to diabetes. *Am J Hypertens*, *14*(11 Pt 2), 304S-309S.
- Faeh, D., William, J., Yerly, P., Paccaud, F., & Bovet, P. (2007). Diabetes and pre-diabetes are associated with cardiovascular risk factors and carotid/femoral intima-media thickness independently of markers of insulin resistance and adiposity. *Cardiovasc Diabetol*, *6*, 32.
- Franco-Cereceda, A., & Liska, J. (1998). Neuropeptide Y Y1 receptors in vascular pharmacology. *Eur J Pharmacol*, *349*(1), 1-14.
- Frisbee, J. C. (2004). Enhanced arteriolar alpha-adrenergic constriction impairs dilator responses and skeletal muscle perfusion in obese Zucker rats. *J Appl Physiol*, *97*(2), 764-772.

- Haffner, S. M., Stern, M. P., Hazuda, H. P., Mitchell, B. D., & Patterson, J. K. (1990). Cardiovascular risk factors in confirmed prediabetic individuals. Does the clock for coronary heart disease start ticking before the onset of clinical diabetes? *JAMA*, *263*(21), 2893-2898.
- Hu, Z. W., Shi, X. Y., & Hoffman, B. B. (1996). Insulin and insulin-like growth factor I differentially induce alpha1-adrenergic receptor subtype expression in rat vascular smooth muscle cells. *J Clin Invest*, *98*(8), 1826-1834.
- Huggett, R. J., Hogarth, A. J., Mackintosh, A. F., & Mary, D. A. (2006). Sympathetic nerve hyperactivity in non-diabetic offspring of patients with type 2 diabetes mellitus. *Diabetologia*, *49*(11), 2741-2744.
- Huggett, R. J., Scott, E. M., Gilbey, S. G., Stoker, J. B., Mackintosh, A. F., & Mary, D. A. (2003). Impact of type 2 diabetes mellitus on sympathetic neural mechanisms in hypertension. *Circulation*, *108*(25), 3097-3101.
- Jackson, D. N., Ellis, C. G., & Shoemaker, J. K. (2010). Estrogen modulates the contribution of neuropeptide Y to baseline hindlimb blood flow control in female Sprague Dawley rats. *Am J Physiol Regul Integr Comp Physiol*.
- Jackson, D. N., Milne, K. J., Noble, E. G., & Shoemaker, J. K. (2005a). Gender-modulated endogenous baseline neuropeptide Y Y1-receptor activation in the hindlimb of Sprague-Dawley rats. *J Physiol*, *562*(Pt 1), 285-294.
- Jackson, D. N., Milne, K. J., Noble, E. G., & Shoemaker, J. K. (2005b). Neuropeptide Y bioavailability is suppressed in the hindlimb of female Sprague-Dawley rats. *J Physiol*, *568*(Pt 2), 573-581.
- Jackson, D. N., Noble, E. G., & Shoemaker, J. K. (2004). Y1- and alpha1-receptor control of basal hindlimb vascular tone. *Am J Physiol Regul Integr Comp Physiol*, *287*(1), R228-233.
- Kim, S. H., & Reaven, G. M. (2008a). Insulin resistance and hyperinsulinemia: you can't have one without the other. *Diabetes Care*, *31*(7), 1433-1438.

- Kim, S. H., & Reaven, G. M. (2008b). Isolated impaired fasting glucose and peripheral insulin sensitivity: not a simple relationship. *Diabetes Care*, *31*(2), 347-352.
- Laughlin, M. H., & Armstrong, R. B. (1983). Rat muscle blood flows as a function of time during prolonged slow treadmill exercise. *Am J Physiol*, *244*(6), H814-824.
- Leonard, B. L., Watson, R. N., Loomes, K. M., Phillips, A. R., & Cooper, G. J. (2005). Insulin resistance in the Zucker diabetic fatty rat: a metabolic characterisation of obese and lean phenotypes. *Acta Diabetol*, *42*(4), 162-170.
- Lesniewski, L. A., Donato, A. J., Behnke, B. J., Woodman, C. R., Laughlin, M. H., Ray, C. A., et al. (2008). Decreased NO signaling leads to enhanced vasoconstrictor responsiveness in skeletal muscle arterioles of the ZDF rat prior to overt diabetes and hypertension. *Am J Physiol Heart Circ Physiol*, *294*(4), H1840-1850.
- Lovejoy, J., Newby, F. D., Gebhart, S. S., & DiGirolamo, M. (1992). Insulin resistance in obesity is associated with elevated basal lactate levels and diminished lactate appearance following intravenous glucose and insulin. *Metabolism*, *41*(1), 22-27.
- Lundberg, J. M. (1996). Pharmacology of cotransmission in the autonomic nervous system: integrative aspects on amines, neuropeptides, adenosine triphosphate, amino acids and nitric oxide. *Pharmacol Rev*, *48*(1), 113-178.
- Lundberg, J. M., Franco-Cereceda, A., Lou, Y. P., Modin, A., & Pernow, J. (1994). Differential release of classical transmitters and peptides. *Adv Second Messenger Phosphoprotein Res*, *29*, 223-234.
- Malmstrom, R. E. (1997). Neuropeptide Y Y1 receptor mechanisms in sympathetic vascular control. *Acta Physiol Scand Suppl*, *636*, 1-55.
- Mancia, G., Grassi, G., Giannattasio, C., & Seravalle, G. (1999). Sympathetic activation in the pathogenesis of hypertension and progression of organ damage. *Hypertension*, *34*(4 Pt 2), 724-728.

- Martin, W. H., 3rd, Tolley, T. K., & Saffitz, J. E. (1990). Autoradiographic delineation of skeletal muscle alpha 1-adrenergic receptor distribution. *Am J Physiol*, 259(5 Pt 2), H1402-1408.
- Matyal, R., Mahmood, F., Robich, M., Glazer, H., Khabbaz, K., Hess, P., et al. (2011). Chronic type II diabetes mellitus leads to changes in neuropeptide Y receptor expression and distribution in human myocardial tissue. *Eur J Pharmacol*, 665(1-3), 19-28.
- Muntzel, M. S., Anderson, E. A., Johnson, A. K., & Mark, A. L. (1995). Mechanisms of insulin action on sympathetic nerve activity. *Clin Exp Hypertens*, 17(1-2), 39-50.
- Okon, E. B., Szado, T., Laher, I., McManus, B., & van Breemen, C. (2003). Augmented contractile response of vascular smooth muscle in a diabetic mouse model. *J Vasc Res*, 40(6), 520-530.
- Scherrer, U., & Sartori, C. (1997). Insulin as a vascular and sympathoexcitatory hormone: implications for blood pressure regulation, insulin sensitivity, and cardiovascular morbidity. *Circulation*, 96(11), 4104-4113.
- Soma, L. R. (1983). Anesthetic and analgesic considerations in the experimental animal. *Ann N Y Acad Sci*, 406, 32-47.
- Terjung, R. L., & Engbretson, B. M. (1988). Blood flow to different rat skeletal muscle fiber type sections during isometric contractions in situ. *Med Sci Sports Exerc*, 20(5 Suppl), S124-130.
- Zukowska-Grojec, Z. (1995). Neuropeptide Y. A novel sympathetic stress hormone and more. *Ann N Y Acad Sci*, 771, 219-233.
- Zukowska-Grojec, Z., Konarska, M., & McCarty, R. (1988). Differential plasma catecholamine and neuropeptide Y responses to acute stress in rats. *Life Sci*, 42(17), 1615-1624.

Zukowska-Grojec, Z., & Wahlestedt, C. (1993). Origin and actions of neuropeptide Y in the cardiovascular system. In *The Biology of Neuropeptide Y and Related Peptide*, ed. Colmers WF & Wahlestedt (pp. pp.315-388). Totowa: Humana Press.

Chapter 3 : Contraction-evoked vasodilation and functional hyperemia are compromised in branching skeletal muscle arterioles of young pre-diabetic mice

A version of this manuscript is under review at *Acta Physiologica*.

Nicole M. Novielli and Dwayne N. Jackson (2013). Contraction-evoked vasodilation and functional hyperemia are compromised in branching skeletal muscle arterioles of young pre-diabetic mice. *Acta Physiologica*, Manuscript No. APH-2013-10-0364.

3.1. Introduction

Pre-diabetes affects approximately 25% of North Americans, and its prevalence continues to rise with increased cases of obesity and sedentary lifestyle (Canadian Diabetes Association, 2011, Disease Control and Prevention, 2011). Inherently, pre-diabetes is associated with impairments in cardiovascular health that manifest prior to the onset of overt type 2 diabetes (Faeh, William, Yerly, Paccaud, & Bovet, 2007; Haffner, Stern, Hazuda, Mitchell, & Patterson, 1990; Shin, Lee, & Lee, 2011). Characterized by hyperinsulinemia, insulin resistance, elevated blood glucose and frequently accompanied by obesity, the pathological metabolic characteristics of pre-diabetes play a role in the initiation of cardiovascular complications centrally and peripherally (DeFronzo & Abdul-Ghani, 2011; Gupta et al., 2012; Schaefer et al., 2010); however, our knowledge regarding the effects of pre-diabetes on skeletal muscle arteriolar function is limited.

Skeletal muscle makes up approximately 40% of body mass and contains the greatest proportion of arterioles than any other organ (Janssen et al., 2000). Comprising approximately 20% of the body's total baseline systemic vascular resistance, skeletal muscle arterioles play a key role in blood pressure regulation at rest and blood flow redistribution during exercise. A hallmark of musculoskeletal health is ability to rapidly match skeletal muscle blood supply to metabolic demand at rest and during physical activity and research in the past decade provides evidence of arteriolar dysregulation in pre-diabetes (Gorczyński et al., 1978, Laughlin and Armstrong, 1982, Fuglevand and Segal, 1997, Lesniewski et al., 2008, Ellis et al., 2010). In 2008, Lesniewski *et al.* reported increases in vasoconstrictor responsiveness to norepinephrine and endothelin-1 in 1st order arterioles isolated from the gastrocnemius of normotensive pre-diabetic

Zucker Diabetic Fatty (ZDF) rats (Lesniewski et al., 2008). In congruence, we have shown that, despite having normal resting blood flow, sympathetic influences on baseline vascular control are augmented in normotensive pre-diabetic ZDF rats *in vivo* (Novielli, Al-Khazraji, Medeiros, Goldman & Jackson, 2012). Taken together, it is reasonable to conclude that skeletal muscle arteriolar dysregulation in early pre-diabetes has little to no effect on systemic blood pressure or bulk blood flow to skeletal muscle under resting conditions. However, the conditions described above may render skeletal muscle microcirculation opposable to arteriolar dilation under exercise conditions, leading to microvascular perfusion deficits.

Studies directly investigating the impact of pre-diabetes on skeletal muscle microvascular control during exercise are limited. Certainly, human and animal studies have illustrated impaired skeletal muscle perfusion and O₂ delivery/uptake, and compromised blood flow regulation at rest and during exercise/muscle contraction in overt type 2 diabetes, the metabolic syndrome, and obesity (Padilla et al., 2006a, Padilla et al., 2006b, Musa, Torrens & Clough, 2014, Blain, Limberg, Mortensen & Schrage, 2012, Vinet et al., 2011, Karpoff et al., 2009, Frisbee, 2003, Frisbee, 2004, MacAnaney, Reilly, O'Shea, Egana & Green, 2011, Kingwell, Formosa, Muhlmann, Bradley & McConell, 2003). However, differences in the experimental models and methodological limitations generally constrain the current understanding of vascular control in metabolic diseases to bulk blood flow measures. Although such studies have merit, measures of bulk blood flow provide no information on the site or nature of arteriolar dysregulation. Furthermore, models of overt type 2 diabetes, metabolic syndrome, and obesity are accompanied by chronic states of cardiovascular compromise and overt vascular disease;

where early pre-diabetes represents the primary stage of diabetic disease progression, where vascular complications may not be as clear-cut.

Direct observations of arteriolar networks using intravital video microscopy (IVVM) illustrate that healthy microvascular responses to contraction are non-uniform, with greater (relative) arteriolar dilation occurring in distal versus proximal regions (Dodd & Johnson, 1991; Marshall & Tandon, 1984; VanTeeffelen & Segal, 2006). As well, it has been shown that arterioles respond differently to vasoactive substances associated with muscle contraction [(e.g. potassium (M. L. Armstrong, Dua, & Murrant, 2007), adenosine (Murrant & Sarelius, 2002), acetylcholine (VanTeeffelen & Segal, 2006), lactate (Chen, Wolin, & Messina, 1996), nitric oxide (Silveira, Pereira-Da-Silva, Juel, & Hellsten, 2003)] depending on where they reside in the network. Distal arterioles closest to the capillaries are the first to dilate, as the sensitivity of these vessels to metabolic vasoactive substances has been shown to be greater than proximal arterioles (Davis, Hill, & Kuo, 2008). Furthermore, distal arterioles are able to dilate and overcome sympathetic activation more readily than proximal arterioles within the muscle (Anderson & Faber, 1991). Finally, studies demonstrate that sympathetic receptors located on arterioles (responsible for vasoconstriction and maintaining arteriolar tone) are differentially distributed at different branch orders of arteriolar networks, indicating distinct spatial sympathetic arteriolar control (Anderson & Faber, 1991; Moore, Jackson, & Segal, 2010). Since these studies illustrate heterogeneous arteriolar regulation in skeletal muscle under healthy conditions, then it would be ideal to investigate arteriolar function at different levels of continuously branching arteriolar networks in pre-diabetes. Interestingly, deficits in post-exercise capillary perfusion have been demonstrated in

overt type 2 diabetic subjects, where blood flow in the supplying conduit artery was not compromised (Womack et al., 2009). These findings suggest that deficiencies in arteriolar regulation may be apparent in the distal microcirculation before impairments of exercise-evoked blood flow can be detected in large vessels (Kingwell et al., 2003; MacAnaney et al., 2011). However, in an effort to determine the effects of early pre-diabetes on the onset of skeletal muscle microvascular dysregulation, an appropriate model enabling concurrent observation of multiple arteriolar orders is needed.

The gluteus maximus (GM) preparation, developed by Bearden *et al.* (Bearden, Payne, Chisty, & Segal, 2004), provides a unique model for investigating skeletal muscle arteriolar control using IVVM. Unlike many other experimental skeletal muscle models, the GM is common to both sexes, is found in all mammalian species, and is recruited during locomotion (Bearden et al., 2004). Furthermore, due to its planar arrangement of microvessels and uniform tissue thinness it is optically ideal for IVVM. These properties enable comprehensive evaluation of complete arteriolar networks within a single focal plane.

In an effort to understand the impact of early pre-diabetes on arteriolar network regulation in skeletal muscle, our lab has refined and adapted the GM preparation in a novel murine model of pre-diabetes, The Pound Mouse. Using this model we investigated the effects of pre-diabetes on GM muscle branching arteriolar network function in response to muscle contraction. Herein, we tested the hypothesis that arteriolar dilation and blood flow in response to single tetanic and rhythmic (steady state) muscle contractions would be blunted in pre-diabetes. Furthermore, we predicted that the greatest

decrements in contraction-evoked vasodilation would occur in distal pre-capillary arterioles versus proximal arterioles.

3.2. Materials and methods

All animal procedures were approved by the Council on Animal Care at The University of Western Ontario (protocol number: 2012-018). All invasive procedures were performed under α -chloralose and urethane anesthetic, and all efforts were made to minimize animal suffering.

3.2.1. Animals

Experiments were performed on male C57BL/6NCrI (CTRL, 7-8 weeks old) and Pound mice (PD, C57BL/6NCrI-*Lepr*^{db-lb}/CrI, 7-8 weeks old). The Pound Mouse (Charles River, Saint-Constant, QC, Canada) is a model of pre-diabetes, where these mice exhibit a novel mutation *Lepr*^{db-lb} in the leptin receptor gene. When fed a high fat diet (i.e. Purina 5008 chow), by 7 weeks of age these mice become obese, hyperinsulinemic, and have elevated blood glucose, characteristic of the pre-diabetic condition in humans (Kim & Reaven, 2008a, 2008b). As these mice are of C57BL/6 background, the male C57BL/6 mouse served as the control group in this study.

Mice were housed in animal care facilities in a temperature (24°C) and light (12 hour cycle)-controlled room and allowed to eat and drink water *ad libitum*. All mice were obtained from Charles River Laboratories (Saint-Constant, QC, Canada) and housed in animal care facilities for at least one week after arrival prior experimentation. Mice were weighted prior to each experiment. After experimentation (in 5 PD and 4 CTRL), GM muscles were excised and weighed (wet muscle mass), then dried in a laboratory oven at

70°C for 3 hours and re-weighed (dry muscle mass). Upon completion of experimental procedures each day, the anesthetized mouse was euthanized with an overdose of α -chloralose and urethane cocktail mix (intraperitoneal injection), and cervical dislocation.

3.2.2. Measurement of blood insulin and glucose levels

Blood insulin values were not determined in this study, as the amount of blood sample necessary to perform the appropriate assay exceeds the ethical amount without sacrificing the animal as specified by Western University Council on Animal Care. Blood insulin values were instead obtained from animal characteristic data reported by Charles River. In order to determine fasting blood glucose, mice were fasted for eight hours and blood glucose was measured from a tail vein blood sample (~10 μ l) using a Bayer Contour® blood glucose analyzer (Bayer, Toronto, ON, Canada). Prior to experimentation, mice were fed *ad libitum* for at least two days following fasting blood glucose measurement.

3.2.3. Anesthesia and muscle preparation

Using an intraperitoneal injection, the mouse was anesthetized with a cocktail of α -chloralose (50 mg/kg) and urethane (750 mg/kg), which was supplemented as needed. This anesthetic was ideal for these experiments as it leaves autonomic, cardiovascular and respiratory function intact (Soma, 1983). Internal body temperature was monitored via a rectal temperature probe and maintained at 37°C with the use of a custom made heated surgical platform. Surgical procedures were viewed through a stereomicroscope. The neck and backside of the mouse was shaved to remove excess fur. The mouse was placed on its back and a mid-neck incision was made. A tracheal cannula (PE-60) was

introduced to facilitate spontaneous respiration and (for experiments involving blood flow measures) the right jugular vein was cannulated (PE-10 tubing) to inject fluorescent RBCs. The neck opening was then closed using sterile stainless steel wound clips (Autoclip 9 mm, Becton Dickinson, Franklin Lakes, NJ, USA). The mouse was then placed in the prone position on a custom built heated stage to prepare the GM for IVVM. Under stereomicroscopic guidance the GM muscle was cut from its origin along the spine and along its rostral and caudal borders (Bearden et al., 2004; Jackson, Moore, & Segal, 2010). With great care taken to preserve its neurovascular supply, the muscle flap was gently reflected away from the mouse, spread evenly onto a transparent Sylgard® (Sylgard 184; Dow Corning, Midland, MI, USA) pedestal to approximate *in situ* dimensions and pinned to secure edges. The exposed tissue was superfused continuously (4–5 ml/min) with bicarbonate-buffered physiological salt solution (PSS, 35°C at tissue, pH 7.4) of the following composition (mM): NaCl 137, KCl 4.7, MgSO₄ 1.2, CaCl₂ 2, NaHCO₃ 18, and equilibrated with 5% CO₂/95% N₂.

3.2.4. Fluorescent labeling of red blood cells

The red blood cell (RBC) staining protocol was adapted from Al-Khazraji *et al.* 2012 (Al-Khazraji, Novielli, Goldman, Medeiros, & Jackson, 2012). One day prior to experimentation, blood was drawn from an anesthetized donor animal via cardiac puncture into a vial containing heparin. Sample was centrifuged at 1300 g for 5 minutes, and the plasma layer and buffy coat were discarded. Red blood cells were then washed in Tris-buffered Ringer's solution (room temperature, pH = 7.4), and incubated in a freshly prepared fluorescein isothiocyanate (FITC, 0.4 mg/mL; Research Organics, Inc., Cleveland, OH, USA) dye solution (FITC mixed into dimethyl sulfoxide and Tris-

buffered Ringer's Albumin [biotechnology grade bovine albumin, 0.005 g/mL; Bioshop® Canada Inc., Burlington, ON, Canada] solution, room temperature, pH = 7.4) for 2 hours. Cells were washed in Tris-buffered Ringer's Albumin solution and stored overnight at 4°C. On the day of experiment, excess dye was removed by washing cells in Tris-buffered Ringer's Albumin solution, and hematocrit was adjusted to ~30–35% with buffer. Prior to injection, fluorescent RBCs were imaged on a microscope and qualitatively evaluated for fluorescence signal and cellular integrity. Prior to IVVM, cells were injected (1% of total animal blood volume) into the animal via the jugular vein and the line was slowly flushed with saline. It has been previously shown that FITC-labeled fresh RBCs (one day or less) do not exhibit adherent or undeformable characteristics in the circulation (Chin-Yee, Gray-Statchuk, Milkovich, & Ellis, 2009). In our experiments, no plugging of capillaries with FITC-labeled RBCs was observed in the muscle preparation.

3.2.5. Intravital video microscopy

Upon completion of microsurgical procedures, the preparation was transferred to the fixed stage of the intravital microscope (Olympus BX51, Olympus, Tokyo, Japan). The preparation was equilibrated with PSS for ~30 minutes. Microvessels were observed under Kohler illumination using a long working distance condenser (NA = 0.80) and long working distance water immersion objectives (Olympus UMPlanFW: 10× NA = 0.30, Olympus UMPlanFW: 20 x NA = 0.50) with illumination from a 100-Watt halogen light source. To enhance contrast of the RBC column, a 450-nm / 20-nm band-pass filter (450BP20; Omega Optical, Brattleboro, VT, USA) was placed in the light path. In an effort to assess microvascular RBC velocities, fluorescent RBCs were epi-illuminated

using a 120-Watt Mercury Vapor Short Arc light source (EXFO, X-Cite 120PC Q, Photonic Solutions Inc., Mississauga, ON, Canada) in line with a FITC (450–490 nm) filter. The optical image was coupled to a front-illuminated interline CCD camera (Qimaging Rolera E=MC²™, Qimaging®, Surrey, BC, Canada) and viewed / stored to a hard drive using specialized imaging software (MetaMorph® 7.6, Molecular Devices Inc., Sunnyvale, CA, USA). Transition between bright-field and fluorescent imaging was performed prior muscle stimulation (to obtain baseline measures) and immediately following stimulation. Bright-field video (.tiff) images were collected (15-17 frames per second [fps]) under Kohler bright-field illumination for off-line analysis of RBC column diameters. Video (.tiff) images were collected (15-17 fps) under epi-illumination for off-line analysis of RBC velocities, and blood flow.

Because second-order arterioles are positioned to control the distribution of blood flow within the GM (Bearden et al., 2004) and terminal (pre-capillary) arterioles play the greatest role in red blood cell distribution to capillaries (Pries, Ley, Claassen, & Gaehtgens, 1989), we chose to study bifurcations at second-order arterioles (2A) to third-order (3A) arterioles and 3A to fourth order (pre-capillary) arterioles (4A). One arteriolar tree (2A-4A) was studied per animal (Figure 3.1). To evaluate the viability of experimental preparations, arterioles were tested for oxygen sensitivity by elevating superfusate O₂ from 0% to 21% (5% CO₂, balance N₂) for 5-8 minutes to elicit vasoconstriction. Upon confirmation of constriction, experiments proceeded and equilibration with 5% CO₂–95% N₂ was restored for the duration of experimental procedures. Following equilibration, a video of the resting (baseline) diameter and fluorescent RBCs was taken. Changes in arteriolar diameter (and blood flow in a subset

of experiments; see Arteriolar and hemodynamic measurements) were evaluated in response to brief maximal tetanic contractions at 100 Hz, as well as 30 seconds of rhythmic muscle contractions (see Skeletal muscle contractions below). For these experiments, each muscle preparation underwent both contraction protocols with the order randomized across experiments.

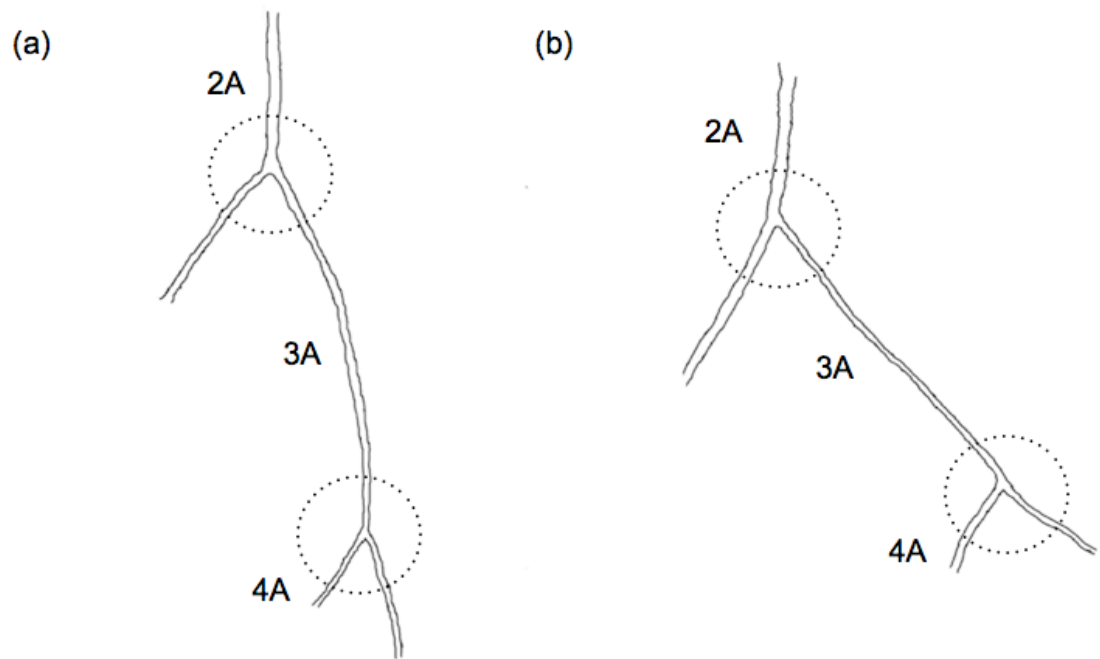


Figure 3.1. Gluteus maximus 2A to 4A arteriolar segments.

Representative tracings of CTRL (a) and PD (b) branching arteriolar segments within the GM demonstrating location of second-order arterioles (2A), third-order arterioles (3A) and fourth-order arterioles (3A). Data was collected from regions of interest at 2A-3A and 3A-4A bifurcations, and are indicated by dotted line. Representative tracings not to scale.

3.2.6. Skeletal muscle contractions

Contractions of the GM were evoked using electrical field stimulation (EFS). For this purpose, wire electrodes (90% Pt–10% Ir; diameter, 250 μM) were positioned in the superfusion solution on either side of the exposed muscle. Monophasic pulses (0.1 ms) were delivered at 10 V through a stimulus isolation unit (SIU5; Grass Technologies; Quincy, MA, USA) driven by a square wave stimulator (S48, Grass Technologies; Quincy, MA, USA). Our experiments and previous work has shown that this voltage elicits reproducible contractions of the GM and of arteriolar responses for the duration of an experiment (Jackson et al., 2010). In control experiments, addition of 10 μM *d*-tubocurarine (nicotinic cholinergic receptor antagonist) inhibited muscle contraction to EFS, confirming that muscle contraction was a result of motor nerve activation and not depolarization of skeletal muscle cells (Jackson et al., 2010).

3.2.6.1. Tetanic contraction and rapid onset vasodilation

A brief maximal tetanic contraction at 100 Hz was used to evoke ROV in each experimental group. Arteriolar dilations were evoked across stimulus train durations of 200, 400, and 800 ms with the order randomized within experiments. Arterioles consistently returned to the initial resting baseline with 2–3 minutes of recovery between contractions. As tissue displacement occurred during tetanic contraction, diameter was measured preceding each stimulus (resting baseline) and immediately following contraction with a delay of ~2-3 seconds that reflected the time the muscle is contracted and field of view out of focus, and the time required to refocus the field of view. Blood flow was calculated from the frames captured under fluorescent excitation prior each

stimulus and immediately following contraction. Diameter of a 2A was tracked per second throughout the video prior and after stimulation to demonstrate a typical arteriolar response to tetanic muscle contraction (Figure 3.2).

3.2.6.2. Rhythmic contraction and steady-state vasodilation

As the nature of vasodilatation can vary with the pattern of muscle fiber activation (Murrant, 2005; VanTeeffelen & Segal, 2000), vasomotor responses to 30 seconds of rhythmic contractions at 2 and 8 Hz (in randomized order) were also evaluated in each experimental group. Stimulation at these frequencies evokes unfused twitch contractions (Bearden et al., 2004). Following each 30 second period of rhythmic twitch contractions, resting baseline was re-established consistently within 5 minutes. Arteriolar diameter was determined preceding contractile activity, throughout the contraction period, and following contractions throughout recovery to demonstrate the typical arteriolar response to rhythmic contraction (Figure 3.3). Blood flow was calculated from the frames captured under fluorescent excitation prior each stimulus and immediately following 30 seconds of rhythmic contraction.

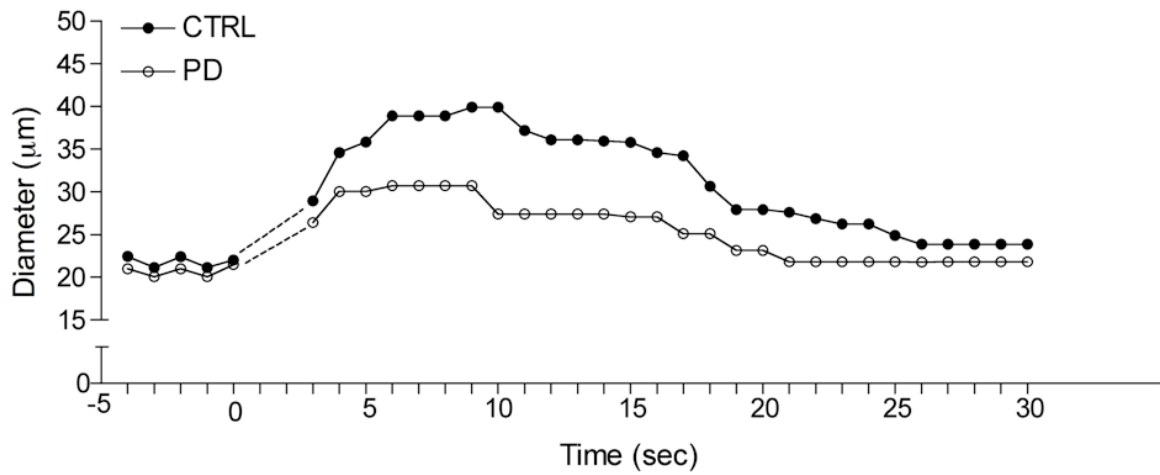


Figure 3.2. Second order arteriolar response to 800 ms tetanic contraction.

Representative 2A diameter tracing of ROV in response to 800 ms single tetanic contraction in CTRL and PD. Dotted line indicates where diameter cannot be resolved due to displacement of the tissue at contraction and refocusing of the field of view. CTRL, control; PD, pre-diabetic.

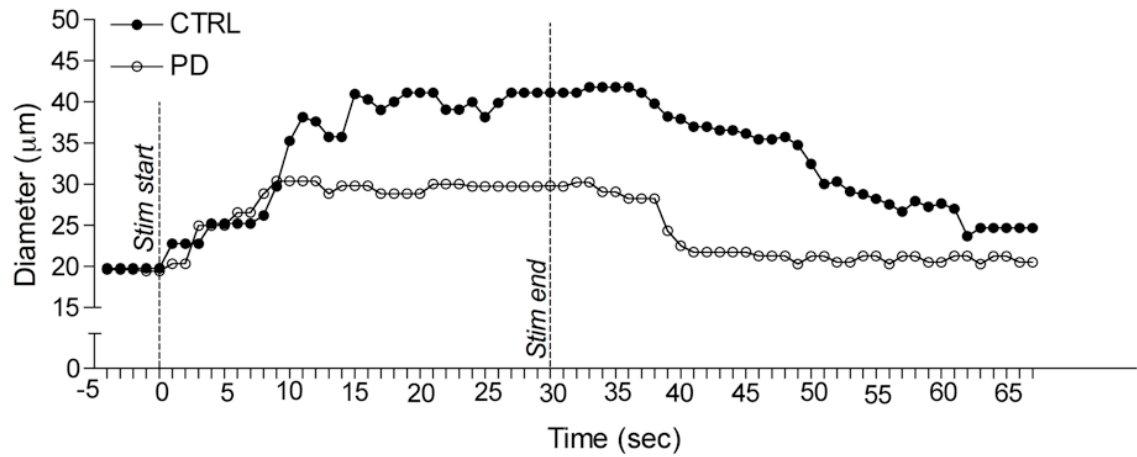


Figure 3.3. Second order arteriolar response to 8 Hz rhythmic contraction.

Representative 2A diameter tracing of steady-state vasodilation in response to 30 seconds of 8 Hz contraction in CTRL and PD. CTRL, control; PD, pre-diabetic.

3.2.7. Arteriolar and hemodynamic measurements

Diameters of 2A, 3A and 4A arterioles were measured manually off-line using ImageJ software (1.43 u; National Institute of Health, Bethesda, MD, USA). Fluorescent frames of 2A and 3A videos were analyzed to determine centerline RBC velocity (V_{RBC}), using the RBC “streak-length method” described in Al-Khazraji *et al.* 2012 (Al-Khazraji *et al.*, 2012). Red blood cell velocity and calculated blood flow were not determined in 4A, as making consistent measurements of ‘centerline streaks’ in 4A (using proper measurement criteria) without moving the field of view and interrupting RCB imaging at 2A and 3A was not possible. Based on exposure times of 10-15 ms for frame rates of 15-17 fps, fluorescent RBCs formed streaks in each frame. Single RBC velocities were calculated using the equation: $V_{RBC} = (RCB \text{ streak length} - RBC \text{ length}) / \text{exposure time}$. Mean velocity (V_m) was then calculated using the equation: $V_m = V_{RBC} / \text{velocity ratio}$. Because velocity ratio has been shown to vary with diameter (Al-Khazraji *et al.*, 2012), the following equation was used to calculate diameter-specific velocity ratios of the vessel the RBC streak is obtained from: $0.0071 \times D + 1.15$, where D is diameter. Blood flow was then calculated as $= \pi(D/2)^2 V_m$.

3.2.8. Statistical analyses and data presentation

Data were analyzed using SigmaStat (version 4, GraphPad Software Inc, La Jolla, CA, USA) and considered significantly different at $p < 0.05$. For ROV data (diameter and blood flow), comparisons of responses between CTRL and PD were made within each stimulus using unpaired t-tests with a Bonferroni correction (3 comparisons) to maintain total $p < 0.05$ over all comparisons. Linear regression was performed to evaluate the correlation between the duration of tetanic contraction and the magnitude of ROV for

each animal group. Slopes of the regression lines determined for responses at 200, 400 and 800 ms represented an index of the sensitivity of ROV responses for each animal group (Jackson et al., 2010). Slopes of these responses were compared between groups using an unpaired t-test. The effect of rhythmic contractions on diameter and blood flow between CTRL and PD was also determined for each stimulus frequency using unpaired t-tests with a Bonferroni correction (2 comparisons) to maintain total $p < 0.05$ over all comparisons. To determine the effect of arteriolar order and animal group on percent change of diameter following tetanic and rhythmic muscle contraction, a two-way analysis of variance was used, followed by Tukey's post-hoc comparison test to determine where differences were significant. Differences between CTRL and PD in tabular data were analyzed using unpaired t-tests. Summary data are presented as mean values \pm standard error, unless otherwise stated.

3.3. Results

3.3.1. Animal characteristics between CTRL and PD

Body mass and fasting blood glucose were approximately 2- and 2.4-fold greater in PD versus CTRL (Table 3.1, $p < 0.05$). Gluteus maximus dry/wet mass ratios were similar among groups (0.2 ± 0.02 g, Table 3.1).

Table 3.1. Body mass, fasting blood glucose and gluteus maximus dry/wet ratio for CTRL and PD.

	CTRL	PD
Body mass (g)	22 ± 0.3	41 ± 0.7*
Fasting blood glucose (mM/L)	5 ± 1	12 ± 1*
Dry/wet muscle mass ratio	0.2 ± 0.02	0.2 ± 0.02

Values are mean ± SEM. CTRL, control, n = 5-14; PD, pre-diabetic, n = 5-10.

* Different from CTRL, $p < 0.05$.

3.3.2. Baseline arteriolar diameter, hemodynamic characteristics and arteriolar O₂ responses of CTRL and PD

Baseline 2A, 3A, and 4A diameters and 2A and 3A blood flows were similar between CTRL and PD (Table 3.2). Arteriolar constriction in response to elevating PSS O₂ to 21% was also similar between groups for all arteriolar orders (Table 3.2).

3.3.3. Rapid onset vasodilation, blood flow and spatial arteriolar reactivity following single tetanic contractions

In PD, ROV (arteriolar diameter) responses to 200, 400, and 800 ms stimulations were attenuated by $45 \pm 8\%$, $53 \pm 8\%$, and $48 \pm 7\%$ respectively in 2A and $36 \pm 11\%$, $49 \pm 7\%$, and $53 \pm 7\%$ respectively in 3A; however, responses in 4A were attenuated only under 400 and 800 ms conditions by $49 \pm 7\%$ and $49 \pm 6\%$ respectively (Figure 3.4 a, b, c, $p < 0.05$). Blood flow responses in PD to 200, 400, and 800 ms stimulations were attenuated by $68 \pm 8\%$, $77 \pm 8\%$, and $81 \pm 6\%$ respectively in 2A. Responses in 3A were attenuated only following 400 and 800 ms stimulations by $60 \pm 11\%$ and $67 \pm 7\%$ respectively in PD versus CTRL (Figure 3.4 d and e, $p < 0.05$).

The slope of the regression line determined for mean peak vasodilatory responses across the range of contraction durations was interpreted as an index of the ROV sensitivity for each experimental group. There was a strong positive correlation between increasing contraction duration on diameter change in 2A, 3A and 4A for both groups; however, ROV sensitivity across arteriolar orders was blunted in PD (Figure 3.5, $p < 0.05$).

In an effort to compare spatial ROV reactivity across arteriolar branch orders, changes in diameter were normalized to respective baselines and presented as % diameter change. In CTRL, relative changes in diameter following 200 and 400 ms single tetanic contractions were greatest in 4A (Figure 3.6 a and b, $p < 0.05$). After 800 ms stimulation, CTRL 3A and 4A were equally reactive, where their responses were greater than CTRL 2A (Figure 3.6 c, $p < 0.05$). As expected, relative changes in diameter following 200, 400, and 800ms tetanic contraction were blunted at all arteriolar orders in PD versus CTRL (Figure 3.6, $p < 0.05$). However, in PD, greater ROV reactivity was only observed in 4A versus 2A, and only after 400 and 800 ms stimulations (Figure 3.6 b and c, $p < 0.05$).

Table 3.2. Gluteus maximus arteriolar baseline diameter, blood flow and responses to elevated O₂ (21%).

	2A		3A		4A	
	CTRL	PD	CTRL	PD	CTRL	PD
Diameter (μm)	19 ± 1	20 ± 1	14 ± 1	13 ± 1	8 ± 1	9 ± 1
Blood flow (nl/sec)	1 ± 0.1	1 ± 0.1	0.5 ± 0.07	0.4 ± 0.04	---	---
O ₂ response (μm)	-5 ± 1	-5 ± 1	-3 ± 1	-4 ± 1	-2.4 ± 0.2	-2.2 ± 0.2

Values are mean ± SEM. CTRL, control, n = 6-14; PD, pre-diabetic, n = 5-10.

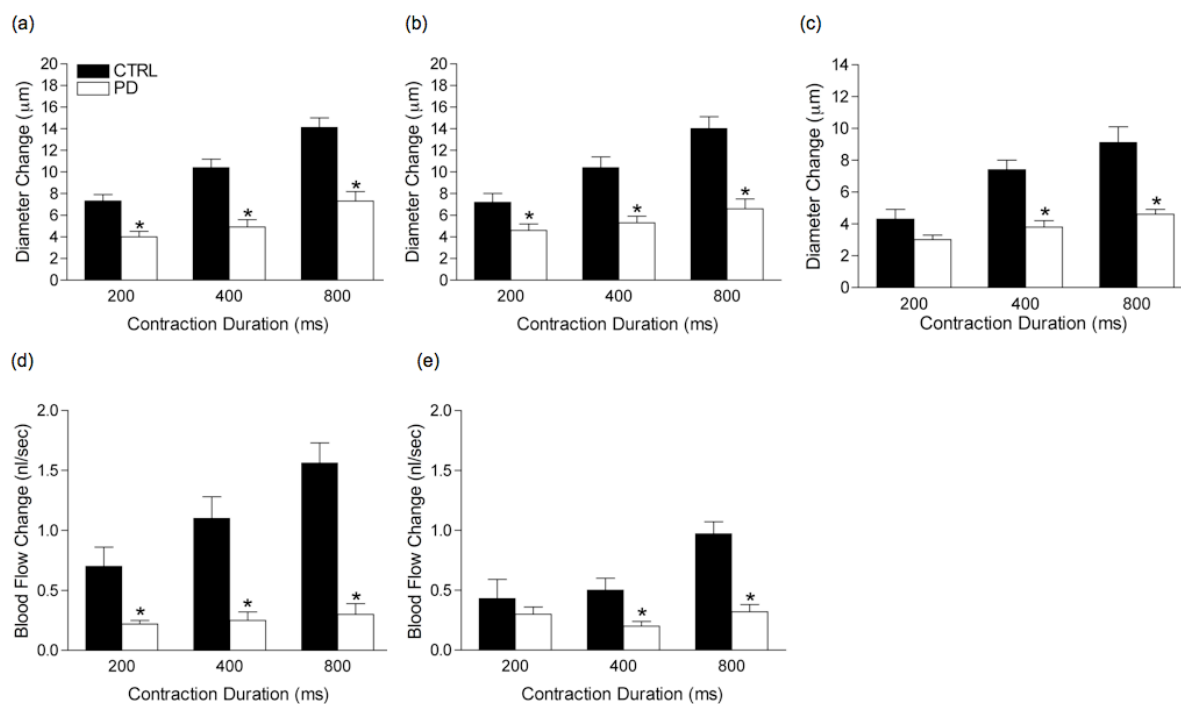


Figure 3.4. Rapid onset vasodilation and blood flow responses of arterioles following tetanic muscle contraction are blunted in PD.

Diameter changes of 2A (a), 3A (b) and 4A (c) following tetanic contraction. Rapid onset vasodilation was blunted in PD (n=5-10) compared to CTRL (n=6-14) following 200, 400 and 800 ms contractions for 2A and 3A, and 400 and 800 ms contractions for 4A. The magnitude of blood flow responses of 2A (d) and 3A (e) following tetanic contractions was also attenuated in PD (n=5-7) compared to CTRL (n=6-7). * Different vs. CTRL, $p < 0.05$. CTRL, control; PD, pre-diabetic.

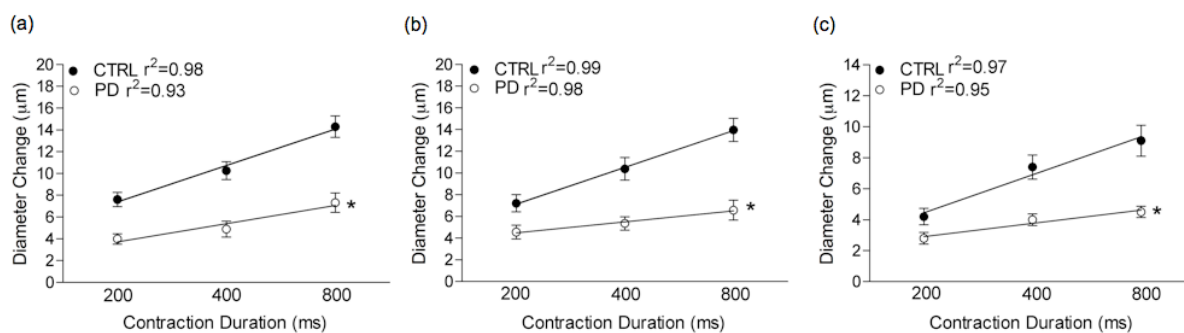


Figure 3.5. Sensitivity of ROV responses to increasing tetanic contraction duration.

For both CTRL and PD, duration of tetanic muscle contraction correlated with the increase in 2A (a), 3A (b) and 4A (c) diameter. The slope of diameter change to increasing tetanic contraction duration was less steep in PD (n = 5-10) compared to CTRL (6-14), demonstrating a decreased sensitivity to increasing duration of tetanic contraction. * Slope different from CTRL, $p < 0.05$. CTRL, control; PD, pre-diabetic.

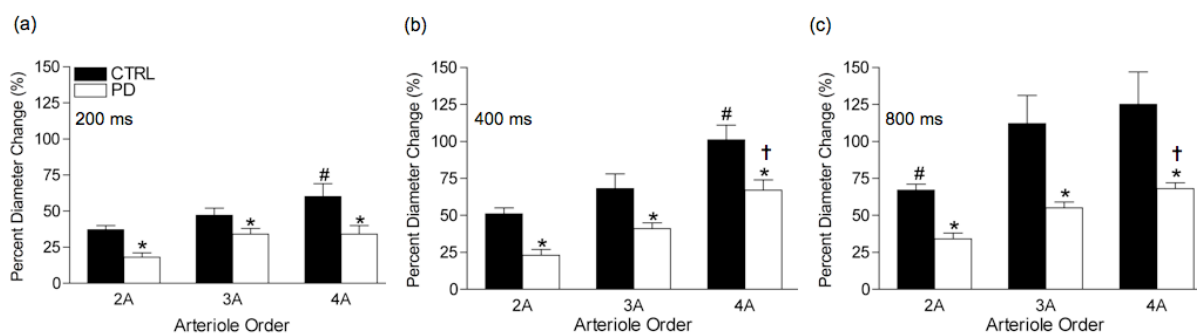


Figure 3.6. Percent diameter change of ROV at arteriolar orders.

Percent change in diameter following brief 200 ms (a), 400 ms (b) and 800 ms (c) tetanic contractions. Across the range of tetanic contractions, the percent change in diameter was attenuated in PD (n= 5-10) compared to CTRL (n=6-14) at 2A, 3A and 4A. Within CTRL, the relative change of 4A diameter was greater compared to 2A and 3A following 200 ms and 400 ms tetanic contractions. Following 800 ms tetanic contraction, the relative change of both 3A and 4A ROV responses were greater than 2A. In contrast, arteriolar order did not have an effect on PD ROV responses following 200 ms tetanic contraction. Following 400 ms and 800 ms tetanic contractions, the relative change in 4A diameter was only greater than 2A. * Different vs. CTRL, $p < 0.05$; # different vs. responses of other arterioles within CTRL, $p < 0.05$; † Different vs. 2A response within PD, $p < 0.05$. CTRL, control; PD, pre-diabetic.

3.3.4. Steady-state vasodilation, blood flow and spatial arteriolar reactivity following rhythmic contractions

In PD, the steady-state arteriolar response to 30 seconds of 2 and 8 Hz rhythmic contractions was attenuated by $45 \pm 9\%$ and $33 \pm 8\%$ respectively in 2A, $48 \pm 6\%$ and $47 \pm 7\%$ respectively in 3A, and $38 \pm 8\%$ and $53 \pm 9\%$ respectively in 4A (Figure 3.7 a, b and c, $p < 0.05$).

Although steady-state blood flow responses in 2A to 2 Hz stimulation were similar between groups, the steady-state blood flow response in 2A to 8 Hz stimulation was attenuated by $61 \pm 9\%$ in PD. In 3A, steady-state blood flow responses were blunted following 2 and 8 Hz stimulation by $70 \pm 7\%$ and $71 \pm 8\%$ respectively (Figure 3.7 d and e, $p < 0.05$).

In an effort to compare spatial reactivity to rhythmic contractions across arteriolar branch orders changes in diameters were normalized to respective baselines and presented as % diameter change. In CTRL, relative changes in diameter following 2 Hz rhythmic contractions were greatest in 3A and 4A (Figure 3.8 a, $p < 0.05$) and reactivity to 8 Hz stimulation was greatest in 4A (Figure 3.8 b, $p < 0.05$). As expected, relative changes in diameter following 2 and 8 Hz rhythmic contractions were blunted at all arteriolar orders in PD versus CTRL (Figure 3.8, $p < 0.05$). In PD, greater reactivity was observed in 4A versus 2A and 3A under 2 Hz stimulation (Figure 3.8 a, $p < 0.05$), but there were no differences among arteriolar orders with 8 Hz stimulation (Figure 3.8 b).

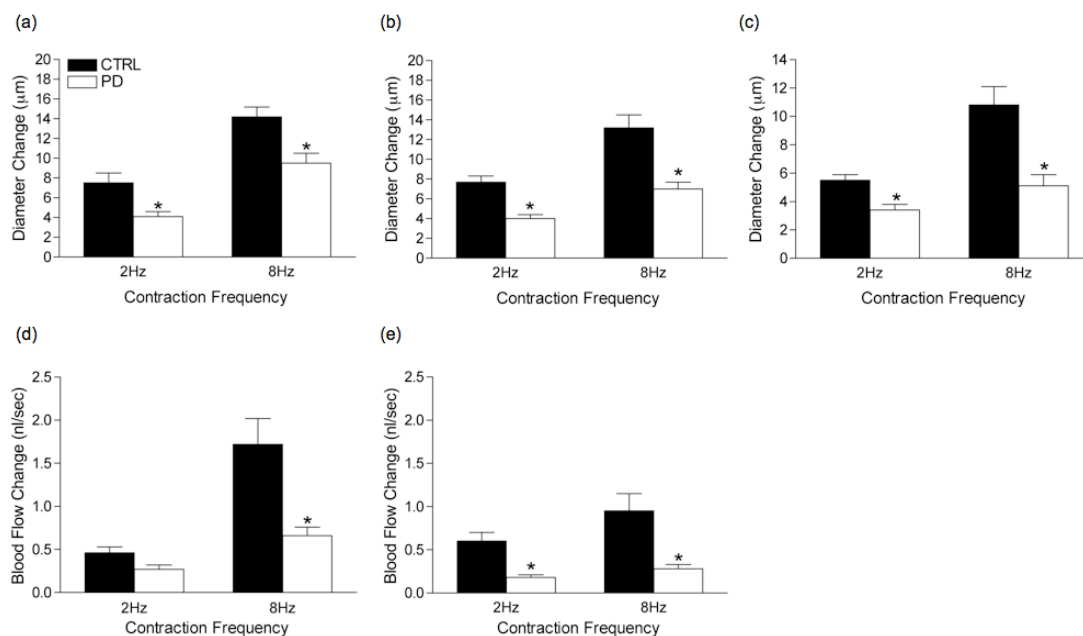


Figure 3.7. Arteriolar dilation and blood flow responses are compromised in PD following rhythmic contraction.

Diameter change of 2A (a), 3A (b) and 4A (c) following 30 seconds of rhythmic contraction. The magnitude of dilation was blunted in PD (n = 5-10) compared to CTRL (n = 5-14) following 2 Hz and 8 Hz rhythmic contractions. 2A (d) and 3A (e) blood flow changes in response to steady-state contraction were also blunted in PD (n = 5-6) compared to CTRL (n = 5-6). * Different vs. CTRL, $p < 0.05$. CTRL, control; PD, pre-diabetic.

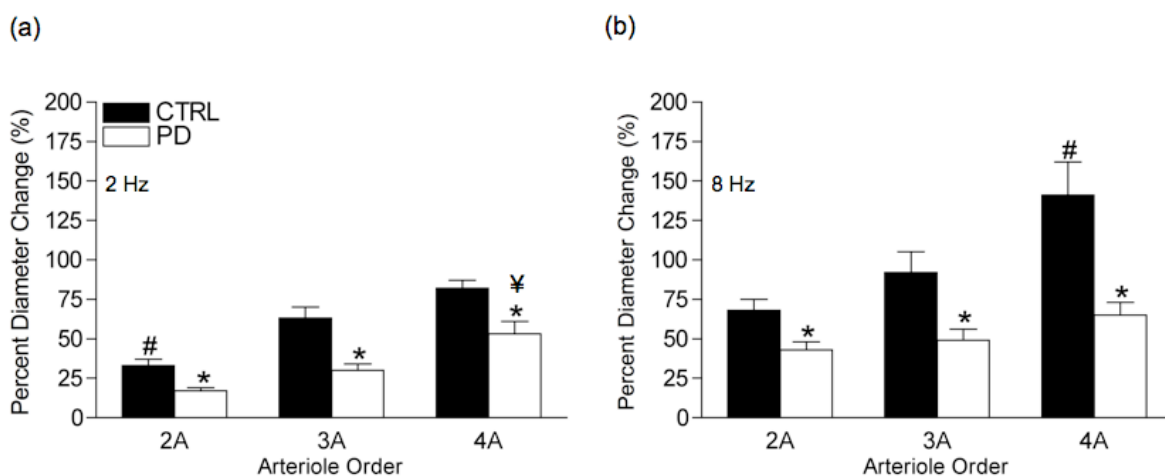


Figure 3.8. Percent diameter change to rhythmic contraction at arteriolar orders.

Percent change in diameter following 30 seconds of 2 Hz (a) and 8 Hz (b) rhythmic contractions. Following 2 and 8 Hz contractions, the percent change in diameter was blunted at 2A, 3A and 4A in PD (n=5-10) compared to CTRL (n=5-14). Within groups, dilatory responses to 2 Hz contraction elicited greater responses at 3A and 4A compared to 2A for CTRL, and greater responses of 4A compared to 3A and 2A for PD. 8 Hz contraction elicited a greater vasodilatory response at 4A compared to 2A and 3A in CTRL. In contrast, the magnitude of PD vasodilatory responses following 8 Hz contraction did not differ between 2A, 3A and 4A. * Different vs. CTRL $p < 0.05$; # different vs. responses of other arterioles within CTRL, $p < 0.05$; ¥ different vs. responses of other arterioles within PD, $p < 0.05$. CTRL, control; PD, pre-diabetic.

3.4. Discussion

Using a novel pre-diabetic murine model (i.e., The Pound Mouse) and an innovative experimental approach, we investigated whether pre-diabetes may modify arteriolar responses to skeletal muscle contraction in branching arteriolar networks. For the first time, we report that pre-diabetes leads to attenuation of vasodilation and blood flow responses in branching arterioles by up to 50% and 80% respectively following single tetanic and rhythmic muscle contraction. Furthermore, as predicted, we observed that the greatest decrements in contraction-evoked vasodilation in pre-diabetes occur in distal versus proximal arterioles.

3.4.1. Pre-diabetes modifies arteriolar responses to muscle contraction

3.4.1.1. Rapid onset vasodilation and blood flow

A rapid increase in blood flow to active muscle fibers is a key determinant of work/exercise tolerance. Upon the initiation of muscle contraction in humans, ROV has been shown to occur almost instantaneously (i.e., within the first few cardiac cycles), eliciting an immediate increase in muscle blood flow (Tschakovsky et al., 2004, Kirby, Carlson, Markwald, Voyles & Dinneno, 2007, Corcondilas, Koroxenidis & Shepherd, 1964, Carlson et al., 2008, Tschakovsky and Sheriff, 2004, Casey and Joyner, 2012). The robust increase in muscle blood flow during ROV serves to initiate a rest-to-exercise transition, such that blood flow can thereafter be maintained at a steady-state level proportional to metabolic demand. In contrast to sustained or repeated muscle contraction, single brief tetanic contraction elicits ROV too quickly to be a result of the accumulation of vasoactive metabolites (Wunsch et al., 2000). Recently, however, studies

using the hamster cremaster muscle have confirmed that the production of both potassium and adenosine occurs rapidly enough following initial contraction to contribute to rapid onset vasodilation (Armstrong et al., 2007, Ross, Mihok & Murrant, 2013). Additionally, cell-to-cell coupling via gap junction channels provides an electrical pathway for rapid coordination of smooth muscle cell relaxation that ascends arteriolar networks (i.e., from terminal to proximal arterioles), known as ascending conducted vasodilation. Ascending conducted vasodilation occurs in normal healthy skeletal muscle microvessels and is necessary for blood flow to quickly meet metabolic demand (Segal, 2005). With the use of animal models, direct observation of the resistance vasculature in cremaster, check pouch retractor and GM muscles have also demonstrated ROV to single brief whole muscle and muscle fiber bundle contraction (VanTeeffelen and Segal, 2006, Jackson et al., 2010, Mihok and Murrant, 2004, Armstrong et al., 2007).

To date, there is a dearth of human and animal studies investigating ROV responses in pre-diabetes. In fact, the only other study to address ROV in metabolic disease was conducted by Blain *et al.* in 2012, where they examined ROV responses (presented as changes in brachial artery vascular conductance) in obese humans (Blain et al., 2012). Our data are in congruence with Blain *et al.*, where they reported deficits in ROV of approximately 40% in obese versus lean adults. As well, they reported that impairments in ROV became greater with increased workloads in obese subjects, which coincides with our finding that the sensitivity of ROV to increasing contraction duration was decreased in PD versus CTRL. The correspondence between data presented by Blain *et al.* in obese humans and the current findings in The Pound Mouse highlights the translational merit of our experimental preparation.

In the current study we used a novel approach to directly measure blood flow at 2A and 3A, where we observed that attenuated ROV in PD resulted in notable decreases in functional hyperemia. The global blunting of ROV and blood flow responses in PD suggests that overall arteriolar network resistance is augmented in this model. Interestingly however, despite observing contraction-duration-dependent increases in arteriolar dilation in PD (Figure 3.4 a, b and c, and Figure 3.5), increasing contraction duration did not result in concomitant increases in arteriolar blood flow (Figure 3.4 d and e). These data suggest that upstream arteriolar resistance restrains overall network blood flow in this model. Such modifications in overall network resistance/control in pre-diabetes may be due to alterations in mechanisms that coordinate (e.g., connexin 40, calcium-activated potassium channels, inward rectifying potassium channels) or restrict (e.g. heightened sympathetic nervous system activity) ascending conducted dilation (Haug & Segal, 2005; Twynstra, Ruiz & Murrant, 2012; VanTeeffelen & Segal, 2003). Indeed, all of the aforementioned modifications in vascular “machinery” may be modified in metabolic diseases (Haddock et al., 2001; Novielli et al., 2012; Young, Hill, Wiehler, Triggle, & Reid, 2008).

3.4.1.2. Steady-state vasodilation and blood flow

In contrast to brief tetanic contraction, sustained rhythmic muscle contraction elicits a gradual and steady-state dilatory response, where muscle blood flow increases and is maintained based on the metabolic demands of the tissue (R. B. Armstrong & Laughlin, 1985; Bockman, 1983; Mohrman & Regal, 1988). This sustained vasodilatory effect is understood to occur due to accumulation of vasoactive metabolites (Clifford & Hellsten, 2004). In the current study, rhythmic contractions elicited robust vasodilation in

2A, 3A and 4A in CTRL; however, responses were attenuated up to 53% in PD. Additionally, 2A and 3A blood flow responses were blunted up to 71% in PD. Although there is a paucity of studies investigating steady-state vasodilation in pre-diabetes, the effects of overt type 2 diabetes on steady-state vasodilation have been relatively well defined and are in congruence with our findings. For example, in type 2 diabetic humans, leg blood flow and forearm capillary perfusion was reported to be attenuated up to 65% following steady-state exercise (Kingwell et al., 2003; Menon et al., 1992; Womack et al., 2009), effects that likely contribute to impaired exercise capacity in this cohort (Seyoum, Estacio, Berhanu, & Schrier, 2006). Decrements in steady-state vasodilation noted in the current study may be due to attenuated nitric oxide-mediated vasodilation (Lesniewski et al., 2008) and/or augmented sympathetic regulation (Novielli et al., 2012), both of which have been reported using *in vitro* and *in vivo* rodent models of pre-diabetes. Indeed, impairments in endothelial function (Bakker, Eringa, Sipkema, & van Hinsbergh, 2009; McVeigh et al., 1992) can contribute to attenuated vasodilatory responses to muscle contraction in overt type 2 diabetes (Kingwell et al., 2003). However, the impact of pre-diabetes on endothelial function remains equivocal (likely due to experimental and temporal differences across studies), as it has been reported that acetylcholine-mediated vascular responses are conserved in these conditions (Ellis et al., 2010; Lesniewski et al., 2008; Novielli et al., 2012). These data highlight the need for future studies which aim to elucidate the mechanisms involved in arteriolar dysregulation in early pre-diabetes.

3.4.2. Pre-diabetes modifies spatial reactivity of vasodilation during contraction

As discussed above, arteriolar responses to muscle contraction are coordinated such that dilation ascends the network from terminal to proximal arterioles. Along the same line, the magnitude of arteriolar vasodilation differs based on the location of the arteriole within the microvascular network where proportional increases in vasodilation are greatest in smaller distal arterioles compared to proximal larger arterioles (Dodd & Johnson, 1991; Marshall & Tandon, 1984; VanTeeffelen & Segal, 2006).

Building on the aforementioned notion of spatially-dependent arteriolar reactivity during muscle contraction, in CTRL we observed that proportional changes in arteriolar dilation increase with contraction duration and frequency, as well as increasing arteriolar order (Figures 3.6 and 3.8). However, as hypothesized, the magnitude and spatially-dependent pattern of arteriolar vasodilation was minimized in PD, where there was little to no delineation between responses across arteriolar orders in either contraction paradigm. As such, the reactivity of terminal arterioles (4A) seems to be affected most in PD, which would have the greatest impact on RBC distribution to capillaries (Pries et al., 1989). Our data are in support of an earlier human study where contraction-evoked increases in forearm capillary blood flow were impaired in type 2 diabetics, despite having normal brachial artery blood flow responses (Womack et al., 2009).

3.5. Conclusions

In conclusion, our data illustrate network-wide arteriolar dysregulation in response to muscle contraction in pre-diabetes, a condition that results in severe decrements in functional hyperemia. Arteriolar dysregulation observed in PD was demonstrated as compromised ROV and steady state vasodilation, as well as blood flow responses, following single tetanic and sustained rhythmic contractions in branching 2A, 3A and 4A. Furthermore, spatial reactivity of PD vasodilatory responses was disrupted compared to CTRL, where distal arterioles were most affected. These data may suggest a spatial and temporal progression of diabetic vascular disease, where impairments in distal microvasculature likely occur before dysfunction can be detected in large conduit vessels. For future studies, the current data underscore the importance of studying multiple levels of the skeletal muscle microcirculation in an effort to elucidate the mechanisms involved in early pre-diabetic arteriolar dysregulation during muscle contraction.

3.6. Acknowledgements

This work was supported by the by Natural Sciences and Engineering Research Council of Canada (NSERC) R4218A03; DNJ.

3.7. References

- Al-Khazraji, B. K., Novielli, N. M., Goldman, D., Medeiros, P. J., & Jackson, D. N. (2012). A simple "streak length method" for quantifying and characterizing red blood cell velocity profiles and blood flow in rat skeletal muscle arterioles. *Microcirculation*, *19*(4), 327-335.
- Anderson, K. M., & Faber, J. E. (1991). Differential sensitivity of arteriolar alpha 1- and alpha 2-adrenoceptor constriction to metabolic inhibition during rat skeletal muscle contraction. *Circ Res*, *69*(1), 174-184.
- Armstrong, M. L., Dua, A. K., & Murrant, C. L. (2007). Potassium initiates vasodilatation induced by a single skeletal muscle contraction in hamster cremaster muscle. *J Physiol*, *581*(Pt 2), 841-852.
- Armstrong, R. B., & Laughlin, M. H. (1985). Rat muscle blood flows during high-speed locomotion. *J Appl Physiol*, *59*(4), 1322-1328.
- Bakker, W., Eringa, E. C., Sipkema, P., & van Hinsbergh, V. W. (2009). Endothelial dysfunction and diabetes: roles of hyperglycemia, impaired insulin signaling and obesity. *Cell Tissue Res*, *335*(1), 165-189.
- Bearden, S. E., Payne, G. W., Chisty, A., & Segal, S. S. (2004). Arteriolar network architecture and vasomotor function with ageing in mouse gluteus maximus muscle. *J Physiol*, *561*(Pt 2), 535-545.
- Blain, G. M., Limberg, J. K., Mortensen, G. F., & Schrage, W. G. (2012). Rapid onset vasodilatation is blunted in obese humans. *Acta Physiol (Oxf)*, *205*(1), 103-112.
- Bockman, E. L. (1983). Blood flow and oxygen consumption in active soleus and gracilis muscles in cats. *Am J Physiol*, *244*(4), H546-551.
- Canadian Diabetes Association. 2011. Diabetes: Canada at the tipping point, Charting a new path. Toronto, Ontario, Canada.

- Carlson, R. E., Kirby, B. S., Voyles, W. F., & Dinunno, F. A. (2008). Evidence for impaired skeletal muscle contraction-induced rapid vasodilation in aging humans. *Am J Physiol Heart Circ Physiol*, *294*(4), H1963-1970.
- Casey, D. P., & Joyner, M. J. (2012). Influence of alpha-adrenergic vasoconstriction on the blunted skeletal muscle contraction-induced rapid vasodilation with aging. *J Appl Physiol*, *113*(8), 1201-1212.
- Chen, Y. L., Wolin, M. S., & Messina, E. J. (1996). Evidence for cGMP mediation of skeletal muscle arteriolar dilation to lactate. *J Appl Physiol*, *81*(1), 349-354.
- Chin-Yee, I. H., Gray-Statchuk, L., Milkovich, S., & Ellis, C. G. (2009). Transfusion of stored red blood cells adhere in the rat microvasculature. *Transfusion*, *49*(11), 2304-2310.
- Clifford, P. S., & Hellsten, Y. (2004). Vasodilatory mechanisms in contracting skeletal muscle. *J Appl Physiol*, *97*(1), 393-403.
- Corcondilas, A., Koroxenidis, G. T., & Shepherd, J. T. (1964). Effect of a Brief Contraction of Forearm Muscles on Forearm Blood Flow. *J Appl Physiol*, *19*, 142-146.
- Davis, M. J., Hill, M. A., & Kuo, L. (2008). Local regulation of microvascular perfusion. In R. F. Tuma, W. N. Duran & L. Klaus (Eds.), *The Handbook of Physiology: Microcirculation* (2 ed., pp. 161-284). Boston: Elsevier/Academic Press.
- DeFronzo, R. A., & Abdul-Ghani, M. (2011). Assessment and treatment of cardiovascular risk in prediabetes: impaired glucose tolerance and impaired fasting glucose. *Am J Cardiol*, *108*(3 Suppl), 3B-24B.
- Disease Control and Prevention. 2011. National Diabetes fact sheet: national estimates and general information on diabetes and prediabetes in the United States, 2011. In: U.S. Department of health and human services. Atlanta, Georgia, USA.

- Dodd, L. R., & Johnson, P. C. (1991). Diameter changes in arteriolar networks of contracting skeletal muscle. *Am J Physiol*, 260(3 Pt 2), H662-670.
- Ellis, C. G., Goldman, D., Hanson, M., Stephenson, A. H., Milkovich, S., Benlamri, A., et al. (2010). Defects in oxygen supply to skeletal muscle of prediabetic ZDF rats. *Am J Physiol Heart Circ Physiol*, 298(6), H1661-1670.
- Faeh, D., William, J., Yerly, P., Paccaud, F., & Bovet, P. (2007). Diabetes and pre-diabetes are associated with cardiovascular risk factors and carotid/femoral intima-media thickness independently of markers of insulin resistance and adiposity. *Cardiovasc Diabetol*, 6, 32.
- Frisbee, J. C. (2003). Impaired skeletal muscle perfusion in obese Zucker rats. *Am J Physiol Regul Integr Comp Physiol*, 285(5), R1124-1134.
- Frisbee, J. C. (2004). Enhanced arteriolar alpha-adrenergic constriction impairs dilator responses and skeletal muscle perfusion in obese Zucker rats. *J Appl Physiol*, 97(2), 764-772.
- Fuglevand AJ & Segal SS. 1997. Simulation of motor unit recruitment and microvascular unit perfusion: spatial considerations. *J Appl Physiol*, 83, 1223-1234.
- Gorzynski, R. J., Klitzman, B., & Duling, B.R. 1978. Interrelations between contracting striated muscle and precapillary microvessels. *Am J Physiol*, 235(5):H494-504.
- Gupta, A. K., Ravussin, E., Johannsen, D. L., Stull, A. J., Cefalu, W. T., & Johnson, W. D. (2012). Endothelial Dysfunction: An Early Cardiovascular Risk Marker in Asymptomatic Obese Individuals with Prediabetes. *Br J Med Med Res*, 2(3), 413-423.
- Haddock, R. E., Grayson, T. H., Morris, M. J., Howitt, L., Chadha, P. S., & Sandow, S. L. (2001). Diet-induced obesity impairs endothelium-derived hyperpolarization via altered potassium channel signaling mechanisms. *PLoS One*, 6(1), e16423.

- Haffner, S. M., Stern, M. P., Hazuda, H. P., Mitchell, B. D., & Patterson, J. K. (1990). Cardiovascular risk factors in confirmed prediabetic individuals. Does the clock for coronary heart disease start ticking before the onset of clinical diabetes? *JAMA*, *263*(21), 2893-2898.
- Haug, S. J., & Segal, S. S. (2005). Sympathetic neural inhibition of conducted vasodilatation along hamster feed arteries: complementary effects of alpha1- and alpha2-adrenoreceptor activation. *J Physiol*, *563*(Pt 2), 541-555.
- Jackson, D. N., Moore, A. W., & Segal, S. S. (2010). Blunting of rapid onset vasodilatation and blood flow restriction in arterioles of exercising skeletal muscle with ageing in male mice. *J Physiol*, *588*(Pt 12), 2269-2282.
- Janssen, I., Heymsfield, S. B., Wang, Z. M., & Ross, R. (2000). Skeletal muscle mass and distribution in 468 men and women aged 18-88 yr. *J Appl Physiol*, *89*(1), 81-88.
- Karpoff, L., Vinet, A., Schuster, I., Oudot, C., Goret, L., Dazat, M., et al. (2009). Abnormal vascular reactivity at rest and exercise in obese boys. *Eur J Clin Invest*, *39*(2), 94-102.
- Kim, S. H., & Reaven, G. M. (2008a). Insulin resistance and hyperinsulinemia: you can't have one without the other. *Diabetes Care*, *31*(7), 1433-1438.
- Kim, S. H., & Reaven, G. M. (2008b). Isolated impaired fasting glucose and peripheral insulin sensitivity: not a simple relationship. *Diabetes Care*, *31*(2), 347-352.
- Kingwell, B. A., Formosa, M., Muhlmann, M., Bradley, S. J., & McConell, G. K. (2003). Type 2 diabetic individuals have impaired leg blood flow responses to exercise: role of endothelium-dependent vasodilation. *Diabetes Care*, *26*(3), 899-904.
- Kirby, B. S., Carlson, R. E., Markwald, R. R., Voyles, W. F., & Dinunno, F. A. (2007). Mechanical influences on skeletal muscle vascular tone in humans: insight into contraction-induced rapid vasodilatation. *J Physiol*, *583*(Pt 3), 861-874.

- Laughlin MH & Armstrong RB. 1982. Muscular blood flow distribution patterns as a function of running speed in rats. *Am J Physiol* **243**, H296-306
- Lesniewski, L. A., Donato, A. J., Behnke, B. J., Woodman, C. R., Laughlin, M. H., Ray, C. A., et al. (2008). Decreased NO signaling leads to enhanced vasoconstrictor responsiveness in skeletal muscle arterioles of the ZDF rat prior to overt diabetes and hypertension. *Am J Physiol Heart Circ Physiol*, *294*(4), H1840-1850.
- MacAnaney, O., Reilly, H., O'Shea, D., Egana, M., & Green, S. (2011). Effect of type 2 diabetes on the dynamic response characteristics of leg vascular conductance during exercise. *Diab Vasc Dis Res*, *8*(1), 12-21.
- Marshall, J. M., & Tandon, H. C. (1984). Direct observations of muscle arterioles and venules following contraction of skeletal muscle fibres in the rat. *J Physiol*, *350*, 447-459.
- McVeigh, G. E., Brennan, G. M., Johnston, G. D., McDermott, B. J., McGrath, L. T., Henry, W. R., et al. (1992). Impaired endothelium-dependent and independent vasodilation in patients with type 2 (non-insulin-dependent) diabetes mellitus. *Diabetologia*, *35*(8), 771-776.
- Menon, R. K., Grace, A. A., Burgoyne, W., Fonseca, V. A., James, I. M., & Dandona, P. (1992). Muscle blood flow in diabetes mellitus. Evidence of abnormality after exercise. *Diabetes Care*, *15*(5), 693-695.
- Mihok, M. L., & Murrant, C. L. (2004). Rapid biphasic arteriolar dilations induced by skeletal muscle contraction are dependent on stimulation characteristics. *Can J Physiol Pharmacol*, *82*(4), 282-287.
- Mohrman, D. E., & Regal, R. R. (1988). Relation of blood flow to VO₂, PO₂, and PCO₂ in dog gastrocnemius muscle. *Am J Physiol*, *255*(5 Pt 2), H1004-1010.
- Moore, A. W., Jackson, W. F., & Segal, S. S. (2010). Regional heterogeneity of alpha-adrenoreceptor subtypes in arteriolar networks of mouse skeletal muscle. *J Physiol*, *588*(Pt 21), 4261-4274.

- Murrant, C. L. (2005). Stimulation characteristics that determine arteriolar dilation in skeletal muscle. *Am J Physiol Regul Integr Comp Physiol*, 289(2), R505-R513.
- Murrant, C. L., & Sarelius, I. H. (2002). Multiple dilator pathways in skeletal muscle contraction-induced arteriolar dilations. *Am J Physiol Regul Integr Comp Physiol*, 282(4), R969-978.
- Musa, M. G., Torrens, C., & Clough, G. F. 2014. The microvasculature: a target for nutritional programming and later risk of cardio-metabolic disease. *Acta Physiol (Oxf)*, 212, 31-45.
- Novielli, N. M., Al-Khazraji, B. K., Medeiros, P. J., Goldman, D., & Jackson, D. N. (2012). Pre-Diabetes Augments Neuropeptide Y(1)- and alpha(1)-Receptor Control of Basal Hindlimb Vascular Tone in Young ZDF Rats. *PLoS One*, 7(10), e46659.
- Padilla, D. J., McDonough, P., Behnke, B. J., Kano, Y., Hageman, K. S., Musch, T. I., & Poole, D. C. 2006a. Effects of Type II diabetes on muscle microvascular oxygen pressures. *Respir Physiol Neurobiol*. 14; 156 (2):187-95.
- Padilla, D. J., McDonough, P., Behnke, B. J., Kano, Y., Hageman, K. S., Musch, T. I., & Poole, D. C. 2006b. Effects of Type II diabetes on capillary hemodynamics in skeletal muscle. *Am J Physiol Heart Circ Physiol*, 291(5): H2439-44.
- Pries, A. R., Ley, K., Claassen, M., & Gaetgens, P. (1989). Red cell distribution at microvascular bifurcations. *Microvasc Res*, 38(1), 81-101.
- Ross, G. A., Mihok, M. L., & Murrant, C. L. 2013. Extracellular adenosine initiates rapid arteriolar vasodilation induced by a single skeletal muscle contraction in hamster cremaster muscle. *Acta Physiol (Oxf)*, 208(1):74-87.
- Schaefer, C., Biermann, T., Schroeder, M., Fuhrhop, I., Niemeier, A., Ruther, W., et al. (2010). Early microvascular complications of prediabetes in mice with impaired glucose tolerance and dyslipidemia. *Acta Diabetol*, 47(Suppl 1), 19-27.

- Segal, S. S. (2005). Regulation of blood flow in the microcirculation. *Microcirculation*, 12(1), 33-45.
- Seyoum, B., Estacio, R. O., Berhanu, P., & Schrier, R. W. (2006). Exercise capacity is a predictor of cardiovascular events in patients with type 2 diabetes mellitus. *Diab Vasc Dis Res*, 3(3), 197-201.
- Shin, J. Y., Lee, H. R., & Lee, D. C. (2011). Increased arterial stiffness in healthy subjects with high-normal glucose levels and in subjects with pre-diabetes. *Cardiovasc Diabetol*, 10, 30.
- Silveira, L. R., Pereira-Da-Silva, L., Juel, C., & Hellsten, Y. (2003). Formation of hydrogen peroxide and nitric oxide in rat skeletal muscle cells during contractions. *Free Radic Biol Med*, 35(5), 455-464.
- Soma, L. R. (1983). Anesthetic and analgesic considerations in the experimental animal. *Ann N Y Acad Sci*, 406, 32-47.
- Tschakovsky, M. E., Rogers, A. M., Pyke, K. E., Saunders, N. R., Glenn, N., Lee, S. J., et al. (2004). Immediate exercise hyperemia in humans is contraction intensity dependent: evidence for rapid vasodilation. *J Appl Physiol*, 96(2), 639-644.
- Tschakovsky, M. E., & Sheriff, D. D. (2004). Immediate exercise hyperemia: contributions of the muscle pump vs. rapid vasodilation. *J Appl Physiol*, 97(2), 739-747.
- Twynstra, J., Ruiz, D. A. & Murrant, C. L. (2012). Functional coordination of the spread of vasodilations through skeletal muscle microvasculature: implications for blood flow control. *Acta Physiol*, 206: 229-241.
- VanTeeffelen, J. W., & Segal, S. S. (2000). Effect of motor unit recruitment on functional vasodilatation in hamster retractor muscle. *J Physiol*, 524 Pt 1, 267-278.

- VanTeeffelen, J. W., & Segal, S. S. (2003). Interaction between sympathetic nerve activation and muscle fibre contraction in resistance vessels of hamster retractor muscle. *J Physiol*, 550(Pt 2), 563-574.
- VanTeeffelen, J. W., & Segal, S. S. (2006). Rapid dilation of arterioles with single contraction of hamster skeletal muscle. *Am J Physiol Heart Circ Physiol*, 290(1), H119-127.
- Vinet, A., Karpoff, L., Walther, G., Startun, A., Obert, P., Goret, L., et al. (2011). Vascular reactivity at rest and during exercise in middle-aged obese men: effects of short-term, low-intensity, exercise training. *Int J Obes (Lond)*, 35(6), 820-828.
- Womack, L., Peters, D., Barrett, E. J., Kaul, S., Price, W., & Lindner, J. R. (2009). Abnormal skeletal muscle capillary recruitment during exercise in patients with type 2 diabetes mellitus and microvascular complications. *J Am Coll Cardiol*, 53(23), 2175-2183.
- Wunsch, S. A., Muller-Delp, J., & Delp, M. D. (2000). Time course of vasodilatory responses in skeletal muscle arterioles: role in hyperemia at onset of exercise. *Am J Physiol Heart Circ Physiol*, 279(4), H1715-1723.
- Young, E. J., Hill, M. A., Wiehler, W. B., Triggle, C. R., & Reid, J. J. (2008). Reduced EDHF responses and connexin activity in mesenteric arteries from the insulin-resistant obese Zucker rat. *Diabetologia*, 51(5), 872-881.

Chapter 4 : Y1- and α 1-adrenergic receptor activation attenuates contraction-evoked vasodilation in branching skeletal muscle arterioles of young pre-diabetic mice

4.1. Introduction

Peripheral vascular complications associated with type 2 diabetes (Creager, Luscher, Cosentino, & Beckman, 2003) are initiated well before manifestation of chronic diabetic disease, but rather in the pre-diabetic state (Ellis et al., 2010; Gupta et al., 2012; Lesniewski et al., 2008; Milman & Crandall, 2011; Reusch, Bridenstine, & Regensteiner, 2013; Schaefer et al., 2010; Tooke & Goh, 1999; Wiernsperger, 1994). Pre-diabetes is a condition of elevated blood glucose, insulin resistance, and hyperinsulinemia that occurs prior to pancreatic β -cell failure and overt type 2 diabetes. Notably, the severity of insulin resistance and elevated plasma insulin has been shown to correlate with the degree of microvascular dysfunction (Jaap, Hammersley, Shore, & Tooke, 1994; Jaap, Shore, & Tooke, 1997). The microvasculature plays an integral role in regulating blood flow distribution throughout tissues, especially skeletal muscle due to its dynamic range of metabolic demand. In exercising muscle, the arterioles play an integral role in modulating tissue blood flow and thereby directing flow to capillary units supplying active skeletal muscle fibers (Fuglevand & Segal, 1997). Most recently, our group has demonstrated blunted rapid onset vasodilation (ROV) and blood flow to brief tetanic contraction, as well as blunted steady-state vasodilation and blood flow to sustained rhythmic twitch contractions in skeletal muscle arterioles of pre-diabetic mice (currently in review). However the mechanisms governing decrements in contraction-evoked arteriolar responses in pre-diabetes are not well defined.

Only few studies have investigated potential contributors to skeletal muscle microvascular dysregulation in pre-diabetes. Earlier studies using isolated arterioles from

the hindlimb of young pre-diabetic Zucker Diabetic Fatty (ZDF) rats demonstrated that vasoconstrictor responsiveness to norepinephrine and endothelin-1 is enhanced (Lesniewski et al., 2008). Additionally, previous work from our group has demonstrated heightened sympathetic neuropeptide Y1 receptor (NPY Y1R) and alpha 1 adrenergic receptor (α 1R) modulation of resting vascular tone in the hindlimb of pre-diabetic ZDF rats, where Y1R, α 1R and NPY expression were upregulated in hindlimb tissue (Novielli et al., 2012). Collectively, these findings provide evidence of elevated sympathetic nervous system influences on vascular control in pre-diabetes. Elevated sympathetic vascular control in pre-diabetes may compromise arteriolar modulation of skeletal muscle blood flow, which may play a role in the reductions of capillary red blood cell supply rate, velocity and oxygen saturations observed in skeletal muscle of pre-diabetic ZDF rats (Ellis et al., 2010). Until recently however, no studies have directly assayed arteriolar function (*in vivo*) throughout microvascular networks in response to skeletal muscle contraction in pre-diabetes.

Physical activity is accompanied by increases in sympathetic nerve activity (SNA), which modifies the distribution of cardiac output to sites of highest metabolic activity (Rowell, 1993). Heightened SNA can limit skeletal muscle arteriolar vasodilation and concomitant increases in blood flow (Thomas & Segal, 2004). In contracting skeletal muscle, direct observations of arterioles confirm that vasodilatory and hyperemic responses override elevated sympathetic activation (Remensnyder, Mitchell, & Sarnoff, 1962). The ability to overcome this effect is termed ‘functional sympatholysis’, which enables arterioles to increase blood flow to active muscle fibers (Strandell & Shepherd, 1967). With the use of microneurography and quantification of plasma catecholamines,

studies have demonstrated that hyperinsulinemia, a result of insulin resistance in pre-diabetes, correlates with elevated SNA (Anderson, Balon, Hoffman, Sinkey, & Mark, 1992; Berne, Fagius, Pollare, & Hjendahl, 1992; DeFronzo & Ferrannini, 1991; Scherrer & Sartori, 1997). As such, heightened sympathetic activity to skeletal muscle arterioles and decreased sympatholysis may contribute to decrements in contraction-evoked vasodilation and hyperemic responses in pre-diabetes (McDaid, Monaghan, Parker, Hayes, & Allen, 1994).

In conditions where heightened SNA is commonly observed, such as aging and the metabolic syndrome, impaired skeletal muscle blood flow has been attributed to enhanced sympathetic α -adrenergic modulation of the vasculature (Casey & Joyner, 2012; Frisbee, 2004; Jackson, Moore, & Segal, 2010). However, it is well established that sympathetic NPY activation of Y1R plays an important role in skeletal muscle microvascular regulation (Jackson, Milne, Noble, & Shoemaker, 2005; Jackson, Noble, & Shoemaker, 2004), where our previous work has demonstrated that heightened Y1R and α 1R modulation of vascular conductance and blood flow in pre-diabetic ZDF rats under resting conditions (Novielli et al., 2012). Thus, it is possible that such conditions may be responsible for blunted contraction-evoked arteriolar responses we recently observed in skeletal muscle (gluteus maximus; GM) arteriolar networks of pre-diabetic mice.

A recent study by our group investigated the effect of pre-diabetes on arteriolar function in contracting skeletal muscle. In pre-diabetic mice, we demonstrated that arteriolar dilation and blood flow responses of GM microvasculature were compromised following both tetanic and steady-state muscle contraction. Evaluating contraction-

evoked vasodilatory responses at multiple locations in the GM arteriolar network revealed that relative changes in arteriolar diameter (relative to baseline diameter) were not identical throughout the network. We found that smaller distal arterioles of healthy control mice dilated to a greater extent compared to larger proximal arterioles, a result corresponding with previous work characterizing vasomotor responses of skeletal muscle microvasculature (Dodd and Johnson, 1991, Marshall and Tandon, 1984, VanTeeffelen and Segal, 2006). In contrast, spatially-dependent arteriolar reactivity to muscle contraction was disrupted in pre-diabetic mice. Interestingly, distal arterioles have been shown to overcome sympatholysis more readily than upstream vasculature (Dodd and Johnson, 1991). Under conditions of heightened sympathetic vascular modulation however, as we have previously demonstrated in pre-diabetic rats, sympatholysis may occur to a lesser extent, and lead to impairments in distinct spatial arteriolar responses to muscle contraction.

Therefore, the purpose of this study was to investigate if attenuated arteriolar dilation in response to brief tetanic and sustained rhythmic muscle contraction in pre-diabetes is a result of heightened arteriolar sympathetic Y1R and α 1R activation. We hypothesized that Y1R and α 1R blockade would restore contraction-evoked arteriolar dilatory responses in pre-diabetic mice (PD) to levels observed in control mice (CTRL). We also hypothesized that impaired spatially-dependent arteriolar responses would be restored via sympathetic Y1R and α 1R blockade. Additionally, we hypothesized that arteriolar vasoconstrictor reactivity to sympathetic agonists phenylephrine (PE) and NPY would be greater in PD compared to CTRL.

4.2. Materials and methods

All animal procedures were approved by the Council on Animal Care at The University of Western Ontario (protocol number: 2008-066). All invasive procedures were performed under α -chloralose and urethane anesthetic, and all efforts were made to minimize animal suffering.

4.2.1. Animal care and use

Experiments were performed on male C57BL/6NCrI (7-8 weeks old) and Pound mice (C57BL/6NCrI-*Lepr*^{db-lb}/CrI, 7-8 weeks old). The Pound mouse is a model of pre-diabetes, where these mice exhibit a novel mutation *Lepr*^{db-lb} in the leptin receptor gene. When fed a high fat diet (i.e. Purina 5008 chow), mice become obese by 7 weeks of age, exhibiting hyperinsulinemia, and elevated blood glucose, characteristic of the pre-diabetic condition in humans (Kim & Reaven, 2008a, 2008b). As these mice are of C57BLK6 background, the male C57BLK6 mouse served as the control group in this study. Mice were housed in animal care facilities in a temperature (24°C) and light (12 hour cycle)-controlled room and allowed to eat and drink water *ad libitum*. All mice were obtained from Charles River Laboratories (Saint-Constant, QC, Canada) and housed in animal care facilities for at least one week after arrival prior experimentation. Mice were weighted prior to each experiment. Upon completion of experimental procedures each day, the anesthetized mouse was euthanized with an overdose of α -chloralose and urethane cocktail mix (intraperitoneal injection), and cervical dislocation.

4.2.2. Measurement of serum insulin levels and blood glucose levels

Blood insulin values were not determined from mice used in this study, as the amount of blood sample necessary to perform the appropriate assay exceeds the ethical amount without sacrificing the animal as specified by the Animal Care Council. Blood insulin values were instead obtained from animal characteristic data reported by Charles River. Fasting blood glucose was sampled from animals no later than two days before experimentation. Mice were fasted for eight hours and blood glucose was sampled from the tail vein (~10 μ l) and determined with a Bayer Contour[®] blood glucose analyzer (Bayer, Toronto, ON, Canada).

4.2.3. Anesthesia and skeletal muscle preparation

Using an intraperitoneal injection, the mouse was anesthetized with a cocktail of α -chloralose (50 mg/kg) and urethane (750 mg/kg), which was supplemented throughout the experiment as needed. This anesthetic was ideal for these experiments as it leaves autonomic, cardiovascular and respiratory function intact (Soma, 1983). Internal body temperature was monitored via a rectal temperature probe and maintained at 37°C with the use of a heating platform. Surgical procedures were viewed through a stereomicroscope. The neck and backside of the mouse was shaved to remove excess fur. The mouse was placed on its back and a mid-neck incision was made. A tracheal cannula (PE-60) was introduced to facilitate spontaneous breathing. The neck opening was then closed using wound clips (Autoclip 9 mm, Becton Dickinson, Franklin Lakes, NJ, USA). The mouse was then placed in the prone position on the heated platform to prepare the GM for intravital microscopy. Under stereomicroscopic guidance the GM muscle was cut

from its origin along the spine and along its rostral and caudal borders (Bearden, Payne, Chisty, & Segal, 2004; Jackson et al., 2010). With great care taken to preserve its neurovascular supply, the muscle flap was gently reflected away from the mouse, spread evenly onto a transparent Sylgard® (Sylgard 184; Dow Corning, Midland, MI, USA) pedestal to approximate *in situ* dimensions and pinned to secure edges. The exposed tissue was superfused continuously (4–5 mL/min) with bicarbonate-buffered physiological salt solution (PSS, 35°C at tissue, pH 7.4) of the following composition (mM): NaCl 137, KCl 4.7, MgSO₄ 1.2, CaCl₂ 2, NaHCO₃ 18, and equilibrated with 5% CO₂/95% N₂.

4.2.4. Intravital video microscopy

Upon completion of microsurgical procedures, the preparation was transferred to the stage of the intravital microscope (Olympus BX51, Olympus, Tokyo, Japan). The preparation was equilibrated with PSS for ~30 minutes. Microvessels were observed under Kohler illumination using a long working distance condenser (NA = 0.80) and long working distance water immersion objectives (Olympus UMPlanFW: 10× NA = 0.30) with illumination from a 100-Watt halogen light source. To enhance contrast of the RBC column, a 450-nm / 20-nm band-pass filter (450BP20; Omega Optical, Brattleboro, VT, USA) was placed in the light path. The optical image was coupled to a front-illuminated interline CCD camera (Qimaging Rolera E=MC²™, Qimaging®, Surrey, BC, Canada) and viewed / stored to a hard drive using specialized imaging software (MetaMorph® 7.6, Molecular Devices Inc., Sunnyvale, CA, USA). Bright-field video (.tiff) images were collected (15-17 fps) under Kohler bright-field illumination for off-line analysis of RBC column diameters.

Bifurcations at second-order arterioles (2A) to third-order (3A) arterioles and 3A to fourth order arterioles (4A) were chosen for study, as these resistance microvessels are positioned to control the distribution of blood flow within the GM and to the capillaries (Bearden et al., 2004; Pries, Ley, Claassen, & Gaehtgens, 1989). One arteriolar tree (2A-4A) was studied per animal. Following equilibration, a video of the resting (baseline) diameter was taken. Arterioles were then tested for oxygen sensitivity by elevating superfusate O₂ from 0% to 21% (5% CO₂, balance N₂) for 5-8 minutes to elicit vasoconstriction. Equilibration with 5% CO₂-95% N₂ was restored for the duration of experimental procedures. Changes in arteriolar diameter were evaluated in response to brief maximal tetanic contractions at 100 Hz as well as 30 seconds of rhythmic muscle contractions (see Skeletal muscle contractions). For these experiments, each muscle preparation underwent both contraction protocols with the order randomized across experiments. At the end of each day's procedures, maximum arteriolar diameter was recorded by adding sodium nitroprusside (SNP, 10 μM) to the superfusate (Bearden et al., 2004; Jackson et al., 2010; VanTeeffelen & Segal, 2006). It was determined however, that vasodilation of PD 2A and 3A to SNP was less than that of CTRL arterioles. Responses of PD arterioles to SNP were then tested with 100nM BIBP3226 (Y1R antagonist) and 100nM prazosin (α1R antagonist) within the PSS. This was performed in an effort to determine if enhanced arteriolar sympathetic receptor activation contributes to decreased vasodilation to SNP in PD.

4.2.5. Skeletal muscle contractions

Contractions of the GM were evoked using electrical field stimulation (EFS). For this purpose, wire electrodes (90% Pt-10% Ir; diameter, 250 μm) were positioned in the

superfusion solution on either side of the exposed muscle. Monophasic pulses (0.1 ms) were delivered at 10 V through a stimulus isolation unit (SIU5; Grass Technologies; Quincy, MA, USA) driven by a square wave stimulator (S48, Grass). Our experiments and previous work has shown that this voltage elicited reproducible contractions of the GM and of arteriolar responses for the duration of an experiment (Jackson et al., 2010).

4.2.5.1. Tetanic contraction and rapid onset vasodilation

A brief maximal tetanic contraction at 100 Hz was used to evoke ROV in each experimental group. Arteriolar dilations were evoked for stimulus train durations of 400 and 800 ms, with the order randomized across experiments. The arteriole consistently returned to the initial resting baseline with 2–3 minutes of recovery between contractions. As tissue displacement occurred during tetanic contraction, diameter was measured preceding each stimulus (resting baseline) and immediately following contraction with a delay of ~2 seconds that reflected the time the muscle is contracted and field of view out of focus, and the time required to refocus the field of view.

4.2.5.2. Rhythmic contraction and steady-state vasodilation

As the nature of vasodilatation can vary with the pattern of muscle fiber activation (Murrant, 2005; VanTeeffelen & Segal, 2000), vasomotor responses to 30 seconds of rhythmic contractions at 2 and 8Hz (in randomized order) were also evaluated in each experimental group. Stimulation at these frequencies evoked unfused twitch contractions (Bearden et al., 2004). Following each 30-second period of rhythmic twitch contractions, resting baseline was re-established consistently within 5 minutes. Arteriolar diameter was determined preceding contractile activity and following contraction period.

4.2.6. Muscle contraction experimental conditions

Arteriolar vasodilatory responses to tetanic and rhythmic contraction were first evaluated under control conditions, where PSS was superfused over the GM. Upon establishing differences in vasodilatory responses between CTRL and PD, we sought to determine whether this difference was attributed to alterations in peripheral sympathetic Y1R and α 1R arteriolar activation. In an effort to recover PD dilatory responses to those of CTRL, i) Y1R, ii) α 1R and iii) Y1R+ α 1R were blocked using BIBP3226 (100nM) and prazosin (100nM) (TOCRIS, Bristol, United Kingdom). Concentrations did not affect resting baseline diameter. Sympathetic antagonist concentrations used were determined based on the ability to reduce arteriolar constriction elicited by supersusion of 10^{-8} M NPY and 10^{-5} M PE (data not shown). In a similar fashion, experiments were performed in CTRL to blunt contraction-evoked arteriolar vasodilation to responses similar to PD. Sympathetic i) Y1R, ii) α 1R and iii) Y1R+ α 1R were activated using neuropeptide Y (100pM) and PE (10nM). Agonist concentrations were determined from concentrations eliciting low arteriolar reactivity, while blunting vasodilatory responses to skeletal muscle contraction. Agents were added to superfusion solution to working concentrations and allowed to equilibrate with the tissue, having little effect on resting baseline arteriolar diameter. The order of drug perturbations per animal group was performed in random order.

4.2.7. Arteriolar reactivity to sympathetic receptor agonists

Vasoconstrictor responses of CTRL and PD 2A, 3A and 4A to sympathetic Y1R and α 1R agonists NPY (Y1R agonist, 10^{-13} - 10^{-8} M) and PE (α 1R agonist, 10^{-9} - 10^{-5} M) were investigated. The order of NPY and PE perturbations were performed in random

order for each experiment, where resting diameter was allowed to recover in between each set of drug perturbations. Baseline diameter prior to the addition of drug to PSS was recorded. At each concentration of NPY or PE, arteriolar diameter was allowed to equilibrate for 5 minutes and a video was recorded before the next increment in drug dose. Working concentrations of drugs were prepared fresh on day of experiment, and diluted in PSS. Arteriolar vasoconstrictor responses were determined from the difference between measures taken prior drug addition to the PSS (baseline diameter) and at each drug concentration.

4.2.8. Statistical analyses and data presentation

Data were analyzed using Sigmastat (Systat Software Inc, San Jose, CA, USA) and differences were accepted as significantly different at $p < 0.05$. In order to compare the effect of sympathetic antagonists on PD arteriolar responses to GM tetanic and steady-state contractions, one way analysis of variance within each stimulus level was performed using a Dunnett post test to compare all conditions to the CTRL condition. In order to compare the effect of sympathetic agonists on CTRL arteriolar responses to GM tetanic and steady-state contractions, one way analysis of variance within each stimulus level was performed using a Dunnett post test to compare all conditions to the PD condition. To determine the effect of arteriolar order on percent change of diameter following tetanic and rhythmic muscle contraction, a one-way analysis of variance was used within each condition (i.e., CTRL, PD, PD BIBP3226, PD prazosin and PD BIBP3226+prazosin) followed by Tukey's post-hoc comparison test. Differences between CTRL and PD responses within each concentration of NPY or PE were compared using unpaired t-tests. Tabular data was also analyzed using unpaired t-tests.

Summary data are presented as mean values \pm standard error (S.E.), unless otherwise stated.

4.3. Results

4.3.1. Characteristics of control and pre-diabetic mice

Body mass and measured fasting blood glucose were greater for PD (42 ± 1 g, 12 ± 1 mmol/L) compared to CTRL (23 ± 1 g, 6 ± 1 mmol/L., $p < 0.05$). Additionally, reported blood insulin levels were also elevated in PD (~ 120 ng/mL) compared to CTRL (< 10 ng/mL, Charles River Laboratories, 2006).

4.3.2. Baseline arteriolar diameter, O₂ response and vasodilatory response to sodium nitroprusside in control and pre-diabetic mice

Baseline 2A, 3A, and 4A diameters were similar between CTRL and PD (Table 4.1). Arteriolar constriction in response to elevating PSS O₂ to 21% was also similar between groups for all arteriolar orders (Table 4.1). Maximal arteriolar diameter elicited by 10 μ M SNP was decreased by $20 \pm 3\%$ and $24 \pm 4\%$ in PD 2A and 3A respectively, *versus* CTRL (Table 4.2, $p < 0.05$). Maximal dilation at 4A was similar between groups. Upon adding both sympathetic antagonists BIBP3226 (100 nM) and prazosin (100 nM) to 10 μ M SNP superfusion solution, maximal vasodilatory responses of PD 2A and 3A were no longer different than CTRL arteriolar responses to SNP (Table 4.2).

Table 4.1. Gluteus maximus arteriolar baseline diameter and responses to elevated O₂ (21%).

	2A		3A		4A	
	CTRL	PD	CTRL	PD	CTRL	PD
Baseline diameter (μm)	21 ± 1	22 ± 1	12 ± 1	13 ± 1	7 ± 1	7 ± 1
O ₂ response (μm)	-6 ± 1	-5 ± 1	-3 ± 1	-4 ± 1	-2.4 ± 0.2	-2.2 ± 0.2

Baseline values were recorded under control conditions (superfusate equilibrated with 5% CO₂-95% N₂). O₂ response indicates the change in diameter in response to elevating superfusate O₂ from 0 to 21%. Values are mean ± SEM. CTRL, control, n = 6-13; PD, pre-diabetic, n = 5-12. * *p* < 0.05 versus CTRL.

Table 4.2. Maximal diameter responses of gluteus maximus arterioles to sodium nitroprusside with and without sympathetic receptor blockade (10 μ M).

	Maximal Dilation CTRL (SNP; 10 μ m)	Maximal Dilation PD (SNP; 10 μ m)	Maximal Dilation PD with sympathetic blockade (SNP; 10 μ m, and BIBP3226+prazosin; 100 μ m)
2A	41 \pm 1	33 \pm 1*	38 \pm 2
3A	29 \pm 1	22 \pm 1*	27 \pm 2
4A	18 \pm 1	17 \pm 1	19 \pm 1

Values are mean \pm SEM. CTRL, control, n = 6-13; PD, pre-diabetic, n = 3-12. * $p < 0.05$ versus CTRL.

4.3.3. Sympathetic receptor blockade and rapid onset vasodilation in pre-diabetic mice

Following 400 and 800 ms tetanic contractions, ROV responses of PD were blunted by $51 \pm 6\%$ and $47 \pm 6\%$ respectively in 2A, $52 \pm 6\%$ and $62 \pm 6\%$ respectively in 3A, and $58 \pm 9\%$ and $59 \pm 6\%$ respectively in 4A (Figure 4.1 a, b and c, $p < 0.05$). In response to 400 ms tetanic contraction, addition of BIBP3226 (Y1R antagonist), prazosin (α 1R antagonist) and BIBP3226 + prazosin to the superfusion solution caused ROV responses of 2A, 3A and 4A to increase such that responses were no longer different from CTRL (Figure 4.1 a, b, c). Following 800 ms tetanic contraction, dual sympathetic Y1R and α 1R blockade (BIBP3226 + prazosin) restored 2A ROV responses of PD to that of CTRL (Figure 4.1 a). Y1R blockade (BIBP3226) and α 1R blockade (prazosin) alone only partially recovered 2A ROV responses of PD (Figure 4.1 a, $p < 0.05$). For 3A, prazosin and BIBP3226+prazosin superfusion conditions increased ROV responses of PD to responses similar to CTRL (Figure 4.1 b); however, BIBP3226 partially recovered the attenuated vasodilatory response of PD (Figure 4.1 b, $p < 0.05$). Alternatively in 4A, BIBP3226 and BIBP3226+prazosin restored ROV to that of CTRL (Figure 4.1 c), where prazosin alone partially recovered the blunted response (Figure 4.1 c, $p < 0.05$).

4.3.4. Sympathetic receptor activation and rapid onset vasodilation in control mice

In addition to testing the effects of sympathetic receptor blockade on ROV in PD, we also tested the effects of sympathetic receptor activation on ROV in CTRL. Following both 400 and 800 ms tetanic contractions, addition of sympathetic agonists NPY (Y1R

agonist), PE (α 1R agonist) or NPY+PE to the superfusion solution decreased ROV responses of CTRL 2A, 3A and 4A to those of PD (Figure 4.2 a, b, c).

4.3.5. Sympathetic receptor blockade and spatial arteriolar reactivity in pre-diabetic mice in response to brief tetanic contraction

Spatial reactivity of ROV responses were investigated based on arteriolar order. Changes in diameter were normalized to respective baselines and presented as percent diameter change. As expected, relative ROV responses to 400 and 800 ms tetanic contractions were attenuated in PD at all arteriolar orders compared to CTRL. Superfusion of sympathetic antagonists restored relative increases in diameter, so they were no longer different from CTRL (Figure 4.3).

4.3.5.1. Effects of sympathetic receptor blockade on relative ROV responses of 2A, 3A and 4A following 400 ms tetanic contraction

In CTRL, relative increases in diameter were greatest in 4A versus 3A and 2A (Figure 4.3 a, $p < 0.05$). In PD, ROV reactivity was also greatest in 4A, but only in comparison to 2A (Figure 4.3 a, $p < 0.05$). In PD, BIBP3226 increased relative change in diameter of 4A specifically, so that 4A responses of PD were different from both 3A and 2A, as demonstrated in CTRL (Figure 4.3 a, $p < 0.05$). Prazosin also increased ROV reactivity; however, α 1R blockade increased both 3A and 4A responses compared to responses of 2A (Figure 4.3 a, $p < 0.05$). Similar to CTRL and effects of BIBP3226, combination Y1R and α 1R blockade (BIBP3226+prazosin condition) caused an increase in ROV reactivity in PD that was greatest at 4A compared to both 3A and 2A (Figure 4.3 a, $p < 0.05$).

4.3.5.2. Effects of sympathetic receptor blockade on relative ROV responses of 2A, 3A and 4A following 800ms tetanic contraction

In CTRL, 800ms tetanic contraction elicited robust increases in relative ROV responses that were greatest in 3A and 4A compared to 2A (Figure 4.3 b, $p < 0.05$). In PD, greatest ROV reactivity was only observed at 4A versus 3A and 2A, demonstrating compromised dilatory reactivity of 3A in PD (Figure 4.3 b, $p < 0.05$). BIBP3226 increased ROV responses of PD, so that relative increases in diameter were greatest in both 3A and 4A compared to 2A, as demonstrated in CTRL (Figure 4.3 b, $p < 0.05$). Both prazosin and BIBP3226+prazosin conditions caused increases in relative ROV reactivity of PD that was greatest in 4A versus 3A and 2A, illustrating a greater effect of sympathetic receptor blockade in most distal arterioles in PD (Figure 4.3 b, $p < 0.05$).

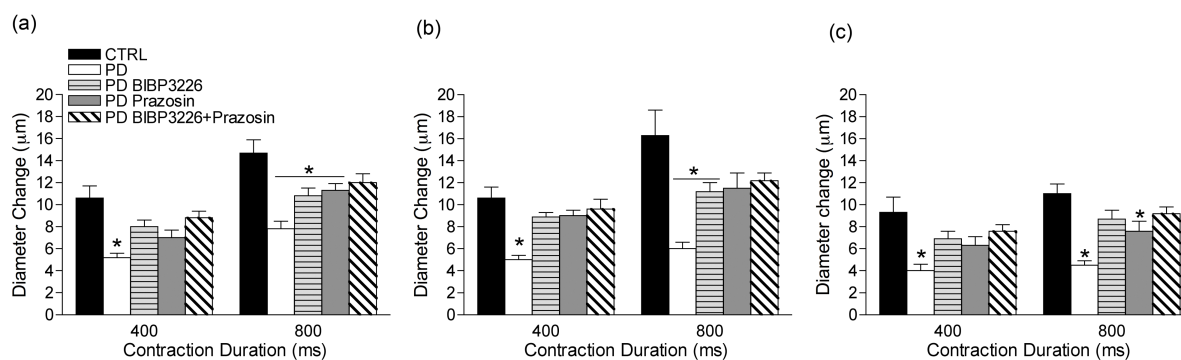


Figure 4.1. Sympathetic Y1R and α 1R blockade restores ROV in PD.

Data are ROV responses of 2A (a), 3A (b) and 4A (c) following brief tetanic contraction in CTRL (n=6-12) and PD (n=6-11). BIBP3226 (Y1R antagonist), prazosin (α 1R antagonist) and BIBP3226+prazosin (dual Y1R and α 1R blockade) were added to the superfusion of PD. Sympathetic receptor blockade enhanced ROV of PD to responses similar to CTRL. * different from CTRL, $p < 0.05$. CTRL, control; PD, pre-diabetic.

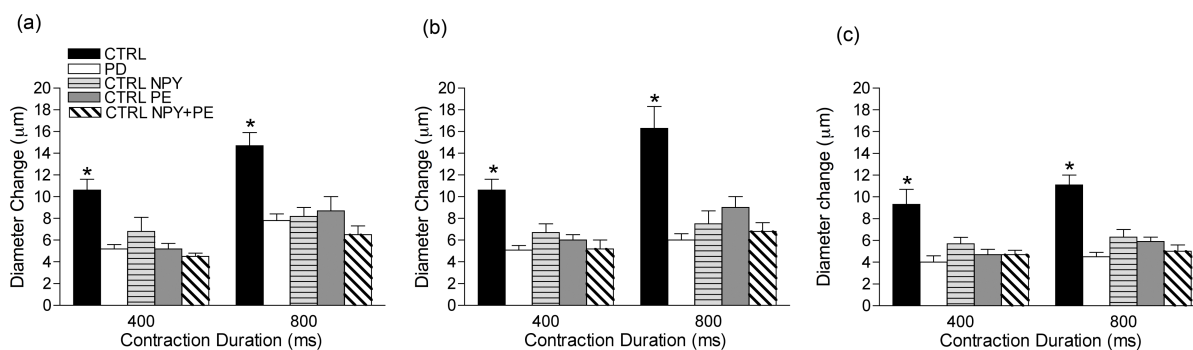


Figure 4.2. Sympathetic Y1R and α 1R activation attenuates ROV in CTRL.

ROV responses of 2A (a), 3A (b) and 4A (c) following brief tetanic contraction in CTRL (n=6-12) and PD (n=6-11). NPY (Y1R agonist), PE (α 1R agonist) and NPY+PE (dual Y1R and α 1R activation) were added to the superfusion of PD. Sympathetic receptor activation decreased ROV of CTRL to responses similar to PD. * different from PD, $p < 0.05$. CTRL, control; PD, pre-diabetic.

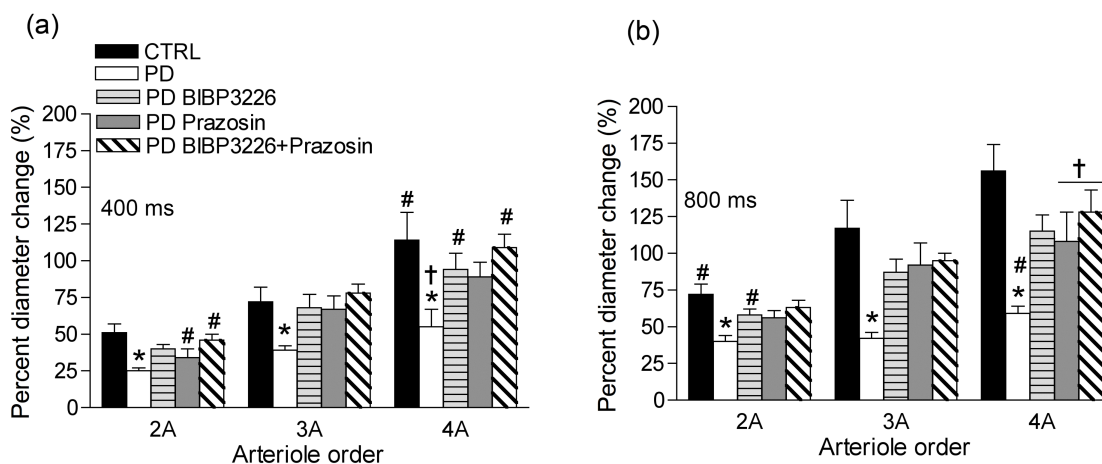


Figure 4.3. Effects of Y1R and α 1R blockade on arteriolar branch order ROV responses following tetanic contraction in PD.

Percent change in diameter following brief 400 ms (a) and 800 ms (b) tetanic contractions. Following both contractions, the percent change in diameter was attenuated in PD (n= 5-11) compared to CTRL (n=6-12) at 2A, 3A and 4A. Superfusion of sympathetic receptor antagonists BIBP3226 and prazosin caused increases in percent diameter change in PD, affecting relative changes of contraction-evoked dilation in distal arterioles the greatest. * Different vs. CTRL, $p < 0.05$; # different vs. responses of other arterioles within condition, $p < 0.05$; † Different vs. 2A response within condition, $p < 0.05$. CTRL, control; PD, pre-diabetic.

4.3.6. Sympathetic receptor blockade and steady-state vasodilation to rhythmic contraction in pre-diabetic mice

Following 2 and 8Hz rhythmic contractions, vasodilatory responses of PD were blunted by $46 \pm 9\%$ and $47 \pm 7\%$ respectively in 2A, $60 \pm 7\%$ and $44 \pm 9\%$ respectively in 3A, and $32 \pm 11\%$ and $53 \pm 11\%$ respectively in 4A (Figure 4.4 a, b and c, $p < 0.05$). In response to 2 Hz rhythmic contraction, vasodilation of 2A in PD was moderately increased with the addition of BIBP3226 to the superfusion (Figure 4.4 a, $p < 0.05$), however prazosin and BIBP3226 + prazosin superfusion conditions increased 2A vasodilation such that responses were no longer different from CTRL (Figure 4.4 a). For 3A, addition of BIBP3226+prazosin to the superfusion also caused an increase in vasodilatory responses to 2 Hz contraction in PD, where diameter change was no longer different to that of CTRL (Figure 4.4 b). BIBP3226 and prazosin alone caused a modest increase in diameter change, however responses were not similar to that of CTRL (Figure 4.4 b, $p < 0.05$). For 4A, superfusion of BIBP3226, prazosin and BIBP3226+prazosin increased PD vasodilatory responses to 2 Hz rhythmic contraction to that of CTRL (Figure 4.4 c). Following 8 Hz rhythmic contraction, vasodilation of PD 2A, 3A and 4A were increased with all three superfusion conditions (BIBP3226, prazosin, BIBP3226+prazosin), where diameter changes were similar to CTRL (Figure 4.4 a, b and c).

4.3.7. Sympathetic receptor activation and steady-state vasodilation to rhythmic contraction in control mice

Sympathetic Y1R and $\alpha 1R$ agonists were also added to the superfusion of CTRL experiments to attenuate CTRL arteriolar vasodilatory responses to rhythmic contractions

(Figure 4.5). Superfusion of NPY, PE and NPY+PE in CTRL decreased vasodilation of 2A, 3A and 4A to 2 and 8 Hz rhythmic contractions so that diameter changes were similar to PD (Figure 4.5 a, b and c).

4.3.8. Sympathetic receptor blockade and spatial arteriolar reactivity in pre-diabetic mice in response to rhythmic contraction

Spatial reactivity of steady-state vasodilatory responses to rhythmic contraction was also investigated based on arteriolar order. Changes in diameter were normalized to respective baselines and presented as percent diameter change. Following 2 Hz rhythmic contraction, relative diameter change was decreased in 2A and 3A of PD, where 4A responses were similar to CTRL. Sympathetic blockade of Y1R, α 1R, and both Y1R and α 1R increased relative dilatory responses of PD in 2A, however only dual Y1R and α 1R blockade increased relative vasodilatory reactivity of 3A (Figure 4.6 a). Following 8 Hz rhythmic contraction however, attenuated dilatory reactivity observed in PD was increased to dilatory responses similar to CTRL in all arterioles, for all conditions of sympathetic receptor blockade (Figure 4.6).

4.3.8.1. Effects of sympathetic receptor blockade on relative dilatory responses of 2A, 3A and 4A following 2 Hz rhythmic contraction

In CTRL, relative increases in diameter were greatest in 4A and 3A compared to 2A (Figure 4.6 a, $p < 0.05$). In PD, only 4A responses were greatest compared to 3A and 2A, demonstrating compromised dilatory reactivity of 3A in PD (Figure 4.6 a, $p < 0.05$). BIBP3226 increased relative vasodilatory responses of PD so that responses of both 4A and 3A were greater than 2A (Figure 4.6 a, $p < 0.05$). Prazosin elicited increases in 4A vasodilatory responses in PD, where relative increases in diameter were greater than 3A

and 2A (Figure 4.6 a, $p < 0.05$). Similar to the effects of BIBP3226 and responses of CTRL, dual Y1R and α 1R blockade increased relative dilatory responses of PD in both 3A and 4A compared to 2A (Figure 4.6 a, $p < 0.05$).

4.3.8.2. Effects of sympathetic receptor blockade on relative dilatory responses of 2A, 3A and 4A following 8Hz rhythmic contraction

In CTRL, relative increases in diameter were greatest in 4A compared to 2A (Figure 4.6 a, $p < 0.05$). Similarly in PD, although reduced in magnitude, 4A responses were greatest compared to 2A (Figure 4.6 b, $p < 0.05$). BIBP3226 and prazosin conditions increased the magnitude of relative dilatory responses of PD, where effects of Y1R and α 1R blockade evoked greatest relative changes in diameter in 4A versus 2A (Figure 4.6 b, $p < 0.05$). Dual sympathetic Y1R and α 1R blockade elicited increases in relative vasodilatory responses in PD that were greater in 3A and 4A compared to 2A, demonstrating a greater contribution of both Y1R and α 1R activation to attenuated dilatory responses of 3A and 4A in PD (Figure 4.6 b, $p < 0.05$).

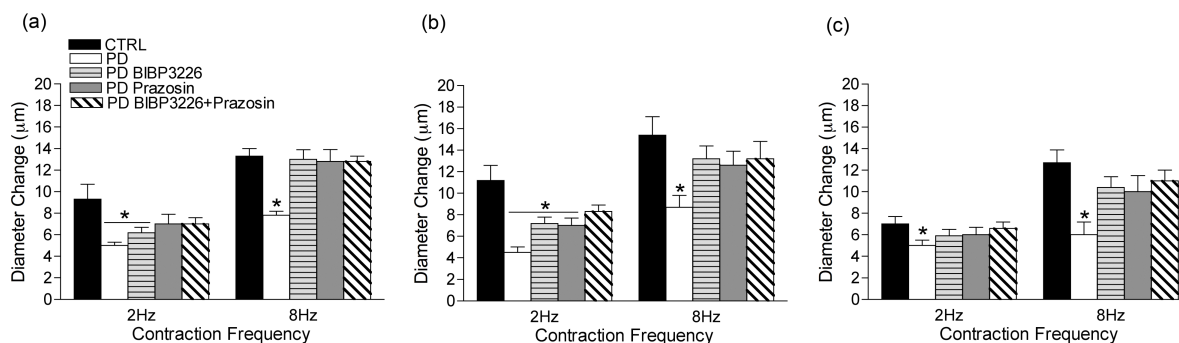


Figure 4.4. Sympathetic Y1R and α 1R blockade restores steady-state vasodilation in PD.

Data are maximal dilatory responses of 2A (a), 3A (b) and 4A (c) following 30 seconds of rhythmic twitch contractions in CTRL ($n=7-12$) and PD ($n=6-11$). BIBP3226 (Y1R antagonist), prazosin (α 1R antagonist) and BIBP3226+prazosin (dual Y1R and α 1R blockade) were added to superfusion of PD. Sympathetic receptor blockade enhanced dilatory responses to rhythmic contractions of PD to responses similar to CTRL. * different from CTRL, $p < 0.05$. CTRL, control; PD, pre-diabetic.

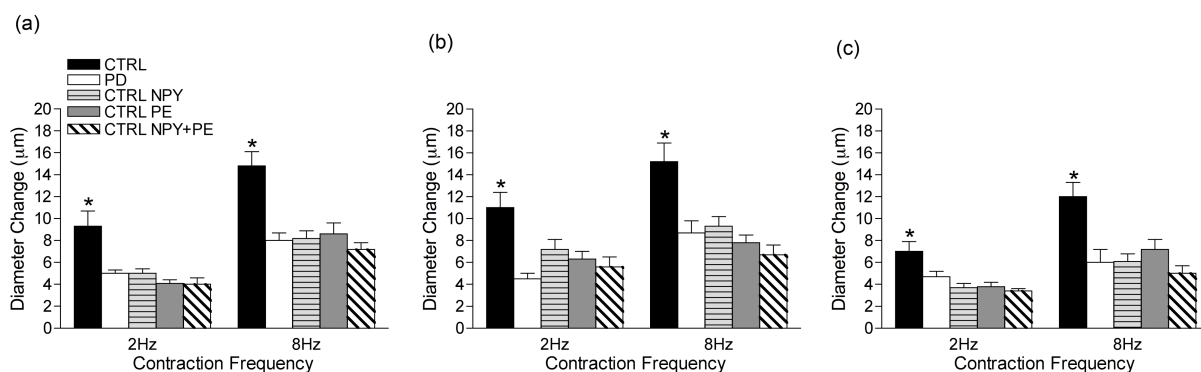


Figure 4.5. Sympathetic Y1R and α 1R activation attenuates steady-state vasodilation in CTRL.

Data are maximal dilatory responses of 2A (a), 3A (b) and 4A (c) following 30 seconds of rhythmic twitch contractions in CTRL (n=7-12) and PD (n=6-11). NPY (Y1R agonist), PE (α 1R agonist) and (dual Y1R and α 1R activation) were added to the superfusion of PD. Sympathetic receptor activation decreased ROV of CTRL to responses similar to PD compared to CTRL. * different from PD, $p < 0.05$. CTRL, control; PD, pre-diabetic.

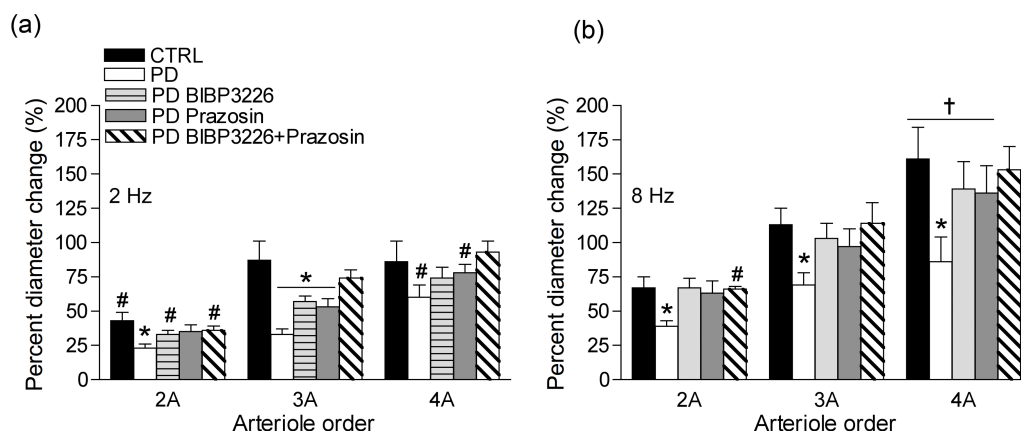


Figure 4.6. Effects of Y1R and α 1R blockade on arteriolar branch order dilatory responses following sustained rhythmic contraction in PD.

Percent change in diameter following 30 seconds of sustained rhythmic contraction at 2 Hz (a) and 8 Hz (b) tetanic contractions. The percent change in diameter was attenuated in PD (n= 6-11) compared to CTRL (n=7-12) at 2A, 3A and 4A, however not in 4A following 2 Hz contraction. Superfusion of sympathetic receptor antagonists BIBP3226 and prazosin caused increases in percent diameter change in PD, affecting relative changes of contraction-evoked dilation in distal arterioles the greatest. * Different vs. CTRL, $p < 0.05$; # different vs. responses of other arterioles within condition, $p < 0.05$; † Different vs. 2A response within condition, $p < 0.05$. CTRL, control; PD, pre-diabetic.

4.3.9. Arteriolar reactivity to sympathetic Y1R and α 1R activation

Increasing concentrations of Y1R agonist NPY (10^{-13} - 10^{-8} M) within the superfusion led to decreases in arteriolar diameter in both CTRL and PD groups (Figure 4.7). Vasoconstrictor responses of 2A to NPY doses were greater in PD *versus* CTRL, especially at NPY 10^{-11} M (Figure 4.7 a, $p < 0.05$). For 3A, vasoconstrictor responses were also greater in PD *versus* CTRL, especially for NPY doses of 10^{-11} – 10^{-8} M (Figure 4.7 b, $p < 0.05$). For 4A, vasoconstrictor responses were similar between groups, however at the highest dose of NPY (10^{-8} M), PD vasoconstrictor responses were greater than those of CTRL (Figure 4.7 c, $p < 0.05$).

Increasing concentrations of α 1R agonist PE (10^{-9} - 10^{-5} M) in the superfusion also led to decreases in arteriolar diameter in both CTRL and PD groups (Figure 4.8). Vasoconstrictor responses of 2A were similar between groups for all PE doses. For 3A and 4A however, vasoconstrictor responses of CTRL and PD were similar for PE doses 10^{-9} - 10^{-6} M, however at 10^{-5} M, vasoconstrictor responses of PD were greater than CTRL (Figure 4.8 b and c, $p < 0.05$).

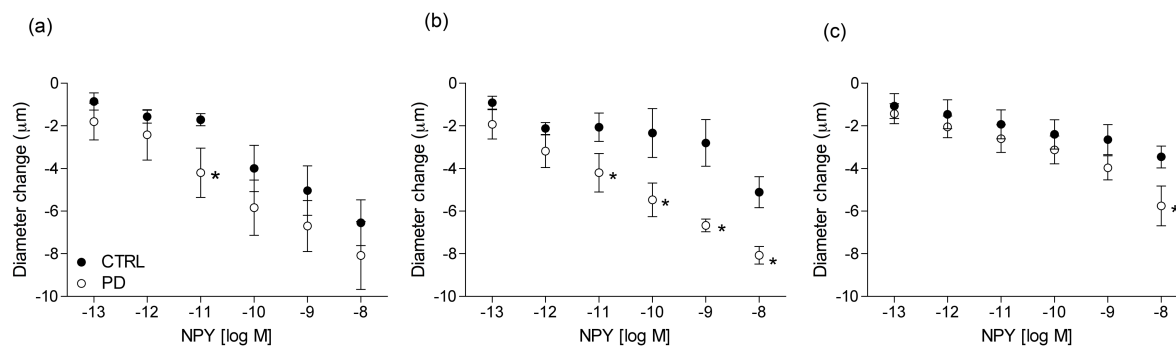


Figure 4.7. Vasoconstriction of gluteus maximus arterioles to NPY.

2A (a), 3A (b) and 4A (c) vasoconstrictor responses to increasing doses of NPY (Y1R agonist) in CTRL (n=7-8) and PD (n=5-7). * different from CTRL within drug dose, $p < 0.05$. CTRL, control; PD, pre-diabetic.

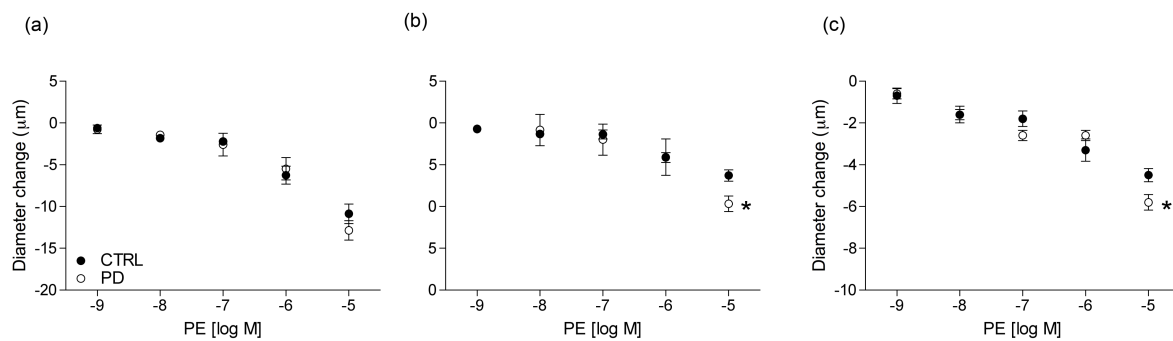


Figure 4.8. Vasoconstriction of gluteus maximus arterioles to PE.

2A (a), 3A (b) and 4A (c) vasoconstrictor responses to increasing doses of PE ($\alpha 1\text{R}$ agonist) in CTRL (n=5-9) and PD (n=5-7). * different from CTRL within drug dose, $p < 0.05$. CTRL, control; PD, pre-diabetic.

4.4. Discussion

Our group has recently demonstrated that pre-diabetes compromises contraction-evoked vasodilation of skeletal muscle arterioles. Prior to this study, we also identified heightened sympathetic regulation of basal vascular tone in pre-diabetic ZDF rats (Novielli et al., 2012). Therefore, in this study, we sought to determine whether enhanced sympathetic Y1R and α 1R receptor activation of skeletal muscle arterioles contributes to decrements in contraction-evoked vasodilation in pre-diabetes. Congruent with our hypotheses, we demonstrated that inhibition of Y1Rs and α 1Rs with BIBP3226 and prazosin increased contraction-evoked vasodilatory responses to levels similar to CTRL. Conversely, blunted contraction-evoked vasodilation observed in PD was reproduced in CTRL via activation of Y1Rs and α 1Rs with NPY and PE. Sympathetic receptor blockade also restored spatially-dependent differences in contraction-evoked vasodilation between arteriolar orders in PD, increasing relative dilatory responses of distal vasculature. In addition, arteriolar vasoconstrictor responsiveness to sympathetic receptor agonists (NPY and PE) appeared to be greater at in PD compared to CTRL, especially at higher concentrations. These findings suggest that Y1R and α 1R activation are enhanced in pre-diabetes, resulting in deficits in arteriolar vasodilation to skeletal muscle contraction.

4.4.1. Sympathetic Y1R- and α 1R-mediated effects on contraction-evoked arteriolar vasodilation in pre-diabetic mice

Rapid onset vasodilation results in the immediate hyperemic response elicited within seconds of muscle contraction at exercise onset. This almost-instantaneous vascular response has been well established in humans and within animal

microcirculatory models (M. L. Armstrong, Dua, & Murrant, 2007; Corcondilas, Koroxenidis, & Shepherd, 1964; Jackson et al., 2010; Kirby, Carlson, Markwald, Voyles, & Dinunno, 2007; Marshall & Tandon, 1984; Mihok & Murrant, 2004; Shoemaker, Tschakovsky, & Hughson, 1998; Tschakovsky et al., 2004; VanTeeffelen & Segal, 2006), and thus is a conserved response in initiating rest-to-exercise transitions to metabolic demand. Until recently, no studies have investigated ROV responses in pre-diabetes. In our most recent study, as well as in the current study, we consistently demonstrated blunted arteriolar ROV responses of 50% or greater following brief tetanic muscle contraction in the GM of pre-diabetic mice, with no differences in baseline arteriolar diameter. When GM arterioles of PD were superfused with sympathetic Y1R antagonist BIBP3226, and α 1R antagonist prazosin, attenuated ROV responses were restored to levels observed in CTRL. Increased ROV responses of PD arterioles following sympathetic blockade prompted experiments testing whether sympathetic activation could do the opposite in CTRL. Without modification of baseline arteriolar diameter, modest activation of Y1R and α 1R with NPY and PE reduced ROV responses of CTRL arterioles following tetanic contraction similar to attenuated responses observed in PD. These novel findings indicate a constitutively higher level of arteriolar smooth muscle cell Y1R and α 1R activation in skeletal muscle microvasculature of pre-diabetic mice, which likely impinge on existing dilatory mechanisms. Past studies of the microcirculation in the hamster cremaster muscle have demonstrated a contributing role of potassium and adenosine to rapid vasodilatory responses elicited by brief tetanic contractions (M. L. Armstrong et al., 2007, Ross, Mihok & Murrant, 2013). In pre-diabetic mice, increased levels of Y1R and α 1R activation, may restrict potassium-

and/or adenosine-mediated VSMC hyperpolarization, thus attenuating ROV to brief tetanic muscle contraction.

Contrary to brief tetanic contraction, sustained rhythmic muscle contraction evokes a progressive increase in arteriolar diameter and blood flow based on the metabolic demands of the tissue (R. B. Armstrong & Laughlin, 1985; Bockman, 1983; Mohrman & Regal, 1988). Studies investigating mechanisms contributing to sustained vasodilation throughout bouts of muscle contraction have identified that the production of local vasoactive metabolites from skeletal muscle tissue and the vasculature contribute to this response (Clifford & Hellsten, 2004). As these signaling events differ from those involved in ROV (Clifford & Hellsten, 2004; Haddy & Scott, 1975; Wunsch, Muller-Delp, & Delp, 2000), it was not known whether decrements in contraction-evoked steady-state dilation, previously demonstrated in PD, was a result of sympathetically-mediated vasoconstriction. In the current study, up to a 60% reduction in steady-state dilation following 30 seconds of rhythmic twitch contractions was observed in PD. Upon sympathetic Y1R and α 1R blockade, arteriolar vasodilatory responses of PD were again restored to levels of CTRL. All sympathetic antagonist conditions were especially effective in restoring PD vasodilatory responses following the greatest contraction frequency (8 Hz). Contrasting experiments determined that activation of arteriolar Y1R and α 1R in CTRL caused decreases in contraction-evoked vasodilatory responses, in turn resembling responses of PD. These findings further demonstrate that increased levels of arteriolar Y1R and α 1R activation in pre-diabetes can restrain vasodilatory responses regardless of the nature of contractile activity.

Blockade of arteriolar Y1R and α 1R activation consistently increased ROV and steady-state vasodilatory responses to respective tetanic and rhythmic contractions across arterioles. Despite the observed 'gain of function', blockade of Y1R or α 1R independently was not always successful in completely restoring contraction-evoked dilatory responses so that they were no longer different than CTRL. ROV responses following 400 ms tetanic contractions were fully restored at all arteriolar orders for all sympathetic antagonist conditions. For longer tetanic contractions (800 ms), evoking greater dilatory responses, 2A ROV could not be restored via independent receptor blockade in PD, where α 1R blockade alone restored ROV of 3A, and Y1R blockade alone restored ROV responses of 4A. Following low frequency rhythmic contractions, 2A dilation of PD was not fully restored via independent Y1R blockade, and 3A dilation was not fully restored via independent blockade of both Y1R and α 1R. Inability to increase ROV or steady-state dilation by blocking sympathetic receptors independently may be due to the vasoconstrictive effects of the outstanding active sympathetic receptor. Interestingly, PD demonstrated elevated arteriolar vasoconstrictor responsiveness to increasing doses of Y1R and α 1R agonists, NPY and PE. These data may suggest greater vasoconstrictive effects of sympathetic receptor activation themselves, or greater vascular expression of sympathetic receptors, as demonstrated previously in the hindlimb of pre-diabetic ZDF rats (Novielli et al., 2012). A potential increase in arteriolar sympathetic receptor density along with reported increases in SNA associated with pre-diabetes may impinge on contraction-evoked dilatory responses in PD, despite blockade of sympathetic receptors independently. Following 8 Hz tetanic contraction, however, all sympathetic antagonist conditions (independent and dual blockade) elicited robust increases in steady-

state vasodilation in PD, similar to levels of CTRL. In conjunction with sympathetic receptor blockade, large accumulation of vasoactive metabolites in response to high frequency muscle contraction likely contributes to the significant increase of arteriolar diameter in PD. As expected however, dual receptor blockade recovered ROV and steady-state vasodilatory responses of PD following all tetanic and rhythmic contractions, at all arteriolar orders studied. Interaction between Y1R and α 1R activation has been established, where NPY and NE can act together to cause greater vasoconstriction compared to responses elicited alone, especially under conditions of increased sympathetic activation (Dahlof, Dahlof, & Lundberg, 1985; Jackson et al., 2005; Revington & McCloskey, 1988). Independent of exercise, we also investigated maximal arteriolar vasodilatory responses elicited by GM superfusion of SNP. We demonstrated decreased arteriolar dilation to SNP in PD, however this response was restored following dual blockade of Y1R and α 1R in the presence of SNP. These findings suggest that endogenous vasodilatory mechanisms contributing to dilation during muscle contraction, as well as direct smooth muscle cell relaxation, can be disrupted by constitutively enhanced dual Y1R and α 1R activation in pre-diabetes.

4.4.2. Emphasis on NPY-mediated neurovascular modulation in pre-diabetes

This is the first study to demonstrate sympathetically-mediated reductions of both ROV and steady-state dilation of arterioles in pre-diabetes. In conditions such as aging and the metabolic syndrome, studies investigated whether decrements in functional hyperemia and vasodilatory responses following muscle contraction was a result of enhanced α -adrenergic modulation of vascular responses (Casey & Joyner, 2012;

Dinunno, Masuki, & Joyner, 2005; Frisbee, 2004; Jackson et al., 2010; Naik, Xiang, Hodnett, & Hester, 2008). In accordance with findings of the current study, α -adrenergic receptor blockade resulted in increased contraction-evoked vasodilation in aged and obese groups. Conversely, peptidergic-mediated modulation of contraction-evoked vasodilation was not considered. In addition to NE, it is well recognized that NPY contributes to sympathetically-mediated vascular regulation at rest, as well as during muscle contraction (Buckwalter, Hamann, & Clifford, 2005; Buckwalter, Hamann, Kluess, & Clifford, 2004; DeLorey et al.; Evanson et al.; Jackson et al., 2005; Jackson et al., 2004; Novielli et al., 2012). Under conditions of greater SNA, neuronal NPY release and its effects on arteriolar constriction become more apparent (Bartfai, Iverfeldt, Fisone, & Serfozo, 1988; De Camilli & Jahn, 1990; Lundberg, Franco-Cereceda, Lou, Modin, & Pernow, 1994). Therefore greater NPY-mediated Y1R vasoconstrictor restraint on contraction-evoked vasodilatory responses was anticipated in pre-diabetic mice of the present study.

4.4.3. Spatially-dependent arteriolar dilation and sympathetic receptor blockade

Skeletal muscle contraction elicits vasodilatory responses that differ based on the location of the arteriole within the microvascular network, where proportional increases in vasodilation are greatest in smaller distal arterioles compared to proximal larger arterioles (Dodd & Johnson, 1991; Marshall & Tandon, 1984; VanTeeffelen & Segal, 2006). This was demonstrated in the current study, where in CTRL, ROV and steady-state dilatory reactivity to tetanic and rhythmic muscle contraction was greatest in distal

arterioles (4A and 3A). In PD, however, spatially-dependent arteriolar responses were almost indistinguishable, where relative diameter changes of only 4A were affected by both types of muscle contraction. In turn, sympathetic receptor antagonist conditions elicited increases in relative diameter responses, restoring appropriate arteriolar reactivity from distal to proximal arterioles. Interestingly, effects of each sympathetic antagonist condition differed between arteriolar orders. Within-condition differences between arterioles in PD may suggest heterogeneous Y1R and α 1R-mediated attenuation of contraction-evoked dilation throughout the arteriolar network. This may be a result of differences in sympathetic receptor distribution or differences in neural innervation density at the distal microvasculature (Cowley & Franchini, 1996). It has been confirmed that α -adrenergic receptor subtype distribution in arteriolar networks in the mouse GM varies with vessel branch order, where α 1Rs are located more distally (Moore, Jackson, & Segal, 2010). Additionally, studies of feline skeletal muscle microvasculature demonstrated that NPY's vasoconstrictor effects are greatest at distal arterioles (Ekelund & Erlinge, 1997). Thus we expected sympathetic receptor blockade to affect vasodilatory responses of distal arterioles in PD.

4.4.4. Experimental considerations

In the current study, we investigated whether constitutively enhanced arteriolar Y1R and α 1R activation contributed to decrements in contraction-evoked vasodilation in pre-diabetic mice. The use of BIBP3226 and prazosin allowed us to specifically block Y1R and α 1R, therefore the effects of endogenous NPY and norepinephrine (NE) on arteriolar modulation of dilatory responses could be resolved in pre-diabetes. Although α 2-adrenergic receptors (α 2R) and NPY Y2 receptors (Y2R) are present post-junctionally

on the vasculature and contribute to sympathetically-mediated vasoconstriction (Jie, van Brummelen, Vermeij, Timmermans, & van Zwieten, 1984; Kiowski, Hulthen, Ritz, & Buhler, 1983), they are also located pre-junctionally and modulate NE and NPY release via a negative feedback mechanism (Ruffolo, Nichols, Stadel, & Hieble, 1991; Wahlestedt et al., 1990). In order to reduce potentially confounding effects of pre- and post- junctional α 2R and Y2R activity on sympathetic vascular modulation in pre-diabetes, we investigated α 1R- and Y1R- mediated effects, as it is understood that they are located post-junctionally on VSMCs. In addition, a recent study has demonstrated heterogeneous distribution of α -adrenergic receptor subtypes throughout the arteriolar network of the mouse GM. It was observed that distal arterioles (e.g. 3As) exhibited the greatest vasoconstrictor responses to α 1R agonist PE, confirming a greater contribution of α 1Rs to sympathetic vascular control in the arterioles examined in the current study. Vasoconstriction elicited by the α 2R agonist UK14304 was greatest in 1As, an area of the arteriolar tree we did not directly examine in the current study. Although there are no studies characterizing NPY Y receptor distribution throughout microvascular networks, past experiments have demonstrated greater effects of Y1R-mediated vasoconstriction compared to Y2Rs in distal vasculature of cat hindlimb skeletal muscle (Ekelund & Erlinge, 1997). Therefore we feel that increased sympathetic activity at the level of skeletal muscle arterioles in pre-diabetic mice is predominantly an effect of enhanced Y1R and α 1R activation.

4.5. Conclusions

In the current study, we demonstrated that ROV and steady-state vasodilation in response to tetanic and rhythmic muscle contraction were blunted in branching arterioles of the GM in pre-diabetic mice. Since Y1R and α 1R blockade restored contraction-evoked vasodilatory responses in PD, and Y1R and α 1R activation attenuated contraction-evoked vasodilatory responses in CTRL, our data suggest that pre-diabetes is associated with greater sympathetic modulation of arteriolar function via elevated levels of Y1R and α 1R activation. Furthermore, disrupted spatial reactivity of PD vasodilatory responses to muscle contraction was also restored following superfusion of sympathetic Y1R and α 1R antagonists, increasing relative diameter changes of distal arterioles. In addition, VSMC relaxation elicited by superfusion of SNP was also attenuated in arterioles of PD, where dual Y1R and α 1R blockade in the presence of SNP increased maximal arteriolar dilatory responses of PD to levels similar to CTRL. The present study provides evidence that pre-diabetes is associated with microvascular impairments related to increased sympathetic receptor activation throughout skeletal muscle branching arteriolar networks.

4.6. References

- Anderson, E. A., Balon, T. W., Hoffman, R. P., Sinkey, C. A., & Mark, A. L. (1992). Insulin increases sympathetic activity but not blood pressure in borderline hypertensive humans. *Hypertension*, *19*(6 Pt 2), 621-627.
- Armstrong, M. L., Dua, A. K., & Murrant, C. L. (2007). Potassium initiates vasodilatation induced by a single skeletal muscle contraction in hamster cremaster muscle. *J Physiol*, *581*(Pt 2), 841-852.
- Armstrong, R. B., & Laughlin, M. H. (1985). Rat muscle blood flows during high-speed locomotion. *J Appl Physiol*, *59*(4), 1322-1328.
- Bartfai, T., Iverfeldt, K., Fisone, G., & Serfozo, P. (1988). Regulation of the release of coexisting neurotransmitters. *Annu Rev Pharmacol Toxicol*, *28*, 285-310.
- Bearden, S. E., Payne, G. W., Chisty, A., & Segal, S. S. (2004). Arteriolar network architecture and vasomotor function with ageing in mouse gluteus maximus muscle. *J Physiol*, *561*(Pt 2), 535-545.
- Berne, C., Fagius, J., Pollare, T., & Hjendahl, P. (1992). The sympathetic response to euglycaemic hyperinsulinaemia. Evidence from microelectrode nerve recordings in healthy subjects. *Diabetologia*, *35*(9), 873-879.
- Bockman, E. L. (1983). Blood flow and oxygen consumption in active soleus and gracilis muscles in cats. *Am J Physiol*, *244*(4), H546-551.
- Bradford, M. M. (1976). A rapid and sensitive method for the quantitation of microgram quantities of protein utilizing the principle of protein-dye binding. *Anal Biochem*, *72*, 248-254.
- Buckwalter, J. B., Hamann, J. J., & Clifford, P. S. (2005). Neuropeptide Y1 receptor vasoconstriction in exercising canine skeletal muscles. *J Appl Physiol (1985)*, *99*(6), 2115-2120.
- Buckwalter, J. B., Hamann, J. J., Kluess, H. A., & Clifford, P. S. (2004). Vasoconstriction in exercising skeletal muscles: a potential role for neuropeptide Y? *Am J Physiol Heart Circ Physiol*, *287*(1), H144-149.

- Casey, D. P., & Joyner, M. J. (2012). Influence of alpha-adrenergic vasoconstriction on the blunted skeletal muscle contraction-induced rapid vasodilation with aging. *J Appl Physiol*, *113*(8), 1201-1212.
- Charles River Laboratories (2006). Comparison of insulin levels for c57BL/6NCrl-Lepr(db-lb)/Crl (THE POUND MOUSE™). Technical resources; Baseline data. Charles River, USA.
- Clifford, P. S., & Hellsten, Y. (2004). Vasodilatory mechanisms in contracting skeletal muscle. *J Appl Physiol*, *97*(1), 393-403.
- Corcondilas, A., Koroxenidis, G. T., & Shepherd, J. T. (1964). Effect of a Brief Contraction of Forearm Muscles on Forearm Blood Flow. *J Appl Physiol*, *19*, 142-146.
- Cowley, A. W., & Franchini, K. G. (1996). Neurogenic control of blood vessels. In D. Robertson, P. A. Low & R. J. Polinsky (Eds.), *Primer on the Autonomic Nervous System* (Vol. 1, pp. 49-58). San Diego: Academic Press Inc.
- Creager, M. A., Luscher, T. F., Cosentino, F., & Beckman, J. A. (2003). Diabetes and vascular disease: pathophysiology, clinical consequences, and medical therapy: Part I. *Circulation*, *108*(12), 1527-1532.
- Dahlof, C., Dahlof, P., & Lundberg, J. M. (1985). Neuropeptide Y (NPY): enhancement of blood pressure increase upon alpha-adrenoceptor activation and direct pressor effects in pithed rats. *Eur J Pharmacol*, *109*(2), 289-292.
- De Camilli, P., & Jahn, R. (1990). Pathways to regulated exocytosis in neurons. *Annu Rev Physiol*, *52*, 625-645.
- DeFronzo, R. A., & Ferrannini, E. (1991). Insulin resistance. A multifaceted syndrome responsible for NIDDM, obesity, hypertension, dyslipidemia, and atherosclerotic cardiovascular disease. *Diabetes Care*, *14*(3), 173-194.
- DeLorey, D. S., Buckwalter, J. B., Mittelstadt, S. W., Anton, M. M., Kluess, H. A., & Clifford, P. S. Is tonic sympathetic vasoconstriction increased in the skeletal

- muscle vasculature of aged canines? *Am J Physiol Regul Integr Comp Physiol*, 299(5), R1342-1349.
- Dinenno, F. A., Masuki, S., & Joyner, M. J. (2005). Impaired modulation of sympathetic alpha-adrenergic vasoconstriction in contracting forearm muscle of ageing men. *J Physiol*, 567(Pt 1), 311-321.
- Dodd, L. R., & Johnson, P. C. (1991). Diameter changes in arteriolar networks of contracting skeletal muscle. *Am J Physiol*, 260(3 Pt 2), H662-670.
- Ekelund, U., & Erlinge, D. (1997). In vivo receptor characterization of neuropeptide Y-induced effects in consecutive vascular sections of cat skeletal muscle. *Br J Pharmacol*, 120(3), 387-392.
- Ellis, C. G., Goldman, D., Hanson, M., Stephenson, A. H., Milkovich, S., Benlamri, A., et al. (2010). Defects in oxygen supply to skeletal muscle of prediabetic ZDF rats. *Am J Physiol Heart Circ Physiol*, 298(6), H1661-1670.
- Evanson, K. W., Stone, A. J., Samraj, E., Benson, T., Prisby, R., & Kluess, H. A. Influence of estradiol supplementation on neuropeptide Y neurotransmission in skeletal muscle arterioles of F344 rats. *Am J Physiol Regul Integr Comp Physiol*, 303(6), R651-657.
- Frisbee, J. C. (2004). Enhanced arteriolar alpha-adrenergic constriction impairs dilator responses and skeletal muscle perfusion in obese Zucker rats. *J Appl Physiol*, 97(2), 764-772.
- Fuglevand, A. J., & Segal, S. S. (1997). Simulation of motor unit recruitment and microvascular unit perfusion: spatial considerations. *J Appl Physiol*, 83(4), 1223-1234.
- Gupta, A. K., Ravussin, E., Johannsen, D. L., Stull, A. J., Cefalu, W. T., & Johnson, W. D. (2012). Endothelial Dysfunction: An Early Cardiovascular Risk Marker in Asymptomatic Obese Individuals with Prediabetes. *Br J Med Med Res*, 2(3), 413-423.
- Haddy, F. J., & Scott, J. B. (1975). Metabolic factors in peripheral circulatory regulation. *Fed Proc*, 34(11), 2006-2011.

- Jaap, A. J., Hammersley, M. S., Shore, A. C., & Tooke, J. E. (1994). Reduced microvascular hyperaemia in subjects at risk of developing type 2 (non-insulin-dependent) diabetes mellitus. *Diabetologia*, *37*(2), 214-216.
- Jaap, A. J., Shore, A. C., & Tooke, J. E. (1997). Relationship of insulin resistance to microvascular dysfunction in subjects with fasting hyperglycaemia. *Diabetologia*, *40*(2), 238-243.
- Jackson, D. N., Milne, K. J., Noble, E. G., & Shoemaker, J. K. (2005). Gender-modulated endogenous baseline neuropeptide Y Y1-receptor activation in the hindlimb of Sprague-Dawley rats. *J Physiol*, *562*(Pt 1), 285-294.
- Jackson, D. N., Moore, A. W., & Segal, S. S. (2010). Blunting of rapid onset vasodilatation and blood flow restriction in arterioles of exercising skeletal muscle with ageing in male mice. *J Physiol*, *588*(Pt 12), 2269-2282.
- Jackson, D. N., Noble, E. G., & Shoemaker, J. K. (2004). Y1- and alpha1-receptor control of basal hindlimb vascular tone. *Am J Physiol Regul Integr Comp Physiol*, *287*(1), R228-233.
- Jie, K., van Brummelen, P., Vermey, P., Timmermans, P. B., & van Zwieten, P. A. (1984). Identification of vascular postsynaptic alpha 1- and alpha 2-adrenoceptors in man. *Circ Res*, *54*(4), 447-452.
- Kim, S. H., & Reaven, G. M. (2008a). Insulin resistance and hyperinsulinemia: you can't have one without the other. *Diabetes Care*, *31*(7), 1433-1438.
- Kim, S. H., & Reaven, G. M. (2008b). Isolated impaired fasting glucose and peripheral insulin sensitivity: not a simple relationship. *Diabetes Care*, *31*(2), 347-352.
- Kiowski, W., Hulthen, U. L., Ritz, R., & Buhler, F. R. (1983). Alpha 2 adrenoceptor-mediated vasoconstriction of arteries. *Clin Pharmacol Ther*, *34*(5), 565-569.
- Kirby, B. S., Carlson, R. E., Markwald, R. R., Voyles, W. F., & Dinunno, F. A. (2007). Mechanical influences on skeletal muscle vascular tone in humans: insight into contraction-induced rapid vasodilatation. *J Physiol*, *583*(Pt 3), 861-874.

- Lesniewski, L. A., Donato, A. J., Behnke, B. J., Woodman, C. R., Laughlin, M. H., Ray, C. A., et al. (2008). Decreased NO signaling leads to enhanced vasoconstrictor responsiveness in skeletal muscle arterioles of the ZDF rat prior to overt diabetes and hypertension. *Am J Physiol Heart Circ Physiol*, 294(4), H1840-1850.
- Lundberg, J. M., Franco-Cereceda, A., Lou, Y. P., Modin, A., & Pernow, J. (1994). Differential release of classical transmitters and peptides. *Adv Second Messenger Phosphoprotein Res*, 29, 223-234.
- Marshall, J. M., & Tandon, H. C. (1984). Direct observations of muscle arterioles and venules following contraction of skeletal muscle fibres in the rat. *J Physiol*, 350, 447-459.
- McDaid, E. A., Monaghan, B., Parker, A. I., Hayes, J. R., & Allen, J. A. (1994). Peripheral autonomic impairment in patients newly diagnosed with type II diabetes. *Diabetes Care*, 17(12), 1422-1427.
- Mihok, M. L., & Murrant, C. L. (2004). Rapid biphasic arteriolar dilations induced by skeletal muscle contraction are dependent on stimulation characteristics. *Can J Physiol Pharmacol*, 82(4), 282-287.
- Milman, S., & Crandall, J. P. (2011). Mechanisms of vascular complications in prediabetes. *Med Clin North Am*, 95(2), 309-325, vii.
- Mohrman, D. E., & Regal, R. R. (1988). Relation of blood flow to VO₂, PO₂, and PCO₂ in dog gastrocnemius muscle. *Am J Physiol*, 255(5 Pt 2), H1004-1010.
- Moore, A. W., Jackson, W. F., & Segal, S. S. (2010). Regional heterogeneity of alpha-adrenoreceptor subtypes in arteriolar networks of mouse skeletal muscle. *J Physiol*, 588(Pt 21), 4261-4274.
- Murrant, C. L. (2005). Stimulation characteristics that determine arteriolar dilation in skeletal muscle. *Am J Physiol Regul Integr Comp Physiol*, 289(2), R505-R513.
- Naik, J. S., Xiang, L., Hodnett, B. L., & Hester, R. L. (2008). Alpha-adrenoceptor-mediated vasoconstriction is not involved in impaired functional vasodilation in the obese Zucker rat. *Clin Exp Pharmacol Physiol*, 35(5-6), 611-616.

- Novielli, N. M., Al-Khazraji, B. K., Medeiros, P. J., Goldman, D., & Jackson, D. N. (2012). Pre-Diabetes Augments Neuropeptide Y(1)- and alpha(1)-Receptor Control of Basal Hindlimb Vascular Tone in Young ZDF Rats. *PLoS One*, 7(10), e46659.
- Pries, A. R., Ley, K., Claassen, M., & Gaehtgens, P. (1989). Red cell distribution at microvascular bifurcations. *Microvasc Res*, 38(1), 81-101.
- Remensnyder, J. P., Mitchell, J. H., & Sarnoff, S. J. (1962). Functional sympatholysis during muscular activity. Observations on influence of carotid sinus on oxygen uptake. *Circ Res*, 11, 370-380.
- Reusch, J. E., Bridenstine, M., & Regensteiner, J. G. (2013). Type 2 diabetes mellitus and exercise impairment. *Rev Endocr Metab Disord*, 14(1), 77-86.
- Revington, M., & McCloskey, D. I. (1988). Neuropeptide Y and control of vascular resistance in skeletal muscle. *Regul Pept*, 23(3), 331-342.
- Ross, G. A., Mihok, M. L., & Murrant, C. L. 2013. Extracellular adenosine initiates rapid arteriolar vasodilation induced by a single skeletal muscle contraction in hamster cremaster muscle. *Acta Physiol (Oxf)*, 208(1):74-87.
- Rowell, L. B. (1993). *Human Cardiovascular Control*. New York: Oxford University Press.
- Ruffolo, R. R., Jr., Nichols, A. J., Stadel, J. M., & Hieble, J. P. (1991). Structure and function of alpha-adrenoceptors. *Pharmacol Rev*, 43(4), 475-505.
- Schaefer, C., Biermann, T., Schroeder, M., Fuhrhop, I., Niemeier, A., Ruther, W., et al. (2010). Early microvascular complications of prediabetes in mice with impaired glucose tolerance and dyslipidemia. *Acta Diabetol*, 47(Suppl 1), 19-27.
- Scherrer, U., & Sartori, C. (1997). Insulin as a vascular and sympathoexcitatory hormone: implications for blood pressure regulation, insulin sensitivity, and cardiovascular morbidity. *Circulation*, 96(11), 4104-4113.

- Shoemaker, J. K., Tschakovsky, M. E., & Hughson, R. L. (1998). Vasodilation contributes to the rapid hyperemia with rhythmic contractions in humans. *Can J Physiol Pharmacol*, 76(4), 418-427.
- Soma, L. R. (1983). Anesthetic and analgesic considerations in the experimental animal. *Ann N Y Acad Sci*, 406, 32-47.
- Strandell, T., & Shepherd, J. T. (1967). The effect in humans of increased sympathetic activity on the blood flow to active muscles. *Acta Med Scand Suppl*, 472, 146-167.
- Thomas, G. D., & Segal, S. S. (2004). Neural control of muscle blood flow during exercise. *J Appl Physiol*, 97(2), 731-738.
- Tooke, J. E., & Goh, K. L. (1999). Vascular function in Type 2 diabetes mellitus and pre-diabetes: the case for intrinsic endotheiopathy. *Diabet Med*, 16(9), 710-715.
- Tschakovsky, M. E., Rogers, A. M., Pyke, K. E., Saunders, N. R., Glenn, N., Lee, S. J., et al. (2004). Immediate exercise hyperemia in humans is contraction intensity dependent: evidence for rapid vasodilation. *J Appl Physiol*, 96(2), 639-644.
- VanTeeffelen, J. W., & Segal, S. S. (2000). Effect of motor unit recruitment on functional vasodilatation in hamster retractor muscle. *J Physiol*, 524 Pt 1, 267-278.
- VanTeeffelen, J. W., & Segal, S. S. (2006). Rapid dilation of arterioles with single contraction of hamster skeletal muscle. *Am J Physiol Heart Circ Physiol*, 290(1), H119-127.
- Wahlestedt, C., Grundemar, L., Hakanson, R., Heilig, M., Shen, G. H., Zukowska-Grojec, Z., et al. (1990). Neuropeptide Y receptor subtypes, Y1 and Y2. *Ann N Y Acad Sci*, 611, 7-26.
- Wiernsperger, N. (1994). Vascular defects in the aetiology of peripheral insulin resistance in diabetes. A critical review of hypotheses and facts. *Diabetes Metab Rev*, 10(3), 287-307.

Wunsch, S. A., Muller-Delp, J., & Delp, M. D. (2000). Time course of vasodilatory responses in skeletal muscle arterioles: role in hyperemia at onset of exercise. *Am J Physiol Heart Circ Physiol*, 279(4), H1715-1723.

Chapter 5 : Conclusions

5.1. Summary

The novel findings presented in this thesis contribute to the understanding of vascular dysfunction associated with type 2 diabetic disease progression. Specifically, in pre-diabetes, elevated sympathetic microvascular modulation leads to compromised blood flow regulation in skeletal muscle. The presented studies demonstrate that pre-diabetes promotes an overall increase in basal Y1R and α 1R vascular control in skeletal muscle under resting and active conditions. These studies are also the first to address the impact of augmented peptidergic (neuropeptide Y, NPY) contribution, in addition to noradrenergic contribution, to skeletal muscle vascular dysfunction under resting and active conditions in pre-diabetes. In support of hypothesis 1, it was shown that chronic basal activation of NPY Y1 receptor (Y1R) and α 1 adrenergic receptor (α 1R) was elevated in hindlimb vasculature of pre-diabetic Zucker diabetic fatty (ZDF) rats. In addition, expression of hindlimb tissue NPY and vascular Y1R and α 1R was greater in pre-diabetic compared to control rats, demonstrating changes in sympathetic control system components involved in vascular modulation. These data support heightened sympathetic nerve activity (SNA) associated with pre-diabetes, thus providing impetus for subsequent studies investigating the impact of pre-diabetes and elevated sympathetic receptor activation on skeletal muscle microvascular function.

In contrast to experiments carried out under basal conditions in chapter 2, the experiments of chapter 3 investigated the impact of pre-diabetes on microvascular function in contracting muscle. Using a murine model of pre-diabetes, an adaptation of

the previously established gluteus maximus preparation, and intravital microscopy techniques, experiments from chapter 3 supported hypothesis 2, where arteriolar dilation and blood flow in response to skeletal muscle contraction was blunted in pre-diabetic mice, compared to healthy controls. Analysis of contraction-evoked arteriolar responses throughout continuous branching arterioles also uncovered spatially-dependent changes in arteriolar diameter, where relative dilation of distal arterioles was greater than that of proximal arterioles. In pre-diabetic mice however, this pattern of dilation was disrupted compared to control. In chapter 4, we determined whether elevated sympathetic modulation of vascular control contributed to impaired contraction evoked dilation in pre-diabetic mice. Findings from chapter 4 supported hypothesis 3, as we found that attenuated arteriolar responses to skeletal muscle contraction were a result of enhanced constitutive activation of arteriolar Y1R and α 1R in pre-diabetic mice. Additionally, arteriolar vasoconstrictor responsiveness to sympathetic Y1R and α 1R activation was greater in pre-diabetic mice.

5.2. Merit

The findings of this thesis contribute to further understanding cardiovascular comorbidities associated with diabetic disease progression. Past research has generally focused on microvascular disease as a result of prolonged chronic diabetic conditions. Few studies however, have examined the impact of early pre-diabetes on microvascular function within skeletal muscle. The studies presented herein demonstrate that pre-

diabetes is accompanied by augmented peripheral sympathetic vascular modulation of basal vascular tone and vasodilatory responses to muscle contraction.

Prior to studies performed in this thesis, no previous studies have examined peptidergic vascular control in pre-diabetes, overt type 2 diabetes or any other metabolic condition (i.e., obesity, hypertension, the metabolic syndrome). Sympathetic modulation of skeletal muscle vasculature in health and disease is often examined in light of noradrenergic mechanisms (Frisbee, 2003, 2004; Hodnett, Xiang, Dearman, Carter, & Hester, 2008; Lesniewski et al., 2008; Naik, Xiang, & Hester, 2006; Naik, Xiang, Hodnett, & Hester, 2008; Okon, Szado, Laher, McManus, & van Breemen, 2003; Romanko, Ali, Mintz, & Stepp, 2009; Stepp & Frisbee, 2002). Notably, NPY's role in sympathetic vascular regulation within skeletal muscle has been demonstrated under basal resting and active conditions (Buckwalter, Hamann, & Clifford, 2005; Buckwalter, Hamann, Kluess, & Clifford, 2004; DeLorey et al., 2010; Evanson et al., 2012; Jackson, Milne, Noble, & Shoemaker, 2005a; Jackson, Noble, & Shoemaker, 2004; Novielli, Al-Khazraji, Medeiros, Goldman, & Jackson, 2012). Increased SNA accompanying pre-diabetes supports a greater role of NPY in sympathetic vascular modulation. NPY release is understood to increase under such conditions [in conjunction with norepinephrine (NE)], and its influence on sympathetic vasoconstrictor effects of arterioles become greater (Bartfai, Iverfeldt, Fisone, & Serfozo, 1988; De Camilli & Jahn, 1990; Lundberg, Franco-Cereceda, Lou, Modin, & Pernow, 1994). Experimental findings from chapters 2 and 4 highlight the role of NPY in augmented skeletal muscle vascular control, whereby NPY's contribution to sympathetic regulation of skeletal muscle blood flow and arteriolar diameter was increased in pre-diabetic rats and mice. Therefore, studies examining

sympathetic vascular control mechanisms should consider consequences of NPY-Y1R activation in addition to α -adrenergic mechanisms.

Functional experiments conducted in chapters 2, 3 and 4 were performed *in vivo* with the use of rat and mouse models of pre-diabetes. Using an *in vivo* approach provided the ability to evaluate vascular function within the animal itself, leaving endogenous neural and vascular control mechanisms intact. In chapter 2, *in vivo* blood flow measurements were evaluated at the level of the femoral artery in pre-diabetic ZDF and control rats. Under basal conditions, changes in resting blood flow that were evoked by sympathetic receptor blockade provided a summation of the modifications in downstream resistance within branching microvascular networks of hindlimb skeletal muscle. In chapters 3 and 4 however, the *in vivo* experimental approach was extended into the skeletal muscle microvasculature of the gluteus maximus (GM) in pre-diabetic and healthy mice. Intravital microscopy served to directly assess functional responses of arterioles themselves, where physiological interactions between microvessels, muscle fibers and perivascular neural control could be resolved. The planar geometry and uniform thinness of the GM enables access to its entire microvascular network for imaging and experimental perturbations, where diameter and blood flow measurements (Al-Khazraji, Novielli, Goldman, Medeiros, & Jackson, 2012) can be made within one focal plane. As such, arteriolar responses to both tetanic and rhythmic muscle contraction were evaluated at multiple orders of arterioles. Development of this model was ideal for investigating the impact of early pre-diabetes on arteriolar network regulation in skeletal muscle. This model can be used to address additional regulatory events of the microvasculature that may be compromised in early pre-diabetes.

The use of experimental preparations used in chapters 2, and 3 and 4 allowed for *in situ* evaluation of sympathetic Y1R and α 1R effects on vascular control. With the use of specific Y1R and α 1R antagonists, BIBP3226 and prazosin, autogenous sympathetic receptor-ligand mediated effects were uncovered in chapters 2 and 4. In a contrasting manner, the use of Y1R and α 1R agonists (chapter 4) may determine the existence of receptors and outcomes of receptor activation (i.e. induce vasoconstriction), or activate sympathetic receptors to modify physiological outcomes (i.e. blunting of contraction-evoked arteriolar dilation in control mice). Targeting Y1R and α 1R pharmacologically with the use of antagonists and agonists therefore provided the ability to discern differences in sympathetic vascular control between pre-diabetic and control groups that may have thereby been overlooked, as resting cardiovascular and hemodynamic characteristics were similar between experimental groups.

5.3. Limitations and assumptions

The experiments presented in this thesis have been conducted using rodent models of pre-diabetes, thus limitations may arise when translating results to pre-diabetic humans. Heightened SNA has been observed in pre-diabetic individuals affected by insulin resistance and hyperinsulinemia, however sympathetically-mediated modulation of vascular function remains to be investigated in pre-diabetic humans. Nevertheless, animal models are essential to answering research questions pertaining to physiological processes in health and disease. The ZDF rat expresses a dysfunctional leptin receptor, thus leptin cannot interact with its respective receptor to suppress appetite. When male

ZDF rats are fed a high-fat diet, they develop obesity, insulin resistance, and hyperinsulinemia, and ultimately become full blown diabetic (Lesniewski et al., 2008; Oltman et al., 2006). The ZDF rat represents a model of type 2 diabetic disease progression, where it exhibits a pre-diabetic period, followed by genetically predisposed development of overt type 2 diabetes and pancreatic failure (Etgen & Oldham, 2000). The rat model used in chapter 2 represented the pre-diabetic condition at 7 weeks of age, sharing similar pathological metabolic characteristics to pre-diabetic humans e.g. marked increases in circulating plasma insulin, insulin resistance, elevated blood glucose, obesity (Kim & Reaven, 2008a, 2008b; Lyssenko et al., 2005). Additionally, the rat is the most commonly used species in cardiovascular research, and is characterized by sympathetic nervous system responses and components similar to humans (Montano, Furlan, Guzzetti, McAllen, & Julien, 2009). The pre-diabetic ZDF rat model used in chapter 2 was therefore appropriate to study the impact of pre-diabetes on basal sympathetic vascular modulation of skeletal muscle blood flow.

In chapters 3 and 4, studies were performed using a mouse model of pre-diabetes (the Pound Mouse) of the c57bl6 background, exhibiting the same leptin receptor mutation as the pre-diabetic ZDF rat, as well as similar pathological metabolic characteristics to the pre-diabetic rat and human condition (Lee & Cox, 2011). Conversely however, the pre-diabetic Pound Mouse is not genetically predisposed to developing type 2 diabetes, and therefore does not pose an age restriction on experimental procedures. Previous studies have used the c57bl6 mouse to evaluate sympathetic control mechanisms of arteriolar function in the gluteus maximus (Bearden, Payne, Chisty, & Segal, 2004; Jackson, Moore, & Segal, 2010; Moore, Bearden, & Segal,

2010; Moore, Jackson, & Segal, 2010), thus we adapted this skeletal muscle preparation to the pre-diabetic model used in chapters 3 and 4. Although not demonstrated in pre-diabetes, mouse *versus* human comparisons of vascular function have been highlighted in ageing studies. In aged mice, impaired hemodynamic and arteriolar dilatory responses to contraction of the gluteus maximus muscle was a result of enhanced sympathetic receptor activation (Jackson et al., 2010). Accordingly, aged humans demonstrate elevated SNA, which has also been demonstrated to restrict blood flow responses to exercising limbs (Casey & Joyner, 2012; Dineno & Joyner, 2006; Proctor & Parker, 2006). Findings of chapter 4 demonstrated that enhanced sympathetic receptor activation throughout the microvasculature of the GM results in blunted dilatory responses to muscle contraction in pre-diabetic mice, however this has not been confirmed in humans. Humans affected by insulin resistance or pre-diabetes have indeed demonstrated instances of heightened SNA and impaired functional hyperemic responses to muscle contraction on separate accounts. Based on the findings of this thesis, increased SNA likely contributes to attenuated vascular responses to muscle contraction in pre-diabetic humans, however this remains to be elucidated.

Although it was not measured directly, sympathetic activity was assumed to be elevated in pre-diabetic animals used in studies of this thesis. Experiments were conducted in anesthetized animals, and therefore concerns may be raised regarding the effects of anesthesia on cardiovascular and sympathetic systems. Barbiturates are often used for rodent anesthesia for invasive non-recovery procedures, however prolonged anesthesia and supplemental doses may induce respiratory and cardiovascular depression. The majority of experimental variables within this thesis concerned cardiovascular

measurements. Therefore the appropriate anesthetic that was used for all animals was a cocktail of α -chloralose and urethane. Both α -chloralose and urethane are able to produce long periods of anesthesia, without jeopardizing cardiopulmonary reflexes. Additionally, blood pressure and respiration are not affected, and spinal and baroreceptor reflexes remain intact (Jackson, Milne, Noble, & Shoemaker, 2005b; Jackson et al., 2004; Killip, 1963; Soma, 1983). Experimental outcomes of experiments were therefore determined with confidence that the anesthetic did not confound the validity of cardiovascular measurements obtained in studies of chapters 2, 3, and 4.

5.4. Future Directions

As pre-diabetes affects one quarter of the North American population, dietary modification and increased activity level have become the primary first line of defense against diabetic disease progression. Compliance to such lifestyle changes, specifically increased physical activity, may be low as a result of compromised perfusion of contracting muscle. Insufficient blood flow distribution and supply to working tissues may interfere with muscle performance and may even become painful in extreme conditions. Further investigations using animal models to address microvascular function in pre-diabetes may uncover additional functional mechanisms that may be compromised.

In contracting skeletal muscle, vasodilation can ascend the arteriolar network (Hilton, 1959). Vasodilation is generally initiated at distal arterioles and travels proximally past intramuscular arterioles, decreasing vascular resistance and increasing blood supply to arteriolar networks of working muscle (Folkow, Sonnenschein, &

Wright, 1971; Segal & Jacobs, 2001). Increased SNA has been shown to inhibit the spread of dilation along arterioles and feed arteries (Haug & Segal, 2005; Haug, Welsh, & Segal, 2003; Kurjiaka & Segal, 1995), and thus attenuates conducted vasodilatory responses within arteriolar networks (VanTeeffelen & Segal, 2003). Increased SNA in the pre-diabetic condition may therefore compromise conducted vasodilatory responses, in addition to maximal arteriolar dilatory responses to exercise. Future studies can utilize the arteriolar network of the GM to evaluate the spread of dilation initiated at distal pre-capillary arterioles and propagated upstream. Micropipette pressure pulse ejection of vasoactive substances can be delivered to arterioles locally to evoke conducted dilatory responses. Measurements such as arteriolar dilation, distance of the conducted response and conduction speed could therefore be quantified. Using sympathetic antagonists, potential sympathetically-mediated restrictions of conducted responses can be determined.

In addition to proposed sympathetically-mediated inhibition of conducted vasodilation, the cellular components involved in the conducted dilatory response may also be effected in pre-diabetes. The upward spread of dilation from distal arterioles is an electrical event mediated by cell-to-cell coupling. Activation of endothelial potassium channels leads to hyperpolarization of endothelial cells that is conducted along the vessel and traverses into vascular smooth muscle cells via myoendothelial gap junctions (Bagher & Segal, 2011). Interestingly, previous work has demonstrated that the activity of ATP-sensitive potassium channels of gracilis feed arteries is augmented in obese Zucker rats (Hodnett et al., 2008). These findings may be translated to the pre-diabetic state, as obesity is commonly associated with pre-diabetes. This may cause impairments

in the ability to initiate and sustain conducted dilatory responses throughout arteriolar skeletal muscle networks. Whether expression and/or function of ion channels involved in initiating vasodilatory hyperpolarization is augmented in pre-diabetes remains to be investigated.

In chapter 2, expression of NPY was greater in hindlimb tissue of pre-diabetic rats compared to control rats. Increased neurotransmitter (NT) expression of NPY supports an increase in NT release and increased SNA reported to accompany hyperinsulinemia and insulin resistance in pre-diabetes. Interestingly however, expression of hindlimb tissue Y1R and α 1R was also elevated. Conventionally, an increase in ligand causes internalization and down regulation of receptors, but findings from chapter 2 demonstrated the opposite. Thus modification of sympathetic Y1R and α 1R expression in pre-diabetes may occur via epigenetic influences, despite the increased presence of NTs. Pilot experiments were performed to investigate whether pre-diabetic conditions modify receptor expression of vascular smooth muscle cell (VSMC) Y1R and α 1R. Vascular smooth muscle cells were isolated from aortas of both control and pre-diabetic mice and cultured *in vitro* (see Appendix A for methods). Cultured VSMCs from control and pre-diabetic mice were then treated with media supplemented with glucose, insulin and leptin at concentrations similar to physiological levels observed in pre-diabetic mice. Upon Western blot analysis of Y1R and α 1R VSMC protein expression, novel results indicated that media mimicking 'pre-diabetic conditions' (high glucose, insulin and leptin) could modify sympathetic receptor expression in VSMC of control mice and pre-diabetic mice (Figure 5.1). Although data are preliminary, these novel findings may provide

implications for initiation of sympathetic vascular dysregulation initiated early in pre-diabetes, as a result of pre-diabetic pathological characteristics.

In addition to the aforementioned directions of study, other factors contributing to microvascular dysregulation in pre-diabetes may be considered. Investigation of sympathetic vascular control mechanisms can be extended, where future experiments may address β -adrenergic, as well as purinergic vascular modulation in pre-diabetes. Also, studies may aim to determine whether increased sympathetic receptor expression may be resolved spatially, where heterogeneous receptor distribution may be modified along individual arteriolar segments within skeletal muscle. Furthermore, long-term effects of heightened SNA may be reflected in changes of microvascular morphology, as NPY possesses potent vascular mitogenic properties (Shigeri & Fujimoto, 1993). Nonetheless, the ability to visualize the microvasculature is a powerful tool for investigating modifications in vascular function in pre-diabetes. At this early stage in diabetic disease progression, pathological modifications of vascular control mechanisms can be resolved at the level of the resistance vasculature, and may translate to microvascular complications in the human condition, which may not be resolved.

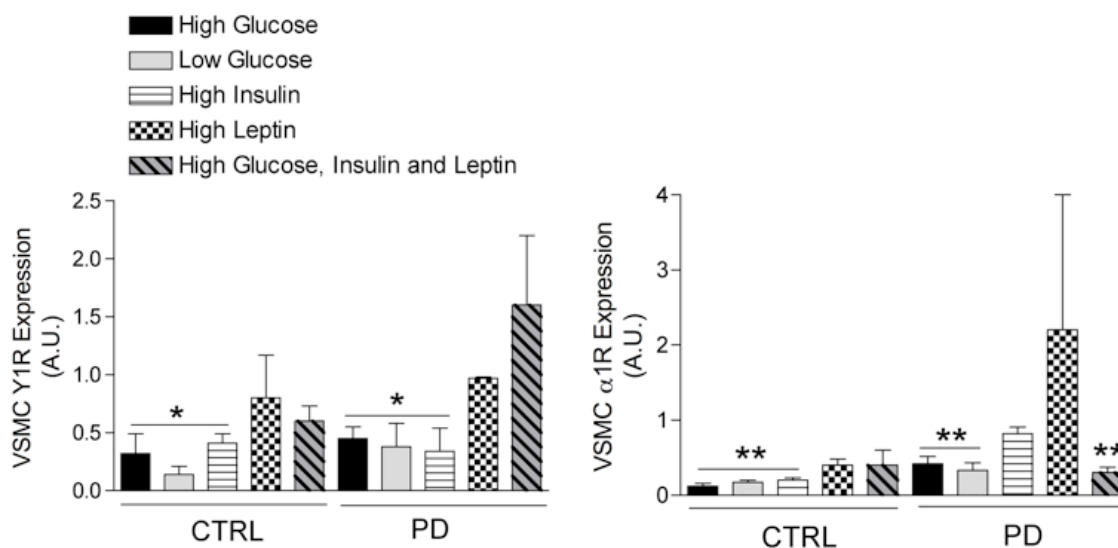


Figure 5.1. Glucose, insulin and leptin modifies vascular smooth muscle cell Y1R and α 1R expression in CTRL and PD.

Protein expression of Y1R and α 1R in aortic VSMCs isolated from control (CTRL n=2-6) and pre-diabetic (PD, n=2-6) mice. VSMCs were exposed to high glucose media (17 mM), low glucose media (5 mM), high insulin media (100 ng/mL), high leptin media (50 ng/mL), and high glucose, insulin and leptin DMEM (mimicking pre-diabetic conditions). * different from PD high glucose, insulin and leptin condition; ** different from PD high leptin condition, 1-way ANOVA. Data represent mean values of Western blot band densities normalized to β -actin \pm SEM.

5.5. References

- Al-Khazraji, B. K., Novielli, N. M., Goldman, D., Medeiros, P. J., & Jackson, D. N. (2012). A simple "streak length method" for quantifying and characterizing red blood cell velocity profiles and blood flow in rat skeletal muscle arterioles. *Microcirculation*, *19*(4), 327-335.
- Bagher, P., & Segal, S. S. (2011). Regulation of blood flow in the microcirculation: role of conducted vasodilation. *Acta Physiol (Oxf)*, *202*(3), 271-284.
- Bartfai, T., Iverfeldt, K., Fisone, G., & Serfozo, P. (1988). Regulation of the release of coexisting neurotransmitters. *Annu Rev Pharmacol Toxicol*, *28*, 285-310.
- Bearden, S. E., Payne, G. W., Chisty, A., & Segal, S. S. (2004). Arteriolar network architecture and vasomotor function with ageing in mouse gluteus maximus muscle. *J Physiol*, *561*(Pt 2), 535-545.
- Buckwalter, J. B., Hamann, J. J., & Clifford, P. S. (2005). Neuropeptide Y1 receptor vasoconstriction in exercising canine skeletal muscles. *J Appl Physiol (1985)*, *99*(6), 2115-2120.
- Buckwalter, J. B., Hamann, J. J., Kluess, H. A., & Clifford, P. S. (2004). Vasoconstriction in exercising skeletal muscles: a potential role for neuropeptide Y? *Am J Physiol Heart Circ Physiol*, *287*(1), H144-149.
- Casey, D. P., & Joyner, M. J. (2012). Influence of alpha-adrenergic vasoconstriction on the blunted skeletal muscle contraction-induced rapid vasodilation with aging. *J Appl Physiol*, *113*(8), 1201-1212.
- De Camilli, P., & Jahn, R. (1990). Pathways to regulated exocytosis in neurons. *Annu Rev Physiol*, *52*, 625-645.
- DeLorey, D. S., Buckwalter, J. B., Mittelstadt, S. W., Anton, M. M., Kluess, H. A., & Clifford, P. S. (2010). Is tonic sympathetic vasoconstriction increased in the skeletal muscle vasculature of aged canines? *Am J Physiol Regul Integr Comp Physiol*, *299*(5), R1342-1349.

- Dinenno, F. A., & Joyner, M. J. (2006). Alpha-adrenergic control of skeletal muscle circulation at rest and during exercise in aging humans. *Microcirculation*, *13*(4), 329-341.
- Etgen, G. J., & Oldham, B. A. (2000). Profiling of Zucker diabetic fatty rats in their progression to the overt diabetic state. *Metabolism*, *49*(5), 684-688.
- Evanson, K. W., Stone, A. J., Samraj, E., Benson, T., Prisby, R., & Kluess, H. A. (2012). Influence of estradiol supplementation on neuropeptide Y neurotransmission in skeletal muscle arterioles of F344 rats. *Am J Physiol Regul Integr Comp Physiol*, *303*(6), R651-657.
- Folkow, B., Sonnenschein, R. R., & Wright, D. L. (1971). Loci of neurogenic and metabolic effects on precapillary vessels of skeletal muscle. *Acta Physiol Scand*, *81*(4), 459-471.
- Frisbee, J. C. (2003). Impaired skeletal muscle perfusion in obese Zucker rats. *Am J Physiol Regul Integr Comp Physiol*, *285*(5), R1124-1134.
- Frisbee, J. C. (2004). Enhanced arteriolar alpha-adrenergic constriction impairs dilator responses and skeletal muscle perfusion in obese Zucker rats. *J Appl Physiol*, *97*(2), 764-772.
- Haug, S. J., & Segal, S. S. (2005). Sympathetic neural inhibition of conducted vasodilatation along hamster feed arteries: complementary effects of alpha1- and alpha2-adrenoreceptor activation. *J Physiol*, *563*(Pt 2), 541-555.
- Haug, S. J., Welsh, D. G., & Segal, S. S. (2003). Sympathetic nerves inhibit conducted vasodilatation along feed arteries during passive stretch of hamster skeletal muscle. *J Physiol*, *552*(Pt 1), 273-282.
- Hilton, S. M. (1959). A peripheral arterial conducting mechanism underlying dilatation of the femoral artery and concerned in functional vasodilatation in skeletal muscle. *J Physiol*, *149*, 93-111.
- Hodnett, B. L., Xiang, L., Dearman, J. A., Carter, C. B., & Hester, R. L. (2008). K(ATP)-mediated vasodilation is impaired in obese Zucker rats. *Microcirculation*, *15*(6), 485-494.

- Jackson, D. N., Milne, K. J., Noble, E. G., & Shoemaker, J. K. (2005a). Gender-modulated endogenous baseline neuropeptide Y Y1-receptor activation in the hindlimb of Sprague-Dawley rats. *J Physiol*, 562(Pt 1), 285-294.
- Jackson, D. N., Milne, K. J., Noble, E. G., & Shoemaker, J. K. (2005b). Neuropeptide Y bioavailability is suppressed in the hindlimb of female Sprague-Dawley rats. *J Physiol*, 568(Pt 2), 573-581.
- Jackson, D. N., Moore, A. W., & Segal, S. S. (2010). Blunting of rapid onset vasodilatation and blood flow restriction in arterioles of exercising skeletal muscle with ageing in male mice. *J Physiol*, 588(Pt 12), 2269-2282.
- Jackson, D. N., Noble, E. G., & Shoemaker, J. K. (2004). Y1- and alpha1-receptor control of basal hindlimb vascular tone. *Am J Physiol Regul Integr Comp Physiol*, 287(1), R228-233.
- Killip, T., 3rd. (1963). Sinus nerve stimulation in the chloralose anesthetized cat: effect on blood pressure, heart rate, muscle blood flow and vascular resistance. *Acta Physiol Scand*, 57, 437-445.
- Kim, S. H., & Reaven, G. M. (2008a). Insulin resistance and hyperinsulinemia: you can't have one without the other. *Diabetes Care*, 31(7), 1433-1438.
- Kim, S. H., & Reaven, G. M. (2008b). Isolated impaired fasting glucose and peripheral insulin sensitivity: not a simple relationship. *Diabetes Care*, 31(2), 347-352.
- Kurjiaka, D. T., & Segal, S. S. (1995). Interaction between conducted vasodilation and sympathetic nerve activation in arterioles of hamster striated muscle. *Circ Res*, 76(5), 885-891.
- Lee, A. W., & Cox, R. D. (2011). Use of mouse models in studying type 2 diabetes mellitus. *Expert Rev Mol Med*, 13, e1.
- Lesniewski, L. A., Donato, A. J., Behnke, B. J., Woodman, C. R., Laughlin, M. H., Ray, C. A., et al. (2008). Decreased NO signaling leads to enhanced vasoconstrictor responsiveness in skeletal muscle arterioles of the ZDF rat prior to overt diabetes and hypertension. *Am J Physiol Heart Circ Physiol*, 294(4), H1840-1850.

- Lundberg, J. M., Franco-Cereceda, A., Lou, Y. P., Modin, A., & Pernow, J. (1994). Differential release of classical transmitters and peptides. *Adv Second Messenger Phosphoprotein Res*, 29, 223-234.
- Lyssenko, V., Almgren, P., Anevski, D., Perfekt, R., Lahti, K., Nissen, M., et al. (2005). Predictors of and longitudinal changes in insulin sensitivity and secretion preceding onset of type 2 diabetes. *Diabetes*, 54(1), 166-174.
- Montano, N., Furlan, R., Guzzetti, S., McAllen, R. M., & Julien, C. (2009). Analysis of sympathetic neural discharge in rats and humans. *Philos Trans A Math Phys Eng Sci*, 367(1892), 1265-1282.
- Moore, A. W., Bearden, S. E., & Segal, S. S. (2010). Regional activation of rapid onset vasodilatation in mouse skeletal muscle: regulation through alpha-adrenoreceptors. *J Physiol*, 588(Pt 17), 3321-3331.
- Moore, A. W., Jackson, W. F., & Segal, S. S. (2010). Regional heterogeneity of alpha-adrenoreceptor subtypes in arteriolar networks of mouse skeletal muscle. *J Physiol*, 588(Pt 21), 4261-4274.
- Naik, J. S., Xiang, L., & Hester, R. L. (2006). Enhanced role for RhoA-associated kinase in adrenergic-mediated vasoconstriction in gracilis arteries from obese Zucker rats. *Am J Physiol Regul Integr Comp Physiol*, 290(1), R154-161.
- Naik, J. S., Xiang, L., Hodnett, B. L., & Hester, R. L. (2008). Alpha-adrenoceptor-mediated vasoconstriction is not involved in impaired functional vasodilation in the obese Zucker rat. *Clin Exp Pharmacol Physiol*, 35(5-6), 611-616.
- Novielli, N. M., Al-Khazraji, B. K., Medeiros, P. J., Goldman, D., & Jackson, D. N. (2012). Pre-Diabetes Augments Neuropeptide Y(1)- and alpha(1)-Receptor Control of Basal Hindlimb Vascular Tone in Young ZDF Rats. *PLoS One*, 7(10), e46659.
- Okon, E. B., Szado, T., Laher, I., McManus, B., & van Breemen, C. (2003). Augmented contractile response of vascular smooth muscle in a diabetic mouse model. *J Vasc Res*, 40(6), 520-530.

- Oltman, C. L., Richou, L. L., Davidson, E. P., Coppey, L. J., Lund, D. D., & Yorek, M. A. (2006). Progression of coronary and mesenteric vascular dysfunction in Zucker obese and Zucker diabetic fatty rats. *Am J Physiol Heart Circ Physiol*, *291*(4), H1780-1787.
- Proctor, D. N., & Parker, B. A. (2006). Vasodilation and vascular control in contracting muscle of the aging human. *Microcirculation*, *13*(4), 315-327.
- Romanko, O. P., Ali, M. I., Mintz, J. D., & Stepp, D. W. (2009). Insulin resistance impairs endothelial function but not adrenergic reactivity or vascular structure in fructose-fed rats. *Microcirculation*, *16*(5), 414-423.
- Segal, S. S., & Jacobs, T. L. (2001). Role for endothelial cell conduction in ascending vasodilatation and exercise hyperaemia in hamster skeletal muscle. *J Physiol*, *536*(Pt 3), 937-946.
- Shigeri, Y., & Fujimoto, M. (1993). Neuropeptide Y stimulates DNA synthesis in vascular smooth muscle cells. *Neurosci Lett*, *149*(1), 19-22.
- Soma, L. R. (1983). Anesthetic and analgesic considerations in the experimental animal. *Ann N Y Acad Sci*, *406*, 32-47.
- Stepp, D. W., & Frisbee, J. C. (2002). Augmented adrenergic vasoconstriction in hypertensive diabetic obese Zucker rats. *Am J Physiol Heart Circ Physiol*, *282*(3), H816-820.
- VanTeeffelen, J. W., & Segal, S. S. (2003). Interaction between sympathetic nerve activation and muscle fibre contraction in resistance vessels of hamster retractor muscle. *J Physiol*, *550*(Pt 2), 563-574.

Appendices

Appendix A

i) Isolation and culture of vascular smooth muscle cells

At the end of a subset of experiments (n=4-6), the CTRL or PD animal was euthanized and placed in the supine position. Under stereomicroscopic guidance and using sterile surgical instruments, a midline incision of the chest was made through the sternum to expose the chest cavity. Cardiac puncture was performed to remove blood volume, followed by cardiac perfusion of 1 mL sterile Hanks buffered saline solution (HBSS 1X, Invitrogen Canada Inc., Burlington, ON, Canada) through the apex of the heart. The lungs were then removed to clearly visualize the heart and aorta. Excess fat surrounding the proximal aorta was also removed. Two incisions were then made to remove the aorta, one below the aortic arch and one above the diaphragm. The isolated aorta was rinsed in HBSS and placed in enzymatic digestion solution (5% collagenase type II [Worthington Biochemical, Lakewood, NJ, USA], 5% soybean trypsin inhibitor [Invitrogen Canada Inc., Burlington, ON, Canada], 0.8 units/mL elastase [Worthington Biochemical, Lakewood, NJ, USA], suspended in HBSS) at 37°C for 10 minutes. The aorta was then moved to and rinsed in a petri dish containing warmed high glucose Dulbecco's minimal essential medium (DMEM), supplemented with 20% fetal bovine serum (FBS) and 1% penicillin-streptomycin (Invitrogen Canada Inc., Burlington, ON, Canada). The outer adventitial layer was carefully removed and the aorta was cut open longitudinally. All remaining blood clots were removed and the endothelial layer was removed by gently scraping the inside of the aorta with forceps. The aorta was then moved to a dish containing fresh warmed DMEM and cut horizontally into pieces, then

placed into enzymatic digestion solution for up to 2 hours, incubated at 37°C and 5% carbon dioxide. Once the pieces of aorta were dissolved, the vascular smooth muscle cell (VSMC) suspension was triturated with a glass pipette and equal volume of warmed DMEM was added to the dish. Cells were collected at 1500 rpm, washed twice, plated and left undisturbed for 5-7 days at 37°C and 5% carbon dioxide. Cells were washed with HBSS and passaged using 0.25% trypsin-EDTA treatment for dissociation. After passage 3-5, cells were weaned to 10% FBS supplemented DMEM.

ii) *Experimental conditions and Western Blot analysis of cultured VSMC*

At passage 8, approximately 1 million cells from each group (i.e. CTRL and PD) were plated into each well of a six well plate. Cells were cultured to approximately 90% confluence, serum starved for 24 hours, and re-incubated with the following media conditions for 48 hours (media was changed every 12 hours): high glucose DMEM (17 mM), low glucose DMEM (5 mM), high insulin DMEM (100 ng/mL), High leptin DMEM (50 ng/mL), High glucose, insulin and leptin DMEM (mimicking pre-diabetic conditions). After 48 hours, media was removed and cells were washed in ice cold HBSS and then lysed in lysis buffer (T-PER Tissue Protein Extraction Reagent, Fisher Scientific Company, Ottawa, ON, Canada) containing protease (104 mM AEBSF, 80 mM aprotinin, 2.1mM leupeptin, 3.6 mM bestatin, 1.5 mM pepstatin A and 1.4 mM E-64) and phosphatase (Halt Phosphatase Inhibitor Cocktail) inhibitors. Cells were scraped and then triturated with a pipette. Cell lysates were centrifuged for 15 min at 14,000 rpm at 4°C. Supernatant was collected and stored at -80°C until protein concentration was determined.

A Bradford assay was performed to determine total protein concentration of samples. Ten micrograms of protein from CTRL or PD samples were loaded on a 4–12% gradient gel and separated by SDS-PAGE. After electrophoresis, proteins were transferred at a constant voltage to polyvinylidene fluoride membranes. To determine Y1R VSMC protein expression, membranes were blocked for 1 hour in 5% bovine serum albumin (BSA) in Tris-Buffered Saline + Tween-20 (0.5%) (TTBS) at room temperature. Membranes were then incubated in primary antibody specific to mouse NPY Y1R (AbCam Inc., Cambridge, MA, USA) in 5% BSA in TTBS at a concentration of 1:1000 at 4°C overnight. Membranes were washed in TTBS then incubated in secondary antibody conjugated to horseradish peroxidase (goat anti-rabbit IgG, 1:20000) in 2.5% BSA in TTBS for 1 hr. To determine VSMC α 1R protein expression, membranes were blocked for 1 hour in 5% non-fat skim milk powder in TTBS at room temperature. Membranes were incubated in primary antibody specific to mouse α 1R (AbCam Inc., Cambridge, MA, USA) in 5% non-fat skim milk powder and Tris buffered saline (TBS) for 1 hour at room temperature. Membranes were washed in TBS and incubated in secondary antibody conjugated to horseradish peroxidase (goat anti-rabbit IgG, 1:20000) in 2.5% BSA in TTBS for 1 hour. Y1R and α 1R membranes were washed three times and bands were detected using an Immun-Star WesternCVC chemiluminescent kit (Bio-Rad, Hercules, CA, USA) and imaged with the ChemiDoc XRS System (Bio-Rad, Hercules, CA, USA). Following imaging, membranes were immediately washed in TTBS, stripped, and blocked in 5% BSA in TTBS for 1 hour at room temperature. Membranes were washed in TTBS and incubated in primary antibody specific to β -actin (loading control, anti-beta actin, rabbit polyclonal, Abcam, Cambridge, MA, USA) for 1

hour at room temperature. Membranes were then washed in TTBS, incubated in secondary antibody and imaged (as above). Densitometric band analysis was performed with Quantity One 1-D Analysis Software (Bio-Rad, Hercules, CA, USA). Quantified protein expression values were normalized to β -actin.

Appendix B

AUP Number: 2012-018 **PI Name:** Jackson, Dwayne **AUP Title:** Microvascular Function In Skeletal Muscle **Approval Date:** 08/08/2012

Official Notice of Animal Use Subcommittee (AUS) Approval: Your new Animal Use Protocol (AUP) entitled "Microvascular Function In Skeletal Muscle" has been APPROVED by the Animal Use Subcommittee of the University Council on Animal Care. This approval, although valid for four years, and is subject to annual Protocol Renewal.2012-018::1

1. This AUP number must be indicated when ordering animals for this project.
2. Animals for other projects may not be ordered under this AUP number.
3. Purchases of animals other than through this system must be cleared through the ACVS office. Health certificates will be required.

The holder of this Animal Use Protocol is responsible to ensure that all associated safety components (biosafety, radiation safety, general laboratory safety) comply with institutional safety standards and have received all necessary approvals. Please consult directly with your institutional safety officers.

**Submitted by: Copeman, Laura on behalf of the Animal Use
Subcommittee University Council on Animal Care**

Curriculum Vitae

Nicole M. Novielli

EDUCATION

Sept 2009- Present Ph.D. Candidate: Department of Medical Biophysics, Schulich School of Medicine and Dentistry, Western University. Project: *Pre-diabetes and arteriolar dysregulation*. Supervisor: Dr. Dwayne N. Jackson, Ph.D.

May 2008 – Aug 2009 M.Sc. Candidate (prior Ph.D status re-classification): Department of Medical Biophysics, Schulich School of Medicine and Dentistry, Western University. Project: *Pre-diabetes augments neuropeptide Y1- and $\alpha 1$ -receptor control of basal hindlimb vascular tone in young ZDF rats*. Supervisor: Dr. Dwayne N. Jackson, Ph.D.

Sept 2004- April 2008 B.M.Sc. (honors): Double Major in Physiology and Medical Sciences. Department of Physiology and Pharmacology, Western Ontario.

AWARDS

- Graduate Thesis Research Award, Western University (\$1,300, Feb. 2013).
- Ontario Graduate Scholarship, Ontario Ministry of Training, Colleges and Universities (\$15,000, May 2012-April 2013).
- Queen Elizabeth II Graduate Scholarship in Science and Technology, Ontario Ministry of Training, Colleges and Universities (\$15,000, May 2011-April 2012).
- Graduate Thesis Research Award, Western University (\$900, April 2011).
- Zweifach Travel Award, The Microcirculatory Society (\$750, April 2010).
- Graduate Thesis Research Award, Western University (\$1,050, April 2010).

- Strategic Training Fellowship in Vascular Research, Canadian Institute of Health Research (\$10,000, Sept. 2008-April 2010).
- Schulich Graduate Scholarship, Schulich School of Medicine and Dentistry, Western University (\$6,672, Sept. 2009 – Aug 2010).

PUBLICATIONS

Manuscripts in review

Novielli N.M. and Jackson D.N. Contraction-evoked vasodilation and functional hyperemia are compromised in branching skeletal muscle arterioles of young pre-diabetic mice. *Acta Physiologica*, October 2013, Manuscript No. APH-2013-10-0364.

Published Manuscripts

Novielli N.M., Al-Khazraji B.K., Medeiros P.J., Goldman D., Jackson D.N. *Pre-diabetes augments neuropeptide Y₁- and α_1 -receptor control of basal hindlimb vascular tone in young ZDF rats.* PLoS One. 2012; 7(10):e46659.

Al-Khazraji B.K., **Novielli N.M.**, Goldman D., Medeiros P.J., and Jackson D.N. *A simple "streak length method" for quantifying and characterizing red blood cell velocity profiles and blood flow in rat skeletal muscle arterioles.* Microcirculation. 2012; 19(4):327-35.

Al-Khazraji B.K., Medeiros P.J., **Novielli N.M.**, Jackson D.N. *An automated cell-counting algorithm for fluorescently-stained cells in migration assays.* Biological Procedures Online. 2011; 13(1):9.

Medeiros P.J., Al-Khazraji B.K., **Novielli N.M.**, Postovit L.M., Chambers A.F., and Jackson D.N. *Neuropeptide Y stimulates proliferation and migration in the 4T1 breast cancer cell line.* International Journal of Cancer. 2012; 131(2): 276-86.

Published Peer Reviewed Abstracts:

Novielli N.M. and Jackson D.N. *Sympathetic mediated microvascular dysregulation in pre-diabetes*. London Health Research Day 2013. London, ON, Canada. Poster presentation.

Novielli N.M., Al-Khazraji B.K., Jackson D.N. *Pre-diabetes and microvascular dysfunction in contracting skeletal muscle*. 2012 CIHR National Student Research Poster Competition. The Canadian Student Health Research Forum 2012. Winnipeg, MB, Canada. Poster presentation.

Al-Khazraji B.K., **Novielli N.M.**, Goldman D., Ellis C.G., Jackson D.N. *Novel video method for acquiring and modeling in vivo hemodynamic data from arteriolar networks of rat gluteus maximus skeletal muscle*. 2011 CIHR National Student Research Poster Competition. The Canadian Student Health Research Forum 2011. Winnipeg, MB, Canada. Poster presentation, recipient of Silver Award.

Novielli N.M., Al-Khazraji B.K., Jackson D.N. *Impaired microvascular control in contracting skeletal muscle in a murine model of prediabetes*. Diabetes Research Day 2011. London, ON, Canada. Poster presentation.

Novielli N.M., Al-Khazraji B.K., Jackson D.N. *Impaired microvascular control in contracting skeletal muscle in a murine model of prediabetes*. Experimental Biology 2011. Washington, DC, USA. Poster presentation.

Novielli. N.M., Al-Khazraji. B.K., Ellis. C.G., Jackson. D.N. *Sympathetic modulation of baseline hindlimb blood flow and vascular conductance in a model of prediabetes using young Zucker Diabetic Fatty rats*. Experimental Biology 2010. Anaheim, CA, USA. Poster presentation.

Medeiros. P.J., **Novielli. N.M.**, Jackson. D.N. *Characterizing the sympathetic neuropeptide Y system in 4T1 mammary carcinoma*. Experimental Biology 2009. New Orleans, LA, USA. Poster presentation.

INVITED PRESENTATIONS

Novielli, N.M. *Impaired microvascular control in contracting skeletal muscle in a murine model of prediabetes.* Presented at London Health Research Day, March 2012. London, ON, Canada. Platform presentation.

Novielli, N.M. *Sympathetic modulation of baseline hindlimb blood flow and vascular conductance in a model of prediabetes using young Zucker Diabetic Fatty rats.* Presented at Diabetes Research Day, Feb. 2010. London, ON, Canada. Platform presentation.

ACTIVITIES AND CONTRIBUTIONS

Teaching:

- *Teaching Assistant:* Sept. 2010-June 2013, Medical Biophysics Graduate Student Seminar Series, Western University.
- *Laboratory Instructor:* Sept. 2009-April 2012, Third-year Medical Biophysics laboratory course (MBP 3970Z), Western University.

Research Mentorship:

- *Elton Ng* (Summer research student): May 2013- Aug 2013, Department of Physiology, Western University.
- *Baraa Al-Khazraji* (Summer research student): May 2009- Aug. 2009, Department of Medical Biophysics, Western University.
- *Kelley Bronson* (Summer research student): May 2009- Aug. 2009, Department of Medical Biophysics, Western University.